



NTNU – Trondheim
Norwegian University of
Science and Technology

Experimental study of water coning phenomenon in perforated pipes geometry

Egor Shevchenko

Natural Gas Technology

Submission date: July 2013

Supervisor: Ole Jørgen Nydal, EPT

Norwegian University of Science and Technology
Department of Energy and Process Engineering

EPT-M-2013-103

MASTER THESIS

For
Egor Shevchenko
Spring 2013

Experimental study of water coning phenomenon in perforated pipes *Eksperimentell studie av vann koning i perforerte rør*

Background

Long horizontal wells require Inflow Control Devices (ICD) to optimize production and to maximize recovery. Water or gas coning have previously led to major losses, so ICDs are always installed in these types of wells.

The ICDs in current use consists of restrictions to create pressure drop and to reduce flow rate locally. However, the flow rate depends on the pressure drop. With depletion the pressure profile will therefore change, and may still cause coning at late production times.

The main target of ICD is to deal with the potential coning phenomenon in the reservoir. Once the water has broken through over the whole area of the well, the coning behavior may happen in the well geometry, the potential of coning formation is larger for more viscous oil field. It is therefore important to understand the mechanism of coning formation in well geometry, and provide important input to improve the design of ICD.

Objectives

Perform an experimental study of the water coning phenomenon in a perforated channel.

The following tasks are to be considered

1. A literature review will be performed on the coning phenomenon.
2. A 2D setup shall be constructed and used for flow visualization experiments made with oil-water flowing between two plates (3 and 7 mm spacing) towards a drainage hole. Two oil viscosities. Measurements of water interface vs. drainage rates. Based on the results, a new setup can be made with pipe geometries instead of flat plates.
3. Data analysis
4. Suggestions for further work

Within 14 days of receiving the written text on the master thesis, the candidate shall submit a research plan for his project to the department.

When the thesis is evaluated, emphasis is put on processing of the results, and that they are presented in tabular and/or graphic form in a clear manner, and that they are analyzed carefully. The thesis should be formulated as a research report with summary both in English and Norwegian, conclusion, literature references, table of contents etc. During the preparation of the text, the candidate should make an effort to produce a well-structured and easily readable report. In order to ease the evaluation of the thesis, it is important that the cross-references are correct. In the making of the report, strong emphasis should be placed on both a thorough discussion of the results and an orderly presentation.

The candidate is requested to initiate and keep close contact with his/her academic supervisor(s) throughout the working period. The candidate must follow the rules and regulations of NTNU as well as passive directions given by the Department of Energy and Process Engineering.

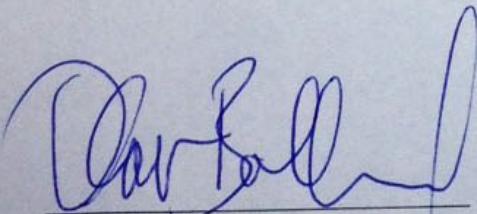
Risk assessment of the candidate's work shall be carried out according to the department's procedures. The risk assessment must be documented and included as part of the final report. Events related to the candidate's work adversely affecting the health, safety or security, must be documented and included as part of the final report.

Pursuant to "Regulations concerning the supplementary provisions to the technology study program/Master of Science" at NTNU §20, the Department reserves the permission to utilize all the results and data for teaching and research purposes as well as in future publications.

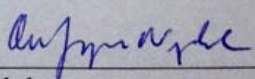
The final report is to be submitted digitally in DAIM. An executive summary of the thesis including title, student's name, supervisor's name, year, department name, and NTNU's logo and name, shall be submitted to the department as a separate pdf file. Based on an agreement with the supervisor, the final report and other material and documents may be given to the supervisor in digital format.

- Work to be done in lab (Multiphase flow laboratory)
 Field work

Department of Energy and Process Engineering, 16 January 2013



Olav Bolland
Department Head



Ole Jørgen Nydal
Academic Supervisor

Co-supervisor: Zhilin Yang, Proff II EPT, Statoil Research Centre

Acknowledgements

Thanks to Statoil Research Center in Rotvoll, Trondheim, for project proposal and especially to Zhilin Yang for supervision and supplying the relevant data.

This research project would not have been possible without the support of NTNU team, Department of Energy and Process Engineering. Sincere gratitude is expressed to co-supervisor, professor Ole Jørgen Nydal, who offered his guidance and assistance invaluable in the creative part of the design. Honorable mention goes to Martin Bustadmo, staff engineer, for operational expertise and manufacturing the facility.

Finally, I would like to thank my family and my friends. Thank you for supporting me in any kind of question throughout my student life!

Contents

| | |
|---|----|
| Abstract | 5 |
| 1 Introduction | 6 |
| 2 Overview of the problem | 7 |
| 2.1 Literature review | 7 |
| 2.2 Statoil input data | 18 |
| 3 Experimental setup design | 21 |
| 3.1 Design principles | 21 |
| 3.2 The finished rig | 25 |
| 4 Preparation stage | 29 |
| 4.1 Risk Assessment | 30 |
| 4.2 Inclined table incident | 32 |
| 5 Running the experiments | 34 |
| 5.1 Operations principles | 34 |
| 5.2 Procedure | 35 |
| 6 Results and discussion | 41 |
| 6.1 Flowrate correlations | 44 |
| 6.2 Liquid “jumps”, WC | 50 |
| 7 Conclusions and recommendations | 58 |
| 8 References | 59 |
| 9 Appendices | 62 |
| 9.1 Appendix A – Full rig design arrangement | 62 |
| 9.2 Appendix B – Drawings for tank manufacturing | 64 |
| 9.3 Appendix C – The parameters of all experimental runs | 66 |
| 9.4 Appendix D – Spreadsheet acronyms’ identification | 68 |
| 9.5 Appendix E – Detailed oils flowrates comparison with a single graph for each gap. | 69 |
| 9.6 Appendix F – “Jump” values vs. flowrate for Nexbase 3080 series and Exxsol D80 series for each gap | 70 |
| 9.7 Appendix G – Detailed oils “jump” comparison with a single graph for each gap. | 73 |
| 9.8 Appendix H – Water cut correlations over flowrate for different water levels | 74 |

Abstract

This Master Thesis is performed in close cooperation between NTNU and Statoil Research Centre in Rotvoll, Trondheim. It focuses on the experimental study of the water coning phenomenon in perforated pipe geometry. This study refers to Statoil data on horizontal well design, geometry of the ICD/AICD housing, production rates and fluid properties.

The experimental facilities were designed during the autumn semester in the project "Experimental setup for water coning in horizontal annular pipe geometries". It is based on the 2D-configuration setup and was used for flow visualization experiments.

The study provides extensive literature review of the problem. It describes existing industry experience and shows available academic research in the area of the coning phenomenon. Detailed hazard identification and risk assessments analysis were performed according to the NTNU and SINTEF safety procedures prior to starting of the work in the lab. The necessary measures for risk reduction were implemented. The event, possibly compromising safety level of the experimental runs, was documented and investigated in order to prevent similar reoccurrences in future.

The total number of 459 experiments with different rig and oil/water flow setup was conducted. Results are presented in clear graphical form in excel spreadsheet attached to the thesis. It shows key trends in oil/water flow behaviour in the gap towards a drainage hole, representing reservoir fluid inflow into the well tubing through the Inflow Control Device (ICD). Discussion part puts emphasis on the explanation of the obtained results and provides important input to improve the design of ICD.

1 Introduction

The average horizontal well is more expensive and technically difficult to drill than the average vertical well. Yet, around the world, horizontal wells are being spudded in ever increasing numbers. In simple terms, horizontal wells allow to do things more efficiently than vertical wells. It would be short-sighted to ignore a technique which offers improved drainage in typical reservoirs and penetrates more of the discrete compartments in complex reservoirs, while helping to reduce gas and water coning (Nurmi et al., 1995).

Statoil is the operator with most long horizontal wells on the Norwegian Continental Shelf. However, increasing the horizontal wellbore length leads to some production challenges. In the early 1990s a number of thin reservoirs required long wells, but to Norsk Hydros surprise (now integrated into Statoil), water breakthrough came very early. The conclusion was that these wells were subjected to water coning.

Long horizontal wells require Inflow Control Devices (ICD) to optimize production and to maximize recovery. Water or gas coning have previously led to major losses, so ICDs are always installed in these types of wells. The ICDs in current use consists of restrictions to create pressure drop and to reduce flow rate locally. However, the flow rate depends on the pressure drop. With depletion the pressure profile will therefore change, and may still cause coning at late production times (Aadnoy, 2008).

The main target of ICD is to deal with the potential coning phenomenon in the reservoir. Once the water has broken through over the whole are of the well, the coning behavior may happen in the well geometry, the potential of coning formation is larger for more viscous oil field. And at the same time, as energy demands grow and the costs of discovering and producing conventional oil goes up, the economics of heavy oil will steadily improve. Heavy crude oil has been defined as any liquid petroleum with an API gravity less than 20° (Dusseault, 2001).

It is therefore important to understand the mechanism of coning formation in well geometry, and provide important input to improve the design of ICD. The picture on the first page shows solar eclipse which is a metaphor referring to water coning in the annulus geometry.

The objective of this Master Thesis is to perform an experimental study of the water coning phenomenon in a perforated channel. The following tasks are considered:

1. A literature review on the coning phenomenon.
2. A 2D setup is to be constructed and used for flow visualization experiments made with oil-water flowing between two plates (5 – 25 mm spacing) towards a drainage hole. Two oil viscosities. Measurements of water interface vs. drainage rates.
3. Data analysis.
4. Suggestions for further work

2 Overview of the problem

2.1 Literature review

A survey of literature shows that coning phenomenon is rather well studied, research work has been done ranging from experimental studies to analytical and numerical simulation studies in order to understand and predict water coning and cresting in vertical and horizontal wells respectively. Several research efforts and solutions have also been developed to mitigate the coning phenomenon and reduce the level of severity of the post water breakthrough performance of the well.

Due to the nature of the Master Thesis an overview of research findings on horizontal well cresting and on placement of Inflow Control Devices (ICD) is presented in this chapter. Literature on water coning, which may happen in the annular well geometry, was not found.

Water coning in a horizontal well

Petroleum reservoirs often have a gas cap and/or an aquifer. In these situations they are subjected to rapid change in oil-water contact (OWC) or gas-oil contact (GOC) profiles as a result of drawdown pressures during production (Schlumberger, 2013). Prior to production, these reservoirs have defined OWC and GOC. Once production commences, the previously defined contacts now become deformed from its plane shape to form a cone or a crest. If a field is developed by vertical wells, the deformation is referred to as a cone (see Figure 2.1). For horizontal wells, it is known as a crest (Makinde et al., 2011).

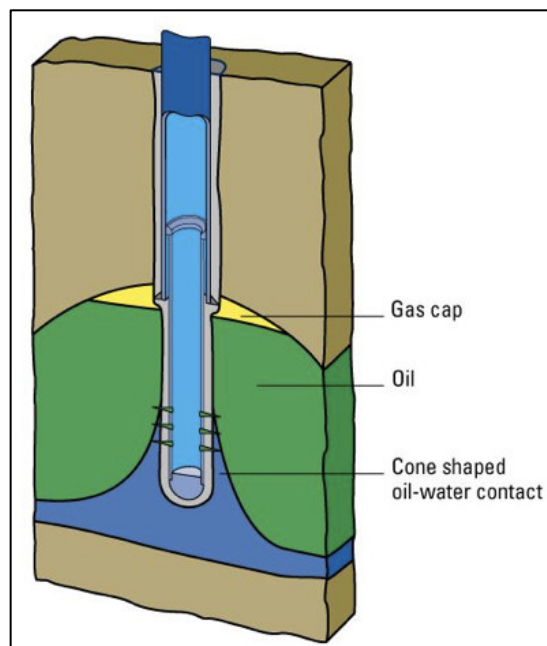


Figure 2.1 – Water coning in an oil well (Schlumberger, 2013).

Cresting occurs in horizontal or highly deviated wells and is affected by the characteristics of the fluids involved and the ratio of horizontal to vertical permeability (Schlumberger, 2013). Figure 2.2 shows cresting in a homogeneous reservoir (left) and heterogeneous (right) with, for example, permeability and other heterogeneity variations along the well trajectory.

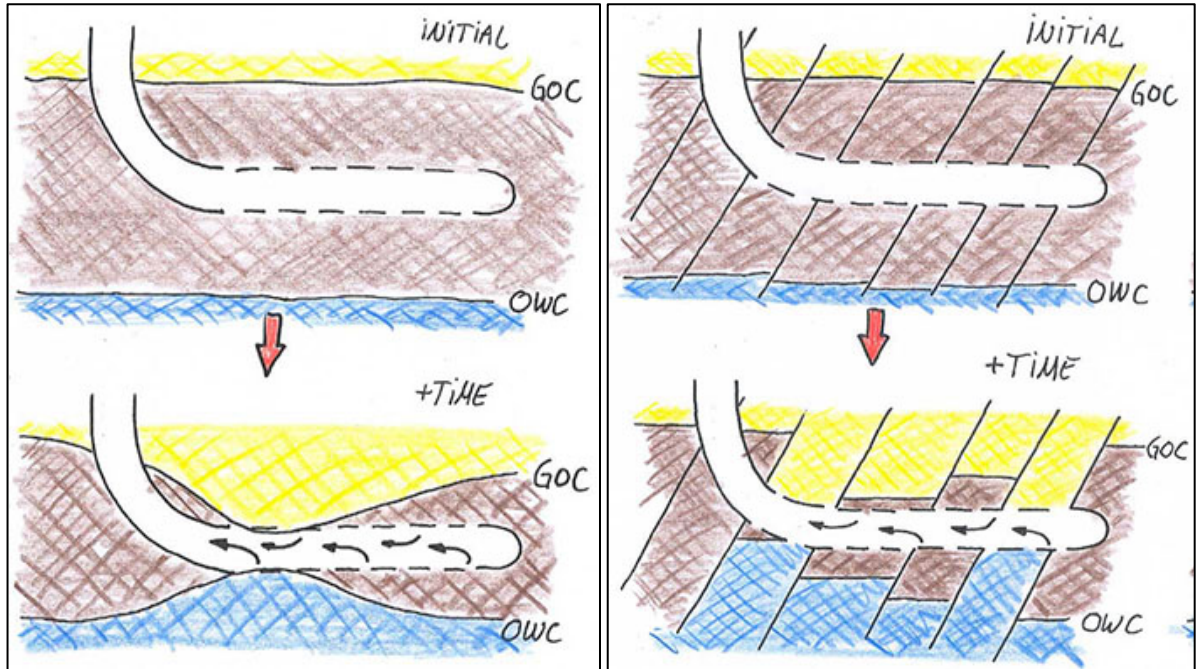


Figure 2.2 – Cresting in different completion scenarios (Porturas et al., 2009).

In many developments, particularly in thin oil rim reservoir (Nurmi et al., 1995), horizontal well drilling is suggested. Horizontal wells have superior production and recovery performance compared to vertical wells because they have more contact with the reservoir. This advantage in terms of fluid production rates, actually becomes a disadvantage when water breaks through into the wellbore causing a very rapid increase in watercut (Inikori, 2002). Another challenge presented by viscous oil is that the pressure drop from frictional loss in the tubing along the horizontal section is higher than in conventional wells. In horizontal wells of low drawdown, this can result in a higher production from the “heel” than from the “toe” of the well (see Figure 2.3 top-left graph, also notice that top-right graph is not a mirror image of bottom-left).

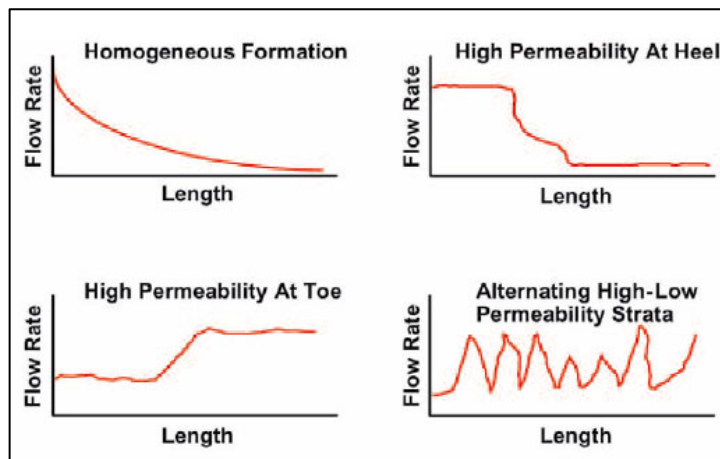


Figure 2.3 – Flux profiles in horizontal wells (Ratterman, 2006).

Therefore these wells are subject to early water and gas coning, usually towards the heel (see Figure 2.4). Moreover, variations in permeability can result in unbalanced inflow along the horizontal section and accelerate early water breakthrough and uneven inflow downhole (see Figure 2.4). These conditions can limit sweep efficiency and reduce hydrocarbon recovery from horizontal wells, leaving bypassed oil (Schlumberger, 2010).

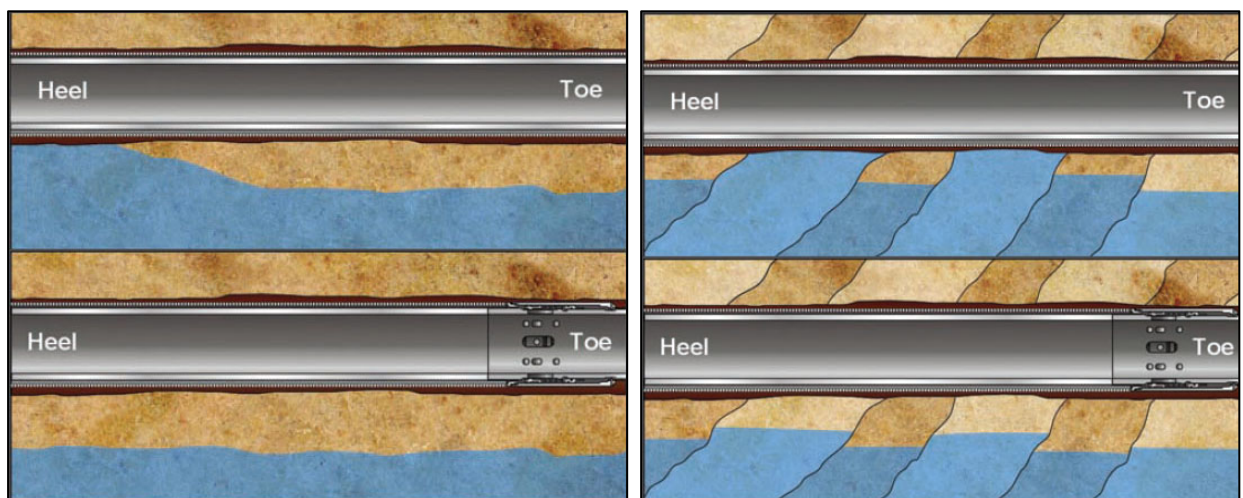


Figure 2.4 – Water coning due to pressure drop in the tubing resulting in higher influx from the reservoir in the “heel” part of the well (left). Uneven influx due to permeability contrasts in the reservoir can result in early water breakthrough of highly mobile water (Halliburton, 2008).

ICD application

Like their vertical well counterpart, the typical critical oil production rates to avoid water influx to the wellbore are also too low for any economic purpose. Thus typical production rates are usually higher than the critical rates for these wells (Inikori, 2002). Although critical rates are typically higher for horizontal wells than for vertical wells and the time to water breakthrough is also longer for horizontal wells than for vertical wells, the typical high production rate expected of horizontal wells soon creates the problem of unwanted water influx.

The experience of water cresting in the horizontal wells over the past years has prompted some level of research into the development of possible solutions. The overview of the research works is well described in the Dissertation by Ikinori (2002).

A way to increase economical attractiveness of horizontal wells is a proper placement of Inflow Control Devices (ICD) along the wellbore. ICD technology acts by automatically balancing the inflow along the well path. This self-adjusting effect works during the entire life of a well, and is achieved by the reservoir to completion interaction; inflow from high mobility reservoir zones is restricted and simultaneously, from low mobility reservoir zones is stimulated, as shown in Figure 2.5. The main objectives for selecting an ICD completion are (Maggs et al., 2008):

- Decrease the influence of flow variations along the wellbore due to geological heterogeneities;
- Increase recoverable reserves due to better sweep efficiency;
- Compensate friction induced heel-toe pressure drop effects;
- Decrease water/gas rates after breakthrough;
- Improve well cleanup.

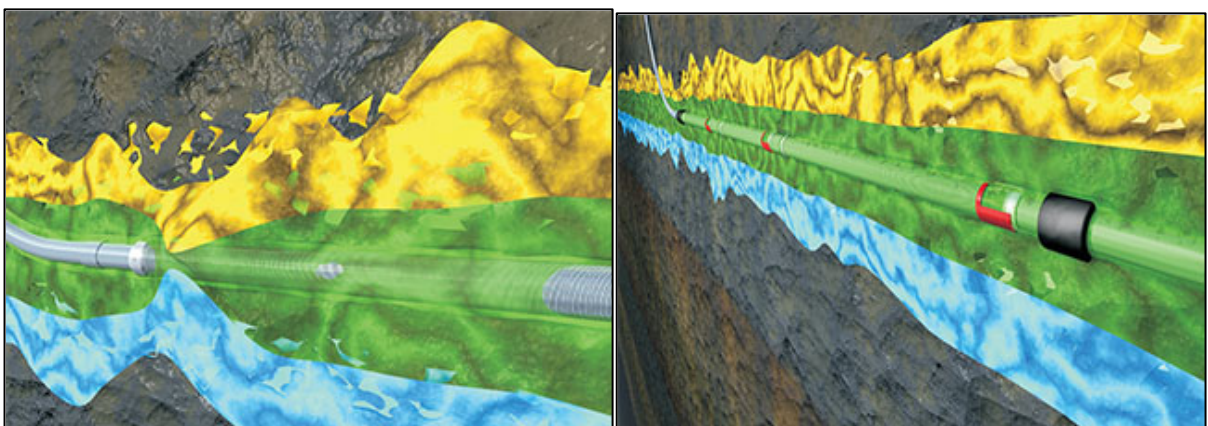


Figure 2.5a – Homogeneous formation without ICD (left) and with FloReq™ ICD (right) (Weatherford, 2010).

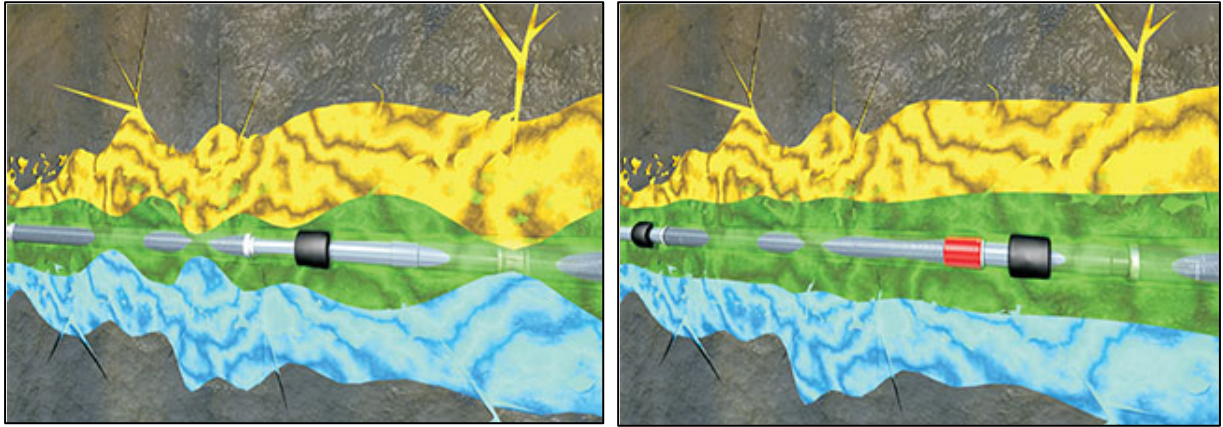


Figure 2.5b – Heterogeneous formation without ICD (left) and with FloReq™ ICD (right) (Weatherford, 2010).

There is no common approach to ICD design, there are different types of ICD (some shown in Figure 2.6): channel type Spiral Inflow Control Device (SICD), nozzle-type ICD, Autonomous Inflow Control Device (AICD), orifice ICD, annular chamber ICD and its combinations. For this project nozzle-based ICD design is of a particular interest.

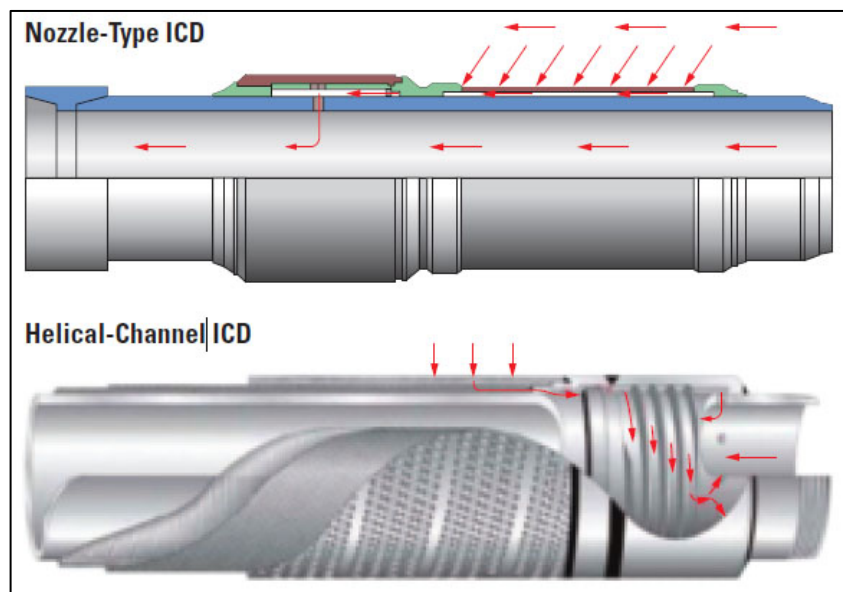


Figure 2.6 – Leading ICD types (Ellis et al., 2010).

Nozzle-type ICDs are self-regulating choking devices that operate through nozzle restriction based on the Bernoulli pressure-drop effect: the higher the velocity of the high-mobile-phase water approaching the nozzles for inflow, the more backpressure was imposed by the nozzles to restrict water influx (Schlumberger, 2010). The pressure drop through a nozzle (between the annulus and the tubing) is a result of the static energy in the fluid being converted into kinetic energy and absorbed in the fluid downstream of the nozzle (Porturas et al., 2009). The pressure drop, generated by the flowing fluid through the nozzles, (see Figure 2.7) is described by a part of the Bernoulli equation:

$$\Delta p_N = C_u \frac{\rho}{2 C_v^2} v^2, \quad v = \frac{q}{A} \quad (\text{Eq. 1})$$

Where: Δp_N – pressure drop across ICD nozzles, C_u – units conversion constant, ρ – density of fluid, v – velocity, C_v – dimensionless flow coefficient for the nozzle, q – rate and A – total cross-section of the nozzles (Maggs et al., 2008).

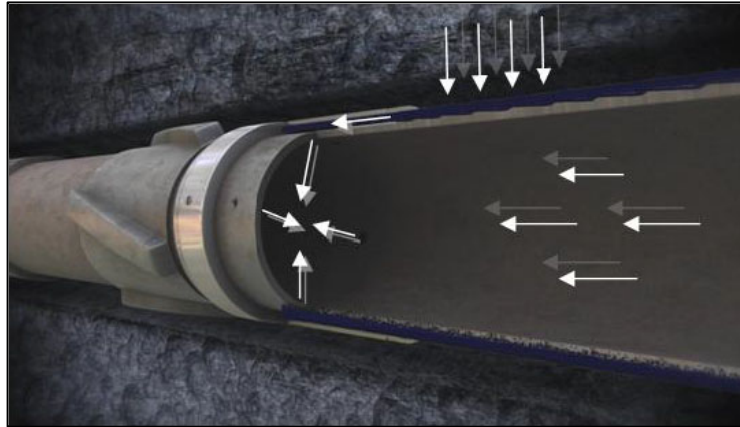


Figure 2.7 – Fluid flowing through the ICD nozzles (Maggs et al., 2008).

An ICD unit is integrated in a sand control screen. The screen ensures sand management and allows fines to be produced through the screen and nozzles (Maggs, 2008). The screen design is based on the fluid flowing through a filtering media and into a drainage layer. The drainage layer allows the fluid to flow from the filter media into the base pipe perforations in a conventional screen or into the ICD housing which is normally located at the end of the screen jacket (Moen, 2008). The fluid flows in through the wrapping of the screen section, along the axial ribs of the drainage layer, into the housing and through the nozzles (see Figure 2.8).

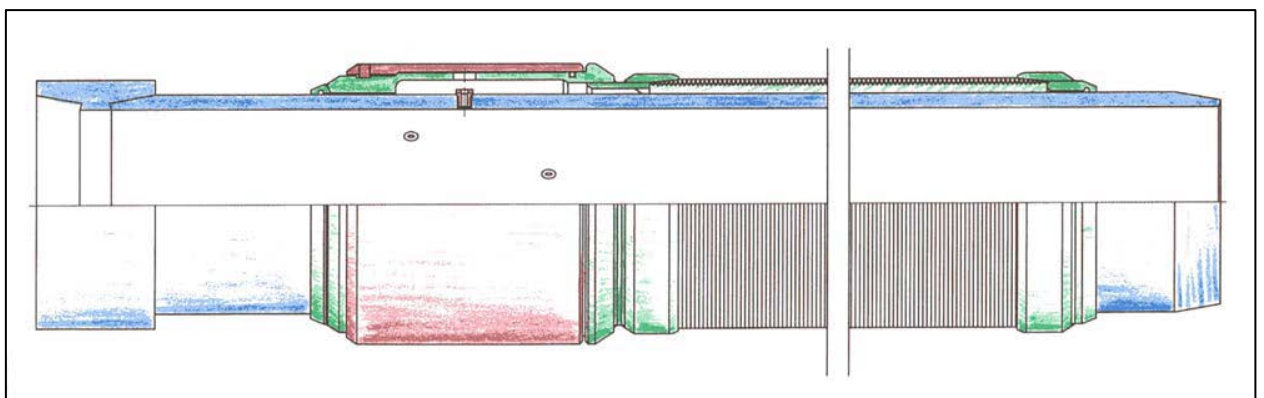


Figure 2.8 – A nozzle based ICD screen (Moen, 2008).

In other words, a nozzle based ICD has an absorbing chamber upstream of the nozzles (see Figure 2.9). Fluid enters the screen and then flows between screen jacket and base pipe into the housing and through the nozzles (Porturas et al., 2009). The similar design is presented by Schlumberger in Figure 2.10.

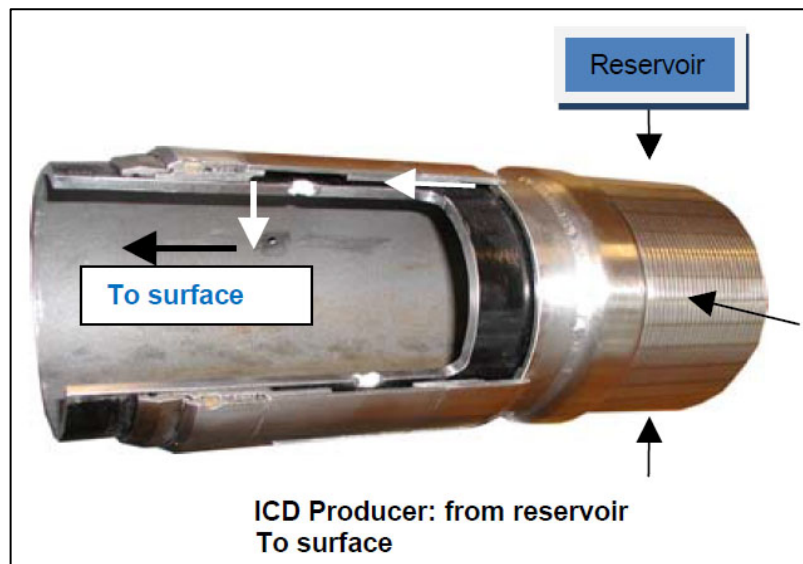


Figure 2.9 – ICD hardware integrated with sand control (Porturas et al., 2009).

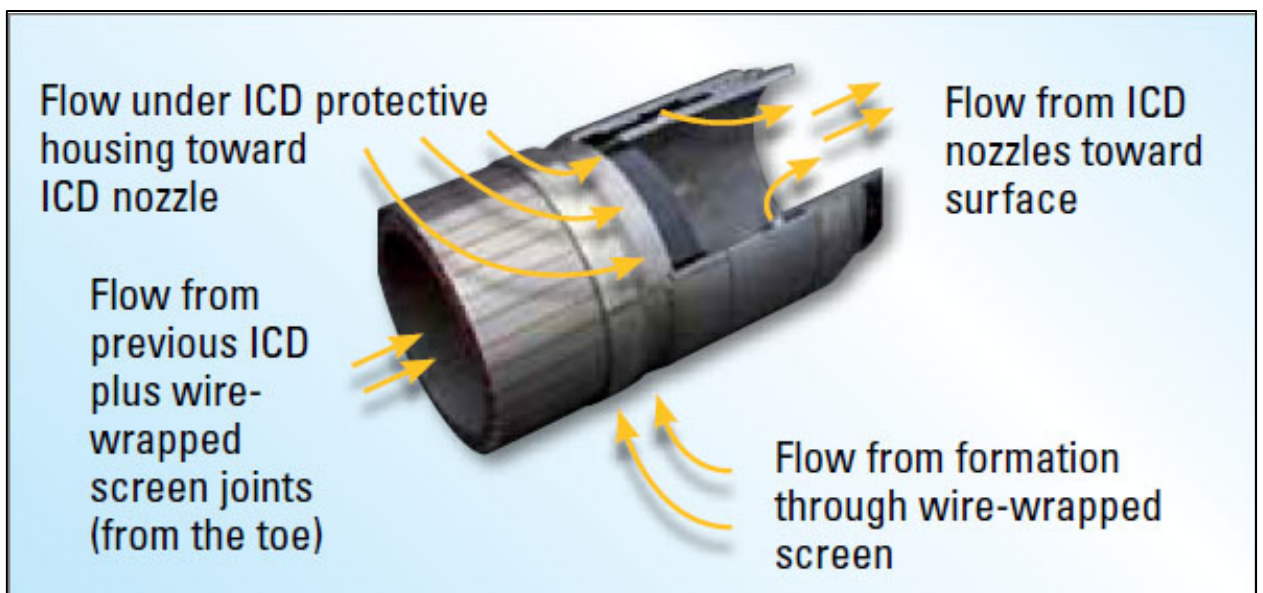


Figure 2.10 – The flow pattern in ResFlow™ ICD (Schlumberger, 2010).

The ICD unit is equipped with two or more nozzles. The pressure drop across the unit is designed based on the reservoir characteristics and flowrates required to achieve the objectives of the well. An advantage with the multiple nozzles is that at least one of the nozzles will be exposed in inflow of fluid. This makes the system reliable for well clean-up, even if the well has been left for some time with dirty fluids downhole before it is put on production (Moen, 2008).

More ICD developments were conducted, since there is a major drawback in current use of ICDs – the flow rate depends on the pressure drop, and this relates to flow changes as the reservoir pressure declines. Clearly the pressure drop flow rate relationship for the well is complex and highly non-linear. It is also sensitive to fluid

viscosity which can vary considerably. When the reservoir pressure declines, the relative flow through the various ICDs will therefore change, the non-linear characteristic is clearly seen in Figure 2.11. It is obvious that the non-linearity of traditional ICDs leads to relative flow change between the heel and the toe of the horizontal well during depletion. Simulations show that coning may still occur during reservoir depletion (Addnoy, 2008).

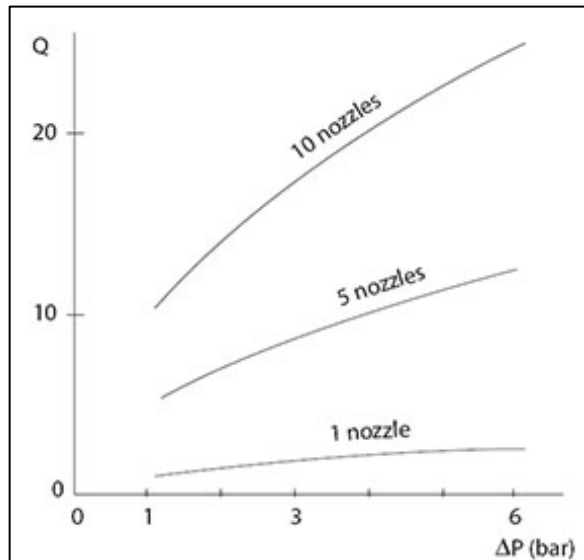


Figure 2.11 –Flowrate vs. pressure drop simulations for the FloReq™ ICD (Aadnoy, 2008).

There is one way to overcome the problem outlined above, and that is to control the flowrate over the entire life of the reservoir. The BECH autonomous control valve provides constant flowrate regardless of the state of the pressures. The valve is actually a constant flow controller (see the simplest version in Figure 2.12). The reservoir pressure is choked through a nozzle, where the required flow rate is set. The oil goes into a chamber where the compensator is consisting of a needle and a nozzle. When the reservoir pressure drops, the needle will open maintaining constant flow (Aadnoy, 2008).

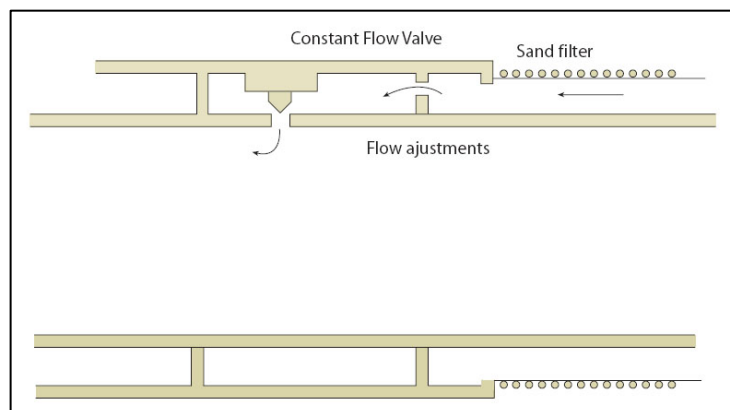


Figure 2.12 – Principle of the BECH autonomous flow control valve (Aadnoy, 2008).

Another autonomous valve design is a passive inflow control devices which automatically chokes back fluids with lower viscosity, thus partially closing sections of the well with high gas or water fraction. For example, in the study by Zadeh et al., 2012, AICD has a floating disk bound between the inlet and outlet of the valve which can move both toward upstream or downstream of the valve based on viscosity of the produced fluid. When a less viscous fluid enters the valve's inlet the floating disk will move towards the upstream and choke back. AICDs have different types with different tuning parameters. Selection between different types of AICDs for implementation depends on rock and fluid properties in a reservoir (Zadeh et al., 2012).

Introducing water coning in the annular pipe geometry

An ICD can equalize the fluids inflow, but it does not eliminate water entirely as shown in Figure 2.13. In addition, OWC continuously rises and water inevitably approaches the production tubing even with ICD as shown in Figure 2.14.

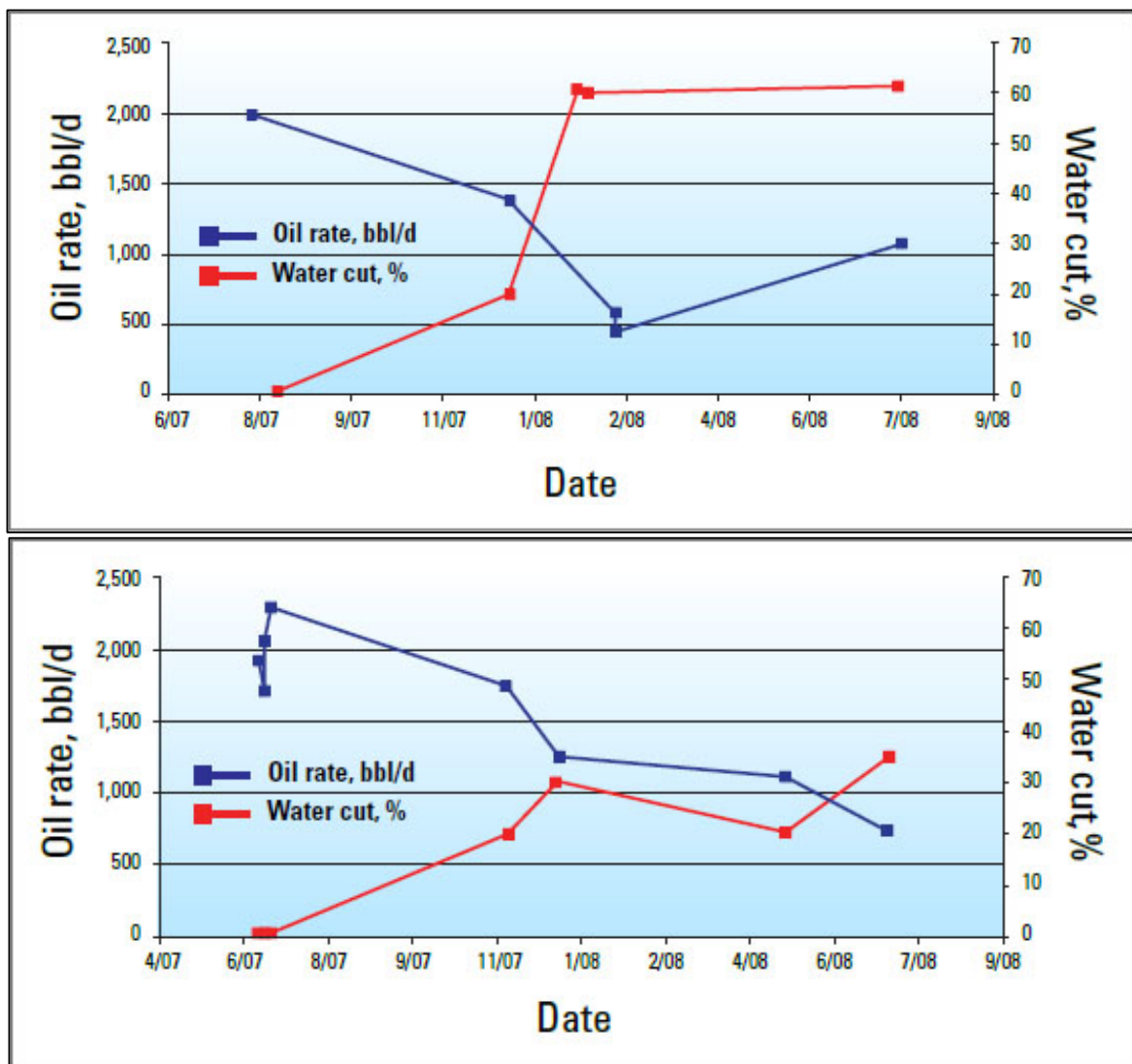


Figure 2.13 – Production profile with no ICDs (top) and with ResFlow™ ICD (bottom). Baram field, east Malaysia (Schlumberger, 2010).

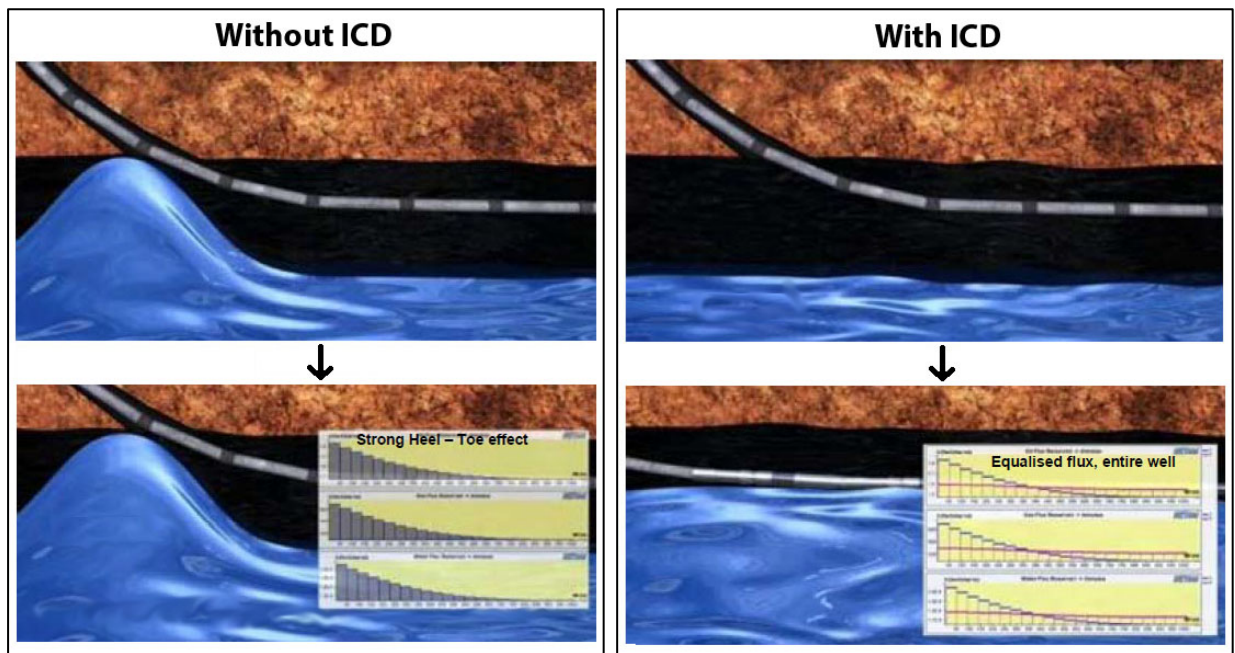


Figure 2.14 – Completions without ICD (left) and with ICD (right) (Porturas et al., 2009).

Oil and water is flowing from the reservoir through the gravel pack and screens into the ICD/AICDs, or simply “valves”. The local velocities are quite small and stratification of oil and water is probable as illustrated in Figure 2.15. In a horizontal well with inflow of oil and water from the reservoir in annular geometry some of the inflow openings/valves will be exposed to a water continuous phase and others to an oil continuous phase (Statoil, 2012).

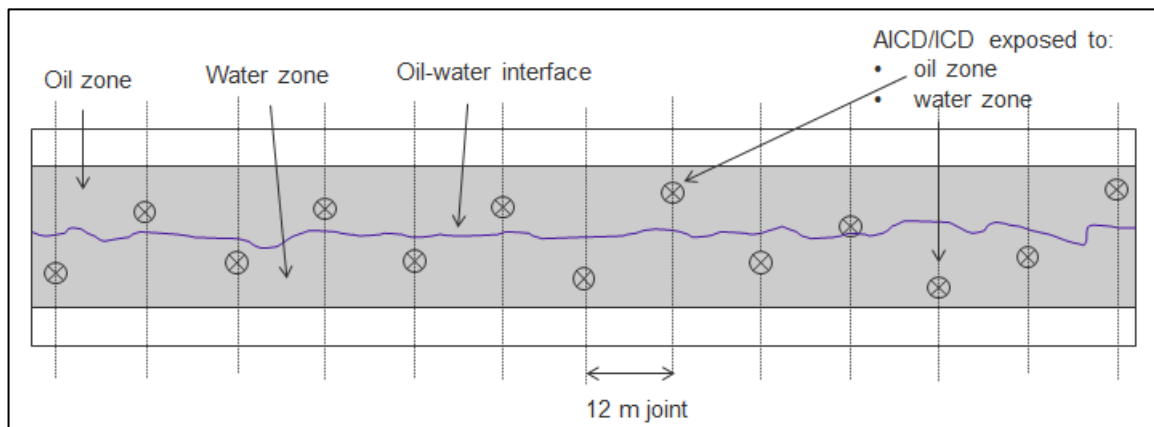


Figure 2.15 –Stratified pattern in the annular geometry outside the base pipe (Statoil, 2012).

The pressure gradient on the inlet of the valve will be much larger for the viscous oil compared with the water. This can lead to water coning to the oil producing pipe’s opening/valves, which can lead to a lower efficiency with regards to keeping the water cut in the well low.

When oil and water are flowing towards the entrance of the valve the pressure gradient will tend to cone in also the second liquid phase on the other side of the oil-water interface. In particular the inflow of viscous oil will have potential to generate high pressure gradients and cone the water into the oil zone (see Figure 2.16).

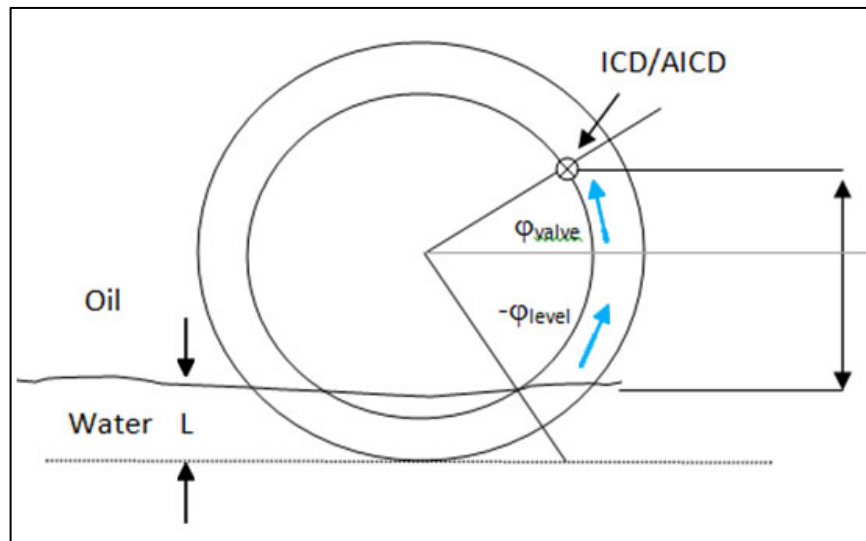


Figure 2.16 – Illustration of coning in annular geometry upstream the valve.

The objective of the work is to perform an experimental study of the water coning phenomenon in a perforated channel of the annular pipe geometry. It is important to understand the mechanism of coning formation in well geometry, and provide important input to improve the design of ICD.

2.2 Statoil input data

The data on the horizontal well design, geometry of the ICD/AICD housing, production rates and fluid properties was provided by Statoil Research Center in Rotvoll, Trondheim. It was used to design the experimental rig in the Industrial Process Technology Specialization Project (3rd semester of the Master Programme) and to estimate its operations conditions in the current Master Thesis.

The typical lower completion design is given in the Figure 2.17 below. Zones of individual length about 200 m are isolated by swell openhole packers. 5.5 inch screen is installed in horizontal 8.5 inch open hole. Each joint of length 12 m includes one or several ICD/AICDs.

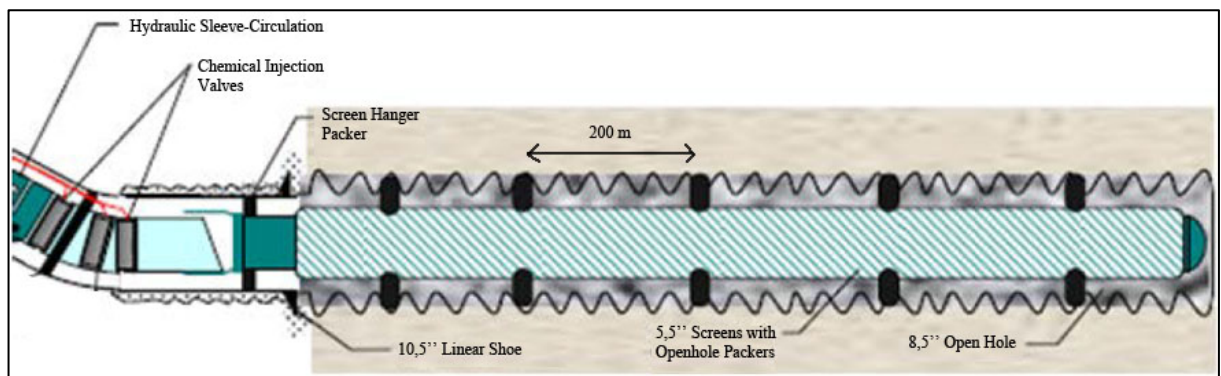


Figure 2.17 – Lower completion design.

The following data is given:

- the length of the horizontal single well: 1271 m;
- number of isolated zones: 6;
- number of joints per zone: 16.

One, two or three valves are installed at each joint of 12 m length. The valves on each joint are arbitrary oriented. This implies that some valves are exposed to a water zone in the lower region of the base pipe and some valves located in the upper region are exposed to oil. For this reason the probability distribution of finding a valve for a specific position around the base pipe wall is assumed to be constant.

The fluids are flowing through the screen into the housing upstream the base pipe and the ICD/AICD as illustrated in the Figures 2.18 and 2.19 below. The following numbers of ICD/AICD per joint are used – 2.

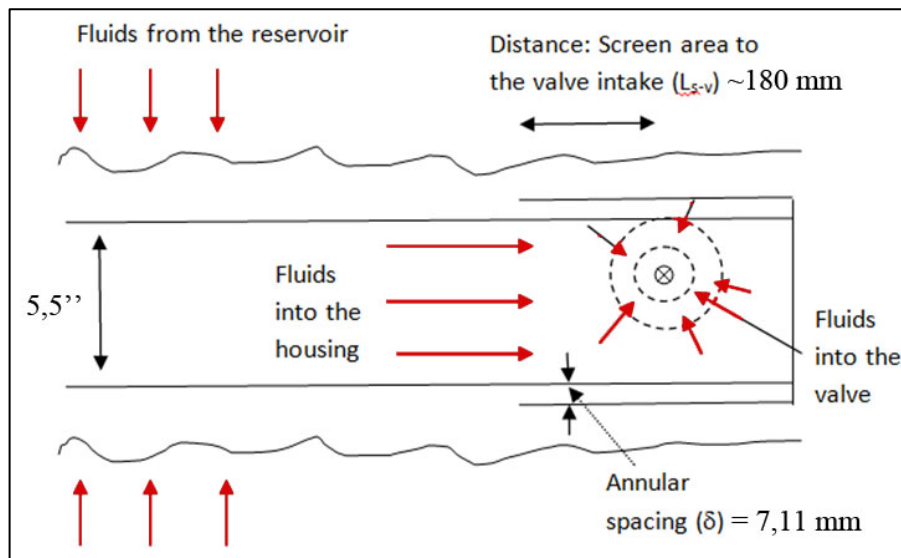


Figure 2.18 – Geometry of the housing upstream design 1.

For the Statoil AICD the fluids are flowing into the valve approximately symmetric around the valve intake. For the other commercial devices the fluid is flowing into valves at the end of the annular housing as illustrated in Figure 2.19.

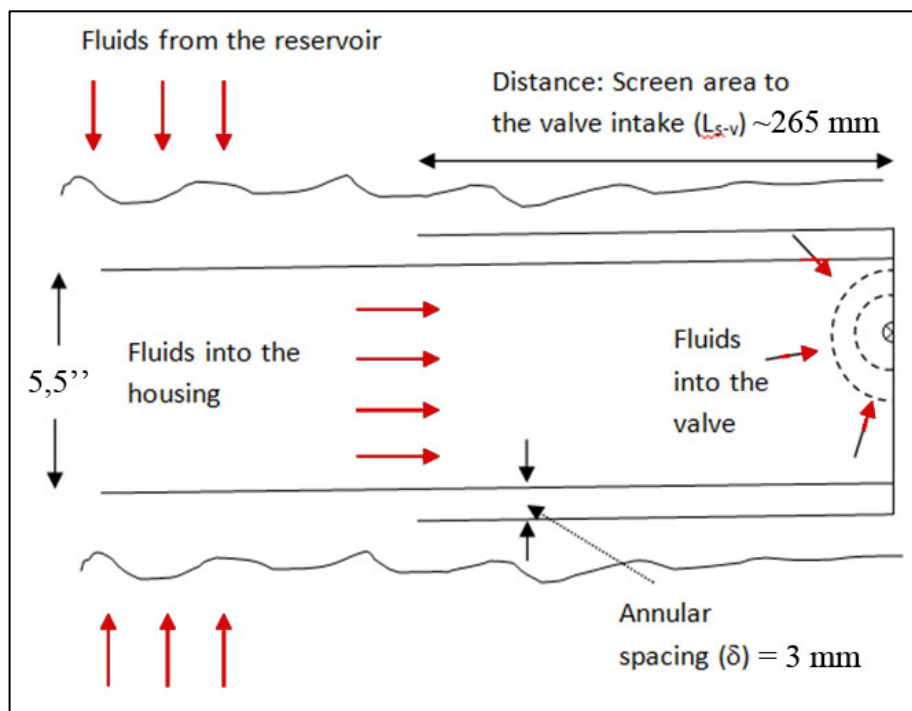


Figure 2.19 – Geometry of the housing upstream design 2.

The inflow geometry from the ICD/AICDs into the main wellbore for each joint are given as follows:

Design 1: in this case the outlet arrangement is not in flush with the inner wall. The flow direction into the main wellbore is perpendicular to the pipe axis. The flow area out of the AICD is calculated to be $3.3338 \cdot 10^{-4} \text{ m}^2$.

Design 2: the hole outlets are flush with the inner pipe wall. Total cross sectional area for the holes is $2.027 \cdot 10^{-3} \text{ m}^2$. This area ends up in a 36 mm for an orifice.

Production rates: 3500 Sm³/d corresponding to a local rate of 1.52 m³/h per joint. For 2 ICDs per joint the rate is halved to 0.76 m³/h.

Oil density: 935 kg/m³

Oil viscosity: 67 cP

Water density: 1031 kg/m³

Water viscosity: 0.72 cP

As said in chapter 2.1 an ICD is equipped with 2 or more nozzles. For the purposes of rig design and adjusting experimental operational parameters it was set up that ICD has 2 nozzles as it was adopted in Baram field, east Malaysia (Maggs et al., 2008). The production rate ends up around 6.2 l/min per orifice. Orifice diameter and flow velocities are calculated as following:

Design 1: orifice diameter 14.6 mm; velocity 0.62 m/s.

Design 2: orifice diameter 36 mm; velocity 0.11 m/s.

3 Experimental setup design

The rig was designed previously in the 3rd semester of the Master Programme. The Industrial Process Technology Specialization Project stated work objective as to design an experimental facility for studies of the water annular coning phenomenon. Here is the key summary of the results.

3.1 Design principles

The design is to imitate the annular geometry between the housing and base pipe upstream of ICD/AICD and account for the flow phenomena which could occur:

1. Annular coning of water caused by the pressure gradient;
2. Oil vs. water velocity difference (slip), occurs when multiphase flow goes through the orifice;
3. Surface tension determined patterns since the annulus is rather narrow.

The facility should have the following functionalities:

- Observe the oil-water interface level for different flowrates;
- Study the coning potential for different annulus width;
- Measure the WC (Water Cut – water vs. total produced fluids percentage) flowing through the base pipe's orifice and the coning influence;
- The components can be easily modified (orifice cross-sectional area, annulus width etc.).

To meet all the described criteria the followings solutions were implemented.

Unbent pipe wall configuration (or so called 2D-configuration) was suggested, its principle is illustrated in Figure 3.1. Only half of the pipe's axial cross-section containing the opening/valve is of interest. Unbending the pipe surface does not eliminate any of the possible flow patterns, but the facility becomes much easier and cheaper to build. Of utmost importance, the configuration makes it much more straightforward to observe and record the results and to modify the setup to a great extent.

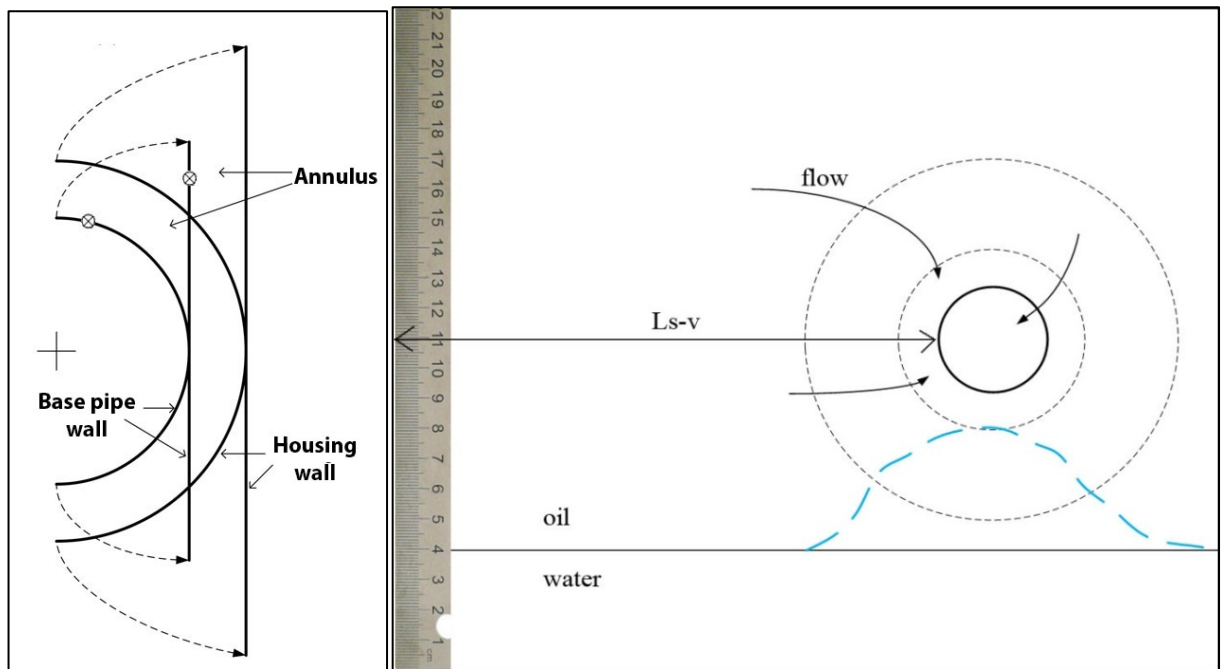


Figure 3.1 – Unbent half-pipe configuration (left) and unbent base pipe wall front view with the coning pattern (right).

The base pipe unbent wall is not fixed but a moveable part of the facility. By displacing the wall a new annulus of a different width is created. The moving wall can be also replaced with a new one with different parameters. In such a manner, depending on the experiment's setup, one is able to modify the facility effortlessly. With this concept different variations are applicable, such as housing distance to the valve intake L_{s-v} ; annulus width; orifice number, its area and vertical position etc.

The housing unbent wall, in its turn, is a fixed wall. It is reasonable to integrate it with the wall of the whole facility box – the fluid tank upstream the unbent annulus. This solution grants extra volume for the fluid and less leakage area. The wall must be made of a transparent material to enable critical visual observation of the process. In the result, the transparent fluid tank wall, standing for the ICD housing, together with the base pipe creates the annulus, as shown in Figure 3.2.

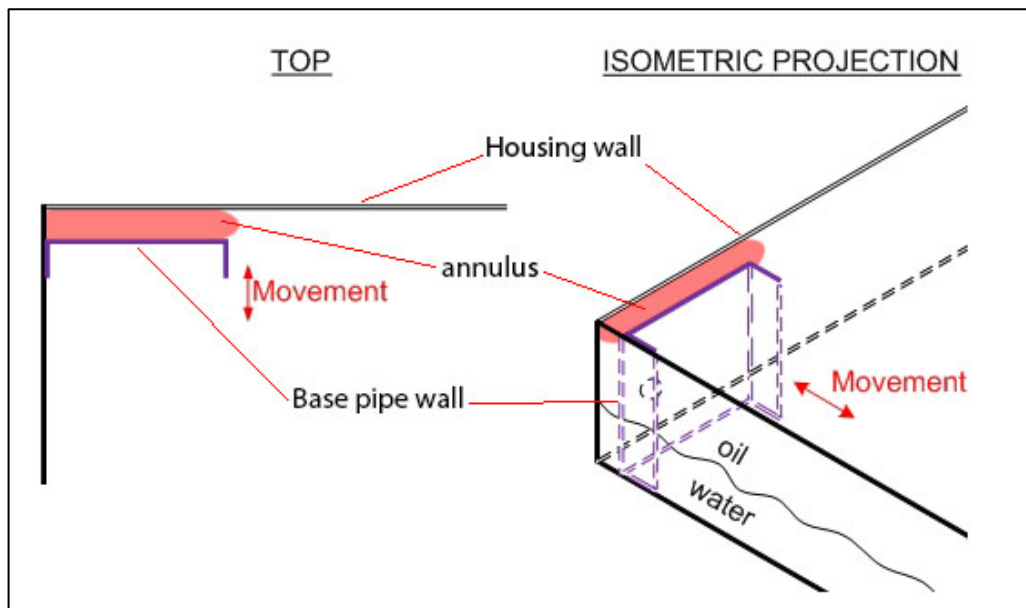


Figure 3.2 – Integration of unbent housing wall with the side of the fluid tank. Top view (left) and isometric view (right).

As shown above, the base pipe wall is to be installed right in the liquid pool. To let the fluid flow it must be directed through the orifice via a flexible tube through a perforation in the tank bottom, as shown in Figure 3.3. The drain goes to a measurement bucket, where fluid volumes can be seen. This will assure the flow, since the input/output pressure difference would appear. For the expected velocity (calculated from Statoil data to be ~ 0.2 m/s for the orifice – the narrowest area) a very small pressure drop is needed, that would be covered by a 1 m tank elevation. Using the tube also makes it possible to better control the desired rate with a valve downstream.

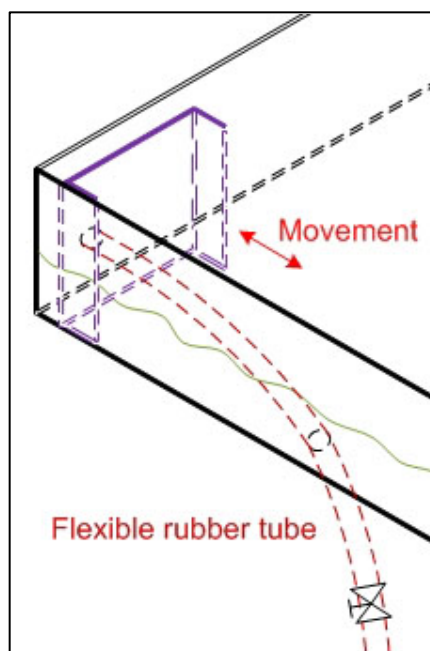


Figure 3.3 – Position of the flexible drain tube.

The fluid tank is required to simulate reservoir inflow, and the larger it is – the more stable pattern would appear. A variable-head liquid flow is a transient flow because flowrate, velocity and head change in time. On the other hand, constant head is very difficult to get with the source lines, keeping up with the discharge, from the design and operations point of view. The supply flowrate would also introduce disturbances, undesired waves etc.

That’s why it was decided to follow the large variable-head tank idea, but not to drop a liquid level more than 1 cm during a single experimental run. Looking ahead at the results it is seen that this concept was reasonable – in Figure 3.4 big head differences (from 170 to 220 mm) in Nexbase case show influence on the total flowrate, while Exxsol picture is more stable under the smaller head differences (from 195 to 208 mm).

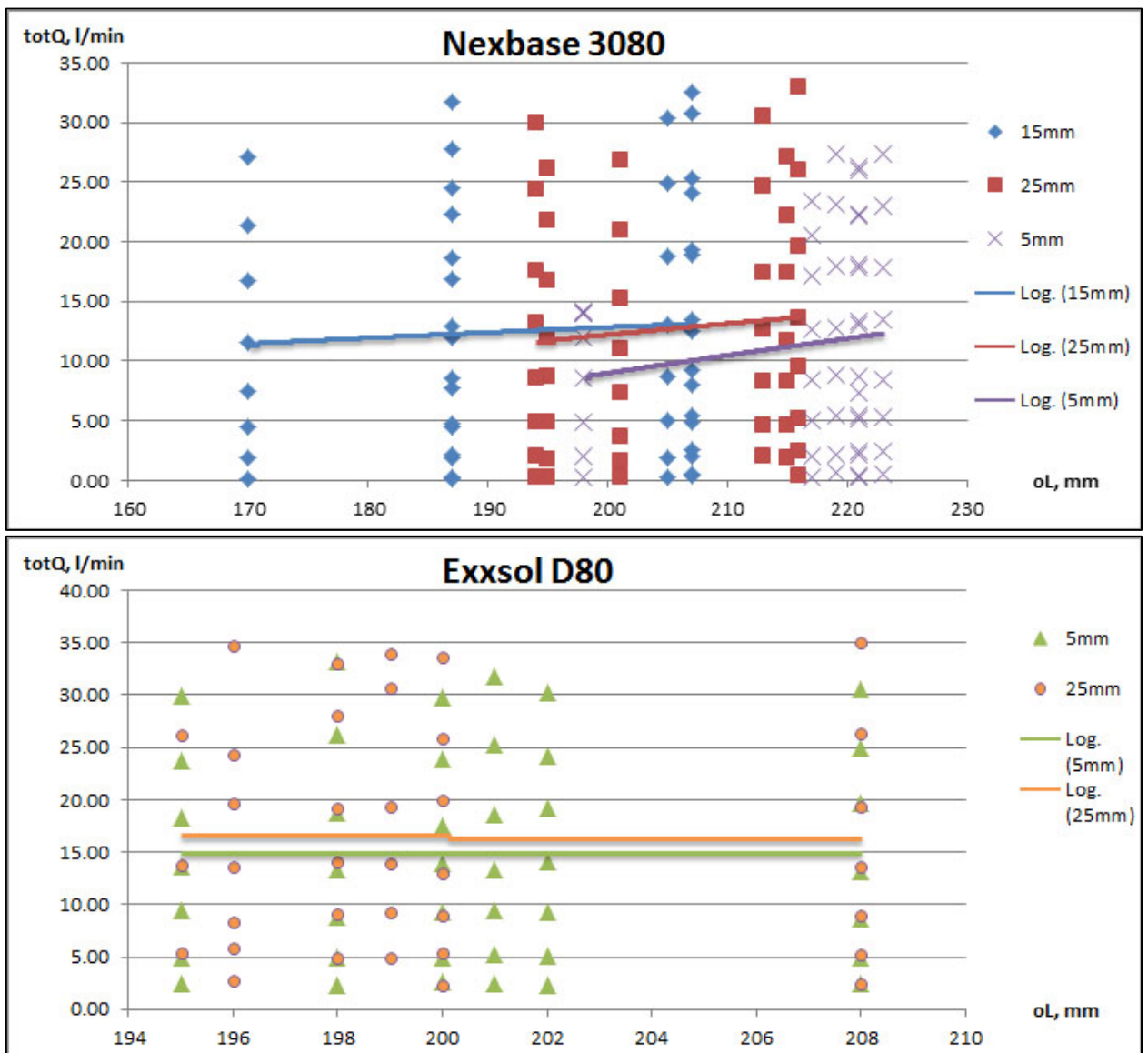


Figure 3.4 – Experimental results plot of total flowrate relative to the oil level with trendlines for Nexbase 3080 oil (top) and Exxsol D80 oil (bottom). 5-25 mm in the legend represent annulus width.

The setup is designed in that way to prevent harm or danger of harm to people, the environment or to financial assets shall in accordance with the legislation relating to health, the environment and safety, including internal requirements and acceptance criteria. Over and above this level the risk shall be further reduced to the extent possible. Assessments on the basis of this provision shall be made in all phases of the manufacturing and experimental activities.

Factors which may cause harm, or nuisance to people, the environment or to financial assets in the activities shall be replaced by factors which in an overall evaluation have less potential for harm, or nuisance.

Manufacturing and experimental activities shall be safe and prudent, both in relation to an individual and an overall consideration of all the factors of importance to planning and implementation of activities as regards health, environment and safety. A high level of health, environment and safety shall be established, maintained and further developed.

3.2 The finished rig

The height of the liquid level was calculated based on the half-pipe cross-section perimeter, what is ~220 mm for a 5.5" pipe. Safety margin of 30 mm above the liquid level was introduced, so the height of the base pipe wall became 250 mm. The width of the base pipe was chosen 250 mm as close to the given maximum screen distance to the valve intake (Statoil input). The orifice diameter was set to 36 mm as calculated from given cross-sectional area in Chapter 2.2, Design 2.

It's important that the height of the base pipe is the same as the fluid tank's height, this allows clamps to be used for sticking the wall to the tank side. Using clamps would fix the part in place and mitigate by-pass leakages. The liquid level would still be set at 220 mm.

It was decided to use standard size tin plates of 1x1 m to manufacture the tank. Each side of the tank should not be composed of multiple plates to avoid long welds (extra work, extra leakage risk, bumpy surfaces). The plates are welded to each other on flanges, which would leave each side 950 mm of real length. The final facility arrangement with dimensions and fluid flow path is presented in Appendix A.

On top the tin sides of the tank are bent into spoilers to reinforce the design, reinforcement ribs can be seen in Figure 3.5. The drawings for the tank manufacturing can be seen in Appendix B. The transparent side is made of lexan. It would have a linear scale marked on, that's how oil/water level would be sustained and any inclination from the horizontal layout would be detected.



Figure 3.5 – The manufactured tank.

The completed rig (see Figure 3.6) can be divided into the following nodes:

1. Fluid tank with the flowlines and valves. The tank is set on a hydraulic table to create a pressure drop needed for the flow. The base pipe wall is installed inside the tank and clamped to its side (seen in Figure 3.7). The flow goes through the orifice in the wall to the flexible flowline (seen in Figure 3.8), which perforates the tanks bottom.
2. Different capacity vessels (see Figure 3.9). The vessels are for measuring (bucket, bottles), auxiliary purposes (drum) and drainage (cubic in the basement).
3. An electric pump.

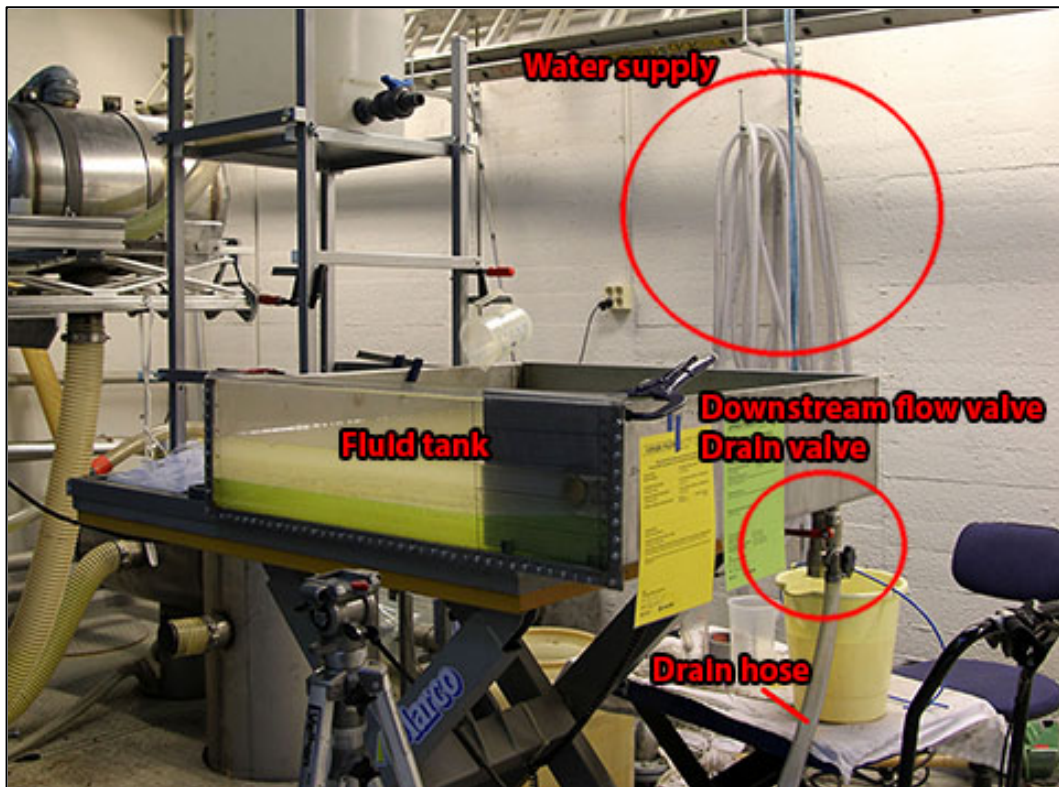


Figure 3.6 – Completed rig front view.

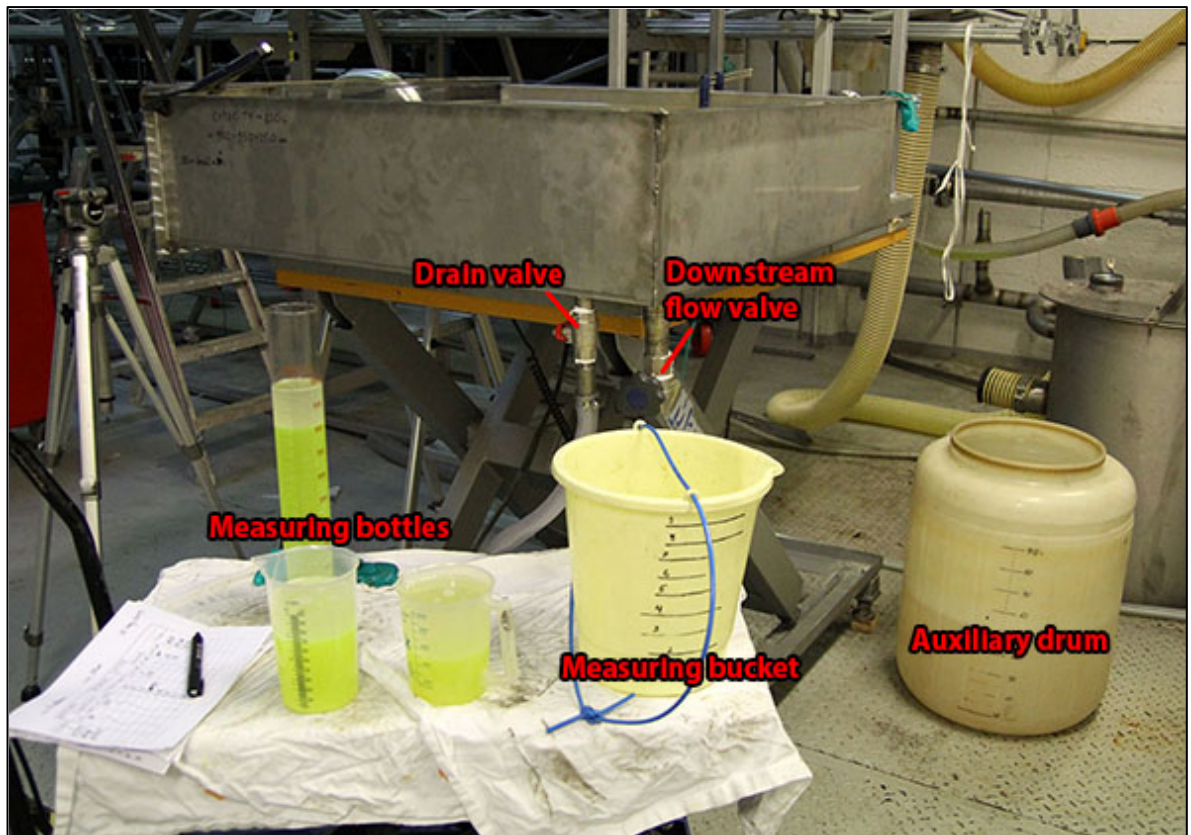


Figure 3.7 – Completed rig back view.

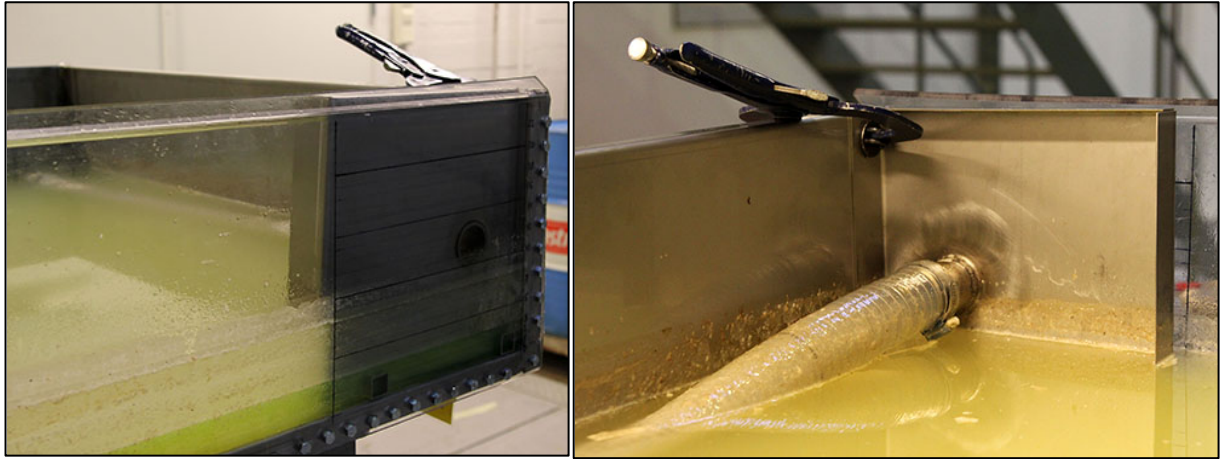


Figure 3.8 – Clamped base pipe wall front (left) and back (right).



Figure 3.9 – Flexible flowline seen in low liquid level.

List of the valves:

- 3 water source valves: 2 upstream of the hose in the house water system, close to the room wall of the lab; 1 at the end of the hose.
- 1 downstream flow valve: attached to the end of the flexible tube flowline, appears below the bottom of the fluid tank. The valve has marks from 0 (closed) to 6 (fully opened) to control the flowrate coming to the measuring bucket (see Figure 3.10).
- 1 drain valve: attached to the tank bottom, connects the fluid tank to the drain hose going down to the drainage cubic in the basement.
- 1 electric pump valve: downstream of electrical pump to control the flowrate.

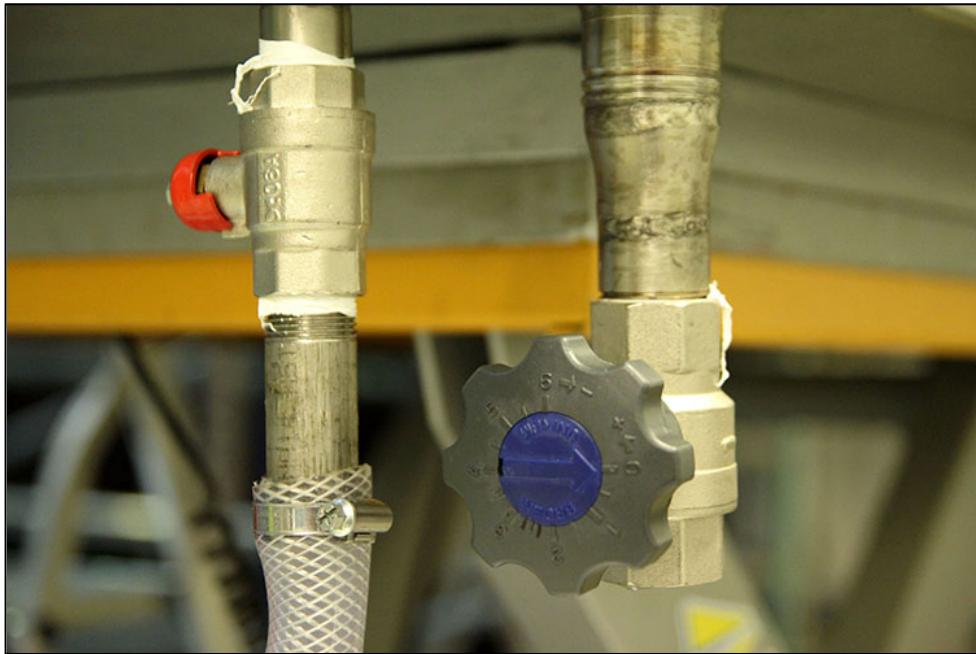


Figure 3.10 – Drain valve (left) and downstream flow valve (right) attached to the tank bottom.

4 Preparation stage

During the preparations a leak test was performed prior to start-up by filling the main tank with water. All welded joints and lexan attachment held the water.

Also a series of water flow runs was conducted to get a rough flowrate vs. valve position pattern. This allowed to estimate what valve positions are of a particular interest by comparing achieved flowrates with the Statoil data of ~6.2 l/min. The positions are 2 – 2.5 as shown in Figure 4.1.

| Rough water flowrates | | | |
|-----------------------|-----------|---------|-----------------|
| Valve open | Amount, l | Time, s | Flowrate, l/min |
| 1 | 5 | 493 | 0.6 |
| 1.5 | 10 | 234 | 2.56 |
| 2 | 10 | 101 | 5.94 |
| 2.5 | 15 | 63 | 9.52 |
| 3 | 15 | 60 | 15 |
| 3.5 | 15 | 38 | 23.68 |
| 4 | 15 | 34 | 26.47 |
| 4.5 | 15 | 26 | 34.61 |
| 5 | 17 | 23 | 44.35 |
| 5.5 | 15 | 20 | 45 |
| 6 | 15 | 17 | 52.94 |

Figure 4.1 – Pre-startup water runs data.

4.1 Risk Assessment

Since the rig is brand new, the new rig Risk Assessment must have been conducted prior to operations. It was done based on NTNU and SINTEF safety standards according to the “Guidance to risk assessment – The approval of test rigs in laboratories at NTNU Department of Energy and Process Engineering and SINTEF Energy – Energy Processes”.

The Risk Assessment report (attached to the Master Thesis) includes description of the setup, operations and emergency shutdown procedure, assessment of technical and operational safety, quantifying of risk. The key summary is the following.

Those oils are to be used – NEXBASE 3080, Marcol 52, EXXSOL D80 FLUID – around 100 liters of each. Oils are stored in drums, handling is done by an electric pump. Disposal is not provided (NTNU, 2012), the oils would go to the separator.

MSDS (Material Safety Data Sheet – attached to the Master Thesis) study shows no/minimal toxicological hazard over exposure. Oils are stable in ambient conditions. Some are combustible materials of low hazard that can burn only on heating above the flash point.

Probable events and risks:

- Skin/eye contact with the chemical causing irritation;
- Liquid spill/overflow introducing slipping hazard.

Both events fall into green A2 zone of the Risk Matrix (see Figure 4.2), which means a small probability of very little consequences. The green zone designates an acceptable risk.

| | | | | | | |
|---------------------|-----------------------|--------------------|--------------|----------------|-------------|-------------------|
| CONSEQUENCES | Svært alvorlig | E1 | E2 | E3 | E4 | E5 |
| | Alvorlig | D1 | D2 | D3 | D4 | D5 |
| | Moderat | C1 | C2 | C3 | C4 | C5 |
| | Liten | B1 | B2 | B3 | B4 | B5 |
| | Svært liten | A1 | A2 | A3 | A4 | A5 |
| | | Svært liten | Liten | Middels | Stor | Svært Stor |
| | | PROBABILITY | | | | |

Figure 4.2 – Colour risk matrix quantifying the residue hazards.

Conclusions and risk mitigations:

- One person must always be present while running experiments, and should be approved as an experimental leader;
- Work carefully to prevent spills and leakages. If a leak appears, it should be cleaned fast, the rags are disposed normally;
- Normal protective safety glasses and gloves are recommended;
- Avoid heat, sparks, open flames and other ignition sources. This is covered by NTNU's No Smoking policy and work restrictions in the particular laboratory room where the rig is installed.

The shutdown procedure was considered:

Emergency shutdown

Shut off all the valves.

If emergency concerns the tank integrity, then open the drain valve and the tank to the cubic tank in the basement.

After the Risk Assessment report with attachments was approved, the UNIT CARD and EXPERIMENT IN PROGRESS CARD were issued allowing the experiments to start (see Figure 4.3).

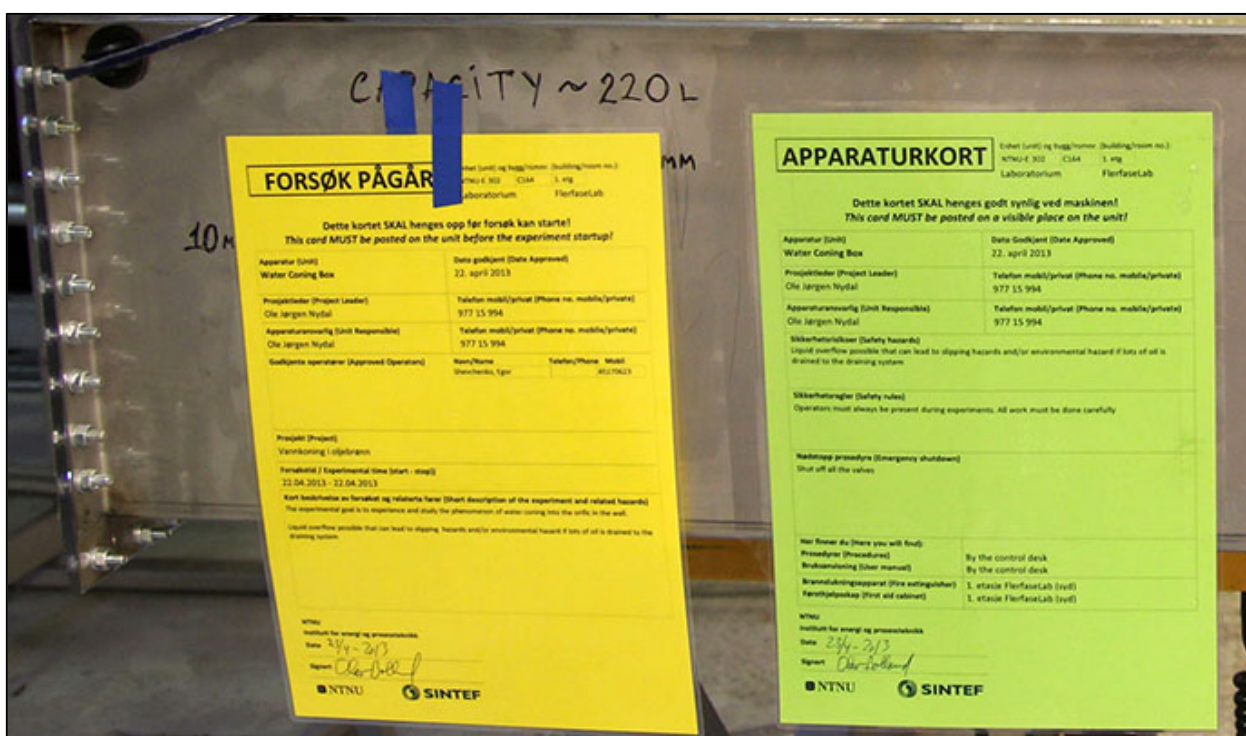


Figure 4.3 – UNIT CARD and EXPERIMENT IN PROGRESS CARD set.

4.2 Inclined table incident

During the preparations an incident occurred resulting in a minor spill. The hydraulic table inclined under the weight of the filled tank and liquid overflow followed (see figure 4.4).



Figure 4.4 – Inclined table incident.

The reason is that the weight balance was not centered. The tank has valves and piping attached to its bottom, and that made the proper placement impossible.

The long term under-stress condition for hydraulic lifts is not recommended, so a safety leg was used. Yet its purpose is to prevent vertical movement, not angular (see figure 4.5). However the leg stopped the further inclination.



Figure 4.5 – The safety leg.

A set of safety measures was introduced such as counterweight and extra safety stoppers. The wood was placed to prevent any movement of the table, thus the weight rested on the wood at all times. In addition the top white drum on the other side of the table was filled with 50 liters of counterweight water (see Figure 4.6).

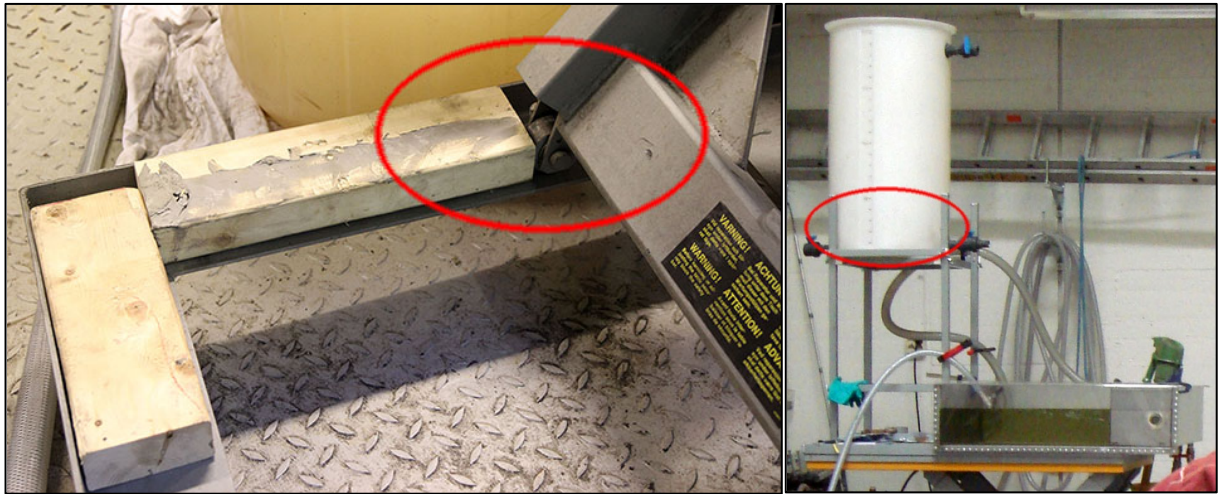


Figure 4.6 – Wooden stoppers (left) and water counterweight (right).

5 Running the experiments

5.1 Operations principles

To thoroughly study the annular coning phenomenon a list of variables, most probably affecting the flow, was prepared. It was cross-referenced to the rig design to establish the methods of controlling those variables. The range of change was determined during the course of the experiments itself. All the discussed is presented in Figure 5.1 below.

| Variables | Control method | Range |
|--|--|--------------------------------------|
| Phase interface distance from the orifice | Controlling water level by pumping fluids in/out | 10 – 110 mm |
| Oil viscosity, density, surface tension | Pumping a new oil in | Nexbase 3080 – Exxsol D80 |
| Annulus width (or gap) | Moving the base pipe wall | 5 – 25 mm |
| Total flowrate | Rotating downstream flow valve | Valve 0 – 6 Flowrate 0 – 45 l/min |
| Orifice cross-sectional area | Applying duct tape to cover the cross-section | ~170 – 1000 mm ² |

Figure 5.1 – Variable experimental parameters.

The changes of the variables were prioritized for the most convenient progress of the experiments in this way:

1. Downstream flow valve rotation (0.5 – 5);
2. Increasing water level (10 – 110 mm);
3. Changing the gap (annulus width) by moving the base pipe wall (5 – 25 mm);
4. Pumping in new oil (Nexbase – Exxsol).

The orifice cross-sectional area was changed for Nexbase (15 mm gap, 10 mm water level) and Exxsol (10 mm gap, 30 mm water level). In such a manner Appendix C shows all the experiments had been done, resulting in 459 runs (including a couple of extra runs).

The key analysis was during visual observation and measuring the amount of each phase. During the runs the following was measured:

- increase of water level (coning, water “jump”), mm;
- decrease of oil level (coning, oil “jump”), mm;
- total amount of flowing liquid, ml;
- amount of water in total fluid, ml;
- orifice cross-section covered by water, %;
- flowing time, s.

5.2 Procedure

The following procedure was used for the runs.

Before the experiment

Post the “Experiment in progress” sign.

Use supply valves and/or electrical pump to fill the tank with oil/water to the desired level.

Before adding water to the tank it was colored fluorescent green to better distinguish it from oil by Fluorescein-Natrium (C.I. 45350) indicator shown in Figure 5.2.



Figure 5.2 – Fluorescein-Natrium can (left) and colored water (right).

During the experiment

Open the downstream valve, obtain the desired flowrate.

Record the flow pattern through the orifice in the plate.

Watch for overflows in any vessel.

Close all the valves when the measuring bucket is full.

Check the time elapsed for filling up the measuring bucket.

Check the amount of different liquids in the bucket.

Empty the measuring bucket back to the tank.

The amount of liquids was measure in measurement bottles where the interphase can be easily seen after a short settling period. The Nexbase 3080 interphase is shown in Figure 5.3.

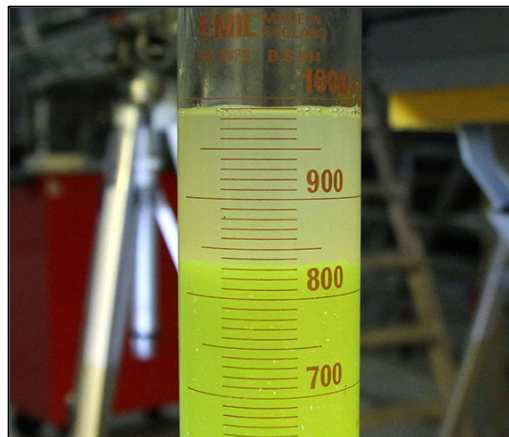


Figure 5.3 – Interphase between water (bottom) and Nexbase 3080 (top).

End of experiment

Remove all obstructions/barriers/signs around the experiment.

Tidy up the work area and return all tools and equipment.

The demobilized rig after all runs is shown in Figure 5.4.



Figure 5.4 – Rig is demobilized.

The procedures for technical modifications are as follows.

Changing experimental conditions (new gap)

Drain the water to the drainage cubic (the water can be contaminated, therefore can't go to sewage).

Drain as much oil as possible to the auxiliary drum by downstream flow valve and manual transfer.

Change the gap between the transparent wall and the base pipe wall.

Use electrical pump to suck oil from the auxiliary drum back to the tank.

Use water supply to fill its level to the desired height.

The gap is piece of metal from 5 mm width to 25 mm. It was decided not to check even bigger gaps since the coning phenomenon practically disappeared at the 25 mm gap. The gap position is shown in Figure 5.5 below.

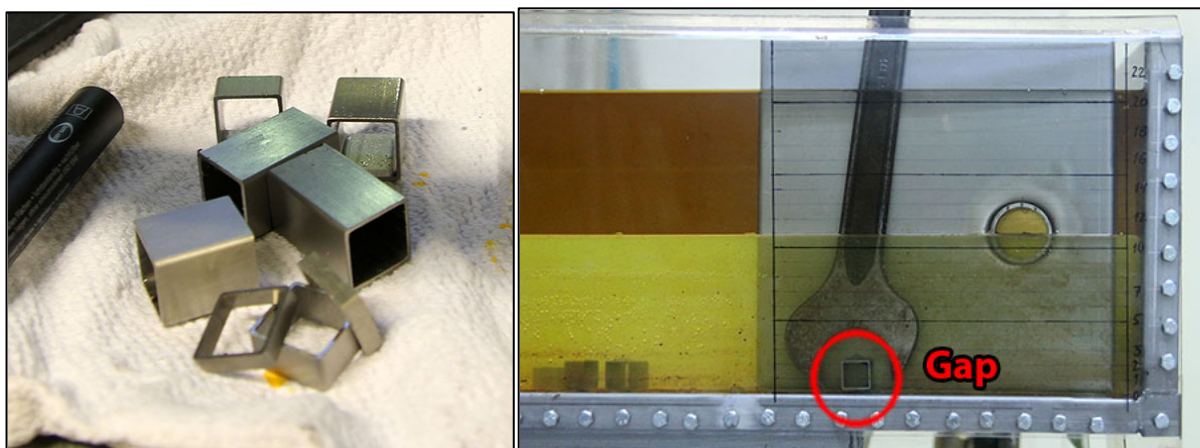


Figure 5.5 – Gap sizes (left) and gap position in the liquid pool (right).

Changing experimental conditions (orifice cross-sectional area)

Drain the water to the drainage cubic (the water can be contaminated, therefore can't go to sewage).

Drain as much oil as possible to the auxiliary drum by downstream flow valve and manual transfer.

Pick the base pipe and set it on the tank corner (see Figure 5.6).

Cover the desired orifice with a duct tape. Install the base pipe back in the pool.

Use electrical pump to suck oil from the auxiliary drum back to the tank.

Use water supply to fill its level to the desired height.

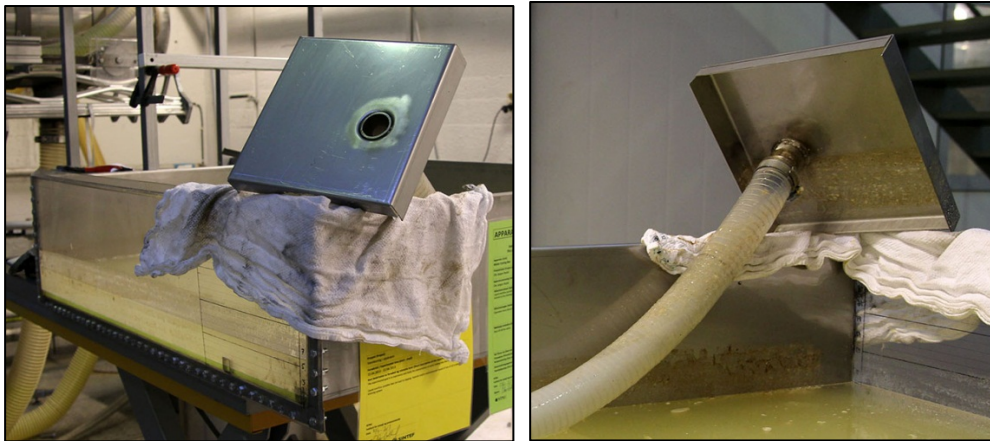


Figure 5.6 – Base pipe wall set on the tank corner, front view (left) and back (right).

The orifice perimeter has markings of 8, 18 and 28 mm out of 36 mm diameter to be covered by the duct tape (see Figure 5.7). That corresponds to 16.5, 50, and 83.5 % of 1017 mm², what is 168, 509 and 849 mm².

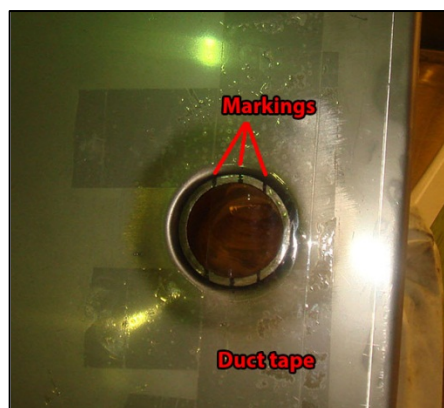


Figure 5.7 – Orifice covered by 83.5 %.

Changing experimental conditions (new oil)

Drain the water to the drainage cubic (the water can be contaminated, therefore can't go to sewage).

Drain as much oil as possible to the oil source drum by downstream flow valve and manual transfer.

Drain the oil leftovers to the drainage cubic.

Clean up all the contaminated surfaces.

Use electrical pump to suck oil from an oil source drum to the tank (see Figure 5.8).

Use water supply to fill its level to the desired height.

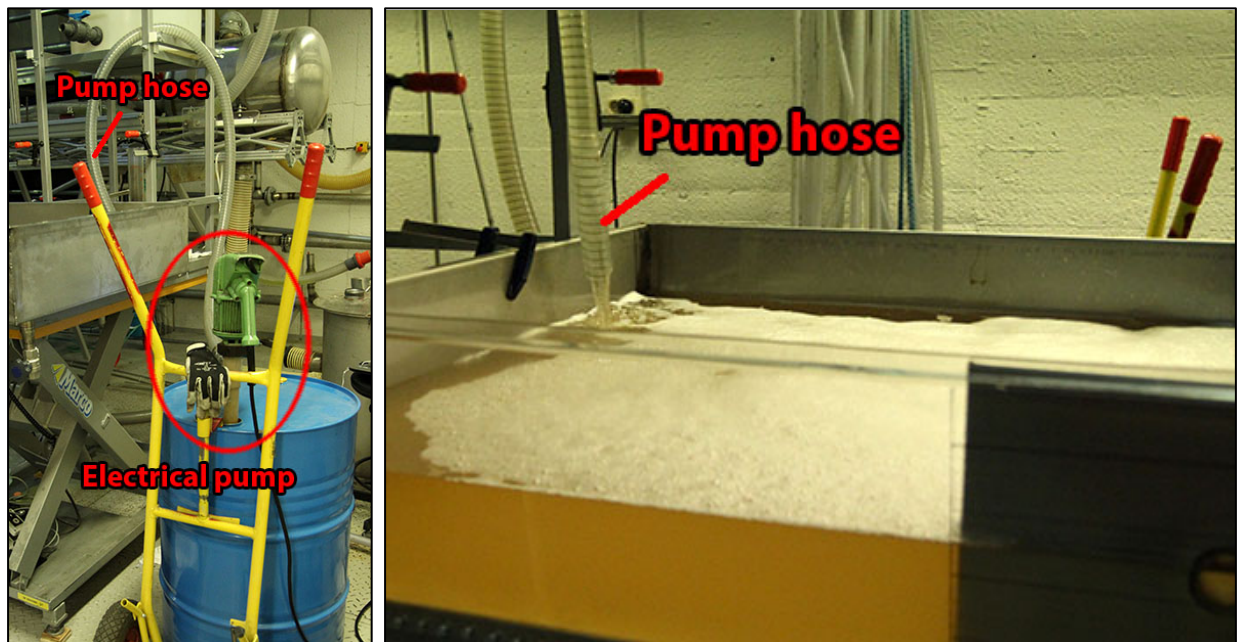


Figure 5.8 – Pumping new Exxsol D80 oil to the tank.

Nexbase 3080 characteristics are the closest to Statoil provided oil density 935 kg/m³ and viscosity 67 cP (~ 72 mm²/s). Due to the workload it was decided not to use Marcol oil because its characteristics sit in between Nexbase and Exxsol (see Figure 5.9), thus Marcol experiments would not provide critical data on the oil influence.

| | Nexbase 3080 | Marcol 52 | Exxsol D80 |
|--|---------------------|------------------|-------------------|
| Density at 15°C, g/ml | 845 | 84 | 798 |
| Viscosity at 100°C, mm ² /s | 7.9 | | |
| Viscosity at 40°C, mm ² /s | 48 | 6.9 | 1.68 |
| Viscosity at 25°C, mm ² /s | | | 2.16 |

Figure 5.9 – Oils characteristics comparison.

6 Results and discussion

The total number of 459 experimental runs was conducted, and every single flow pattern was recorded on video. All the results, including experimental parameters, graphs, trending analyses, were put down in 1 excel spreadsheet (attached to the Master Thesis). The screenshot from the table is available in Figure 6.4. Acronyms identification is presented in Appendix D.

The experimental rig came up reliable and handy. As designed, it was adequate for the planned runs, since water coning was accomplished and flow patterns, to some extent, behaved as expected. Some typical coning photographs are presented in Figure 6.1.



Figure 6.1 – Water coning screenshots in different experimental runs.

In order to conduct a proper data analysis all the experimental parameters were written down and put either to “pre-set” or “observable” section (shown in Figure 6.2). Each parameter in the “observable” section was cross-referenced with each variable in both sections, and each combination pair was checked if it’s either pointless or interesting, if it meets the objectives of the project, and in what form it is better to present the trend.

Pre-set variables

Observable variables

| | |
|--|---|
| <ul style="list-style-type: none"> • Annulus width or gap (δ); • Oil; • Orifice area; • Liquid level ($w_L, o_L, \Delta L$); • Valve rotation (considered to influence only the flowrate $totQ$); • Orifice cross-section in water (w_A). | <ul style="list-style-type: none"> • Flowrate ($totQ$) + velocity ($totU$); • Water cut (WC); • Liquid “jumps” (w_J, o_J); • Liquid levels at flow ($w_L', o_L', \Delta L'$); • Orifice cross-section in water at flow (w_A'); • Flow regime in the tube. |
|--|---|

Figure 6.2 – Variables sorting for easier analysis.

By “jumps” here it is intended the change in liquid level. For example, water “jump” (w_J) is a difference between water levels during the flow and with no flow. In other words a “jump” refers to the annular coning phenomenon itself, therefore its study is of a particular attention. Eventually, those correlations were selected and analyzed:

| Parameter | As a function of |
|---------------------------|---|
| Flowrate, velocity | Valve; Oil; Gap; Orifice area; WC. |
| Liquid “jumps” | Flowrate; Gap; Oil; Orifice area; Liquid level. |
| Water cut | Flowrate; Liquid level. |

Figure 6.3 – Correlations that were selected and analyzed.

| Plate | | Gap | | | | |
|-------|-------|-------|-------|-------|---------------|--|
| H, mm | B, mm | L, mm | h, mm | d, mm | δ , mm | |
| 250 | 250 | 184 | 110 | 36 | 5 | |

| Oil | | Nexbase 3080 | |
|-------------------------------|-----|--------------|--|
| viscosity, mm ² /s | 7.9 | at 100C | |
| | 48 | at 40C | |
| | | at 25C | |
| density, kg/m ³ | 845 | at 15C | |

| BEFORE | | DURING | | | | | AFTER | | | | | Flowrate, l/min | | | Velocity, mm/s | | | | | | |
|---------|------------------|--------|----|--------------|-------|--------------------------|-------|-----|-----|-----|------------|-----------------|------|-------|----------------|--------|-------|-------|---------|------|-------|
| Video # | Liquid level, mm | | | Crosssection | Valve | Liquid level (max Δ), mm | | | | | Amount, ml | | | WC, % | Time, s | wQ | oQ | totQ | Vortex? | totU | |
| | wL | oL | ΔL | wA, % | | wL' | oL' | ΔL' | wJ | oJ | wA', % | wV | oV | totV | | | | | | | |
| 2414 | 10 | 198 | 82 | 0.0 | 1 | 14 | 197 | 78 | 4 | -1 | 0 | 0 | 150 | 150 | 0.0 | 47.48 | 0.00 | 0.19 | 0.19 | | 3.1 |
| 2415 | 10 | 198 | 82 | 0.0 | 1.5 | 90 | 185 | 2 | 80 | -13 | 0 | 0 | 1000 | 1000 | 0.0 | 29.45 | 0.00 | 2.04 | 2.04 | | 33.4 |
| 2416 | 10 | 198 | 82 | 0.0 | 2 | 110 | 179 | -18 | 100 | -19 | 38 | 1940 | 4360 | 6300 | 30.8 | 77.40 | 1.50 | 3.38 | 4.88 | | 80.0 |
| 2417 | 10 | 198 | 82 | 0.0 | 2.5 | 123 | 164 | -31 | 113 | -34 | 40 | 1940 | 3260 | 5200 | 37.3 | 36.72 | 3.17 | 5.33 | 8.50 | | 139.2 |
| 2419 | 10 | 198 | 82 | 0.0 | 3 | 132 | 146 | -40 | 122 | -52 | 30 | 2440 | 5860 | 8300 | 29.4 | 41.78 | 3.50 | 8.42 | 11.92 | vort | 195.3 |
| 2420 | 10 | 198 | 82 | 0.0 | 3.5 | 127 | 127 | -35 | 117 | -71 | 35 | 2040 | 6260 | 8300 | 24.6 | 35.67 | 3.43 | 10.53 | 13.96 | vort | 228.7 |
| 2421 | 10 | 198 | 82 | 0.0 | 4 | 128 | 123 | -36 | 118 | -75 | 35 | 2280 | 6020 | 8300 | 27.5 | 35.72 | 3.83 | 10.11 | 13.94 | vort | 228.4 |
| 2422 | 10 | 198 | 82 | 0.0 | 4.5 | 130 | 127 | -38 | 120 | -71 | 35 | 2010 | 5290 | 7300 | 27.5 | 30.98 | 3.89 | 10.25 | 14.14 | vort | 231.6 |
| 2423 | 30 | 217 | 62 | 0.0 | 1 | 40 | 215 | 52 | 10 | -2 | 0 | 0 | 200 | 200 | 0.0 | 51.39 | 0.00 | 0.23 | 0.23 | | 3.8 |
| 2424 | 30 | 217 | 62 | 0.0 | 1.5 | 99 | 206 | -7 | 69 | -11 | 10 | 70 | 930 | 1000 | 7.0 | 28.95 | 0.15 | 1.93 | 2.07 | | 34.0 |
| 2425 | 30 | 217 | 62 | 0.0 | 2 | 114 | 200 | -22 | 84 | -17 | 40 | 2000 | 3200 | 5200 | 38.5 | 62.30 | 1.93 | 3.08 | 5.01 | | 82.0 |
| 2427 | 30 | 217 | 62 | 0.0 | 2.5 | 117 | 190 | -25 | 87 | -27 | 45 | 2310 | 2890 | 5200 | 44.4 | 36.84 | 3.76 | 4.71 | 8.47 | | 138.7 |
| 2428 | 30 | 217 | 62 | 0.0 | 3 | 123 | 183 | -31 | 93 | -34 | 45 | 2780 | 3520 | 6300 | 44.1 | 29.95 | 5.57 | 7.05 | 12.62 | vort | 206.8 |
| 2429 | 30 | 217 | 62 | 0.0 | 3.5 | 132 | 167 | -40 | 102 | -50 | 45 | 3390 | 3910 | 7300 | 46.4 | 25.58 | 7.95 | 9.17 | 17.12 | vort | 280.5 |
| 2431 | 30 | 217 | 62 | 0.0 | 4 | 140 | 150 | -48 | 110 | -67 | 45 | 3410 | 3890 | 7300 | 46.7 | 21.26 | 9.62 | 10.98 | 20.60 | vort | 337.5 |
| 2432 | 30 | 217 | 62 | 0.0 | 4.5 | 137 | 130 | -45 | 107 | -87 | 70 | 4000 | 4300 | 8300 | 48.2 | 21.22 | 11.31 | 12.16 | 23.47 | vort | 384.5 |
| 0683 | 50 | 221 | 42 | 0.0 | 1 | 59 | 220 | 33 | 9 | -1 | 0 | 0 | 200 | 200 | 0.0 | 47.32 | 0.00 | 0.25 | 0.25 | | 4.2 |
| 0684 | 50 | 221 | 42 | 0.0 | 1.5 | 102 | 214 | -10 | 52 | -7 | 17 | 1320 | 3880 | 5200 | 25.4 | 147.48 | 0.54 | 1.58 | 2.12 | | 34.7 |
| 0685 | 50 | 221 | 42 | 0.0 | 2 | 117 | 210 | -25 | 67 | -11 | 40 | 2690 | 2510 | 5200 | 51.7 | 60.33 | 2.68 | 2.50 | 5.17 | | 84.7 |

Figure 6.4 – Screenshot from the experimental spreadsheet with all data recorded.

6.1 Flowrate correlations

General dependence of flowrate from the downstream flow valve rotation is shown in Figure 6.5. In general, small flow restrictions from the gap can be seen, since the bigger is the gap – the less are frictional losses. The pattern is especially clear in Exxsol oil graph, where trendlines grow up clearly with the increasing gap.

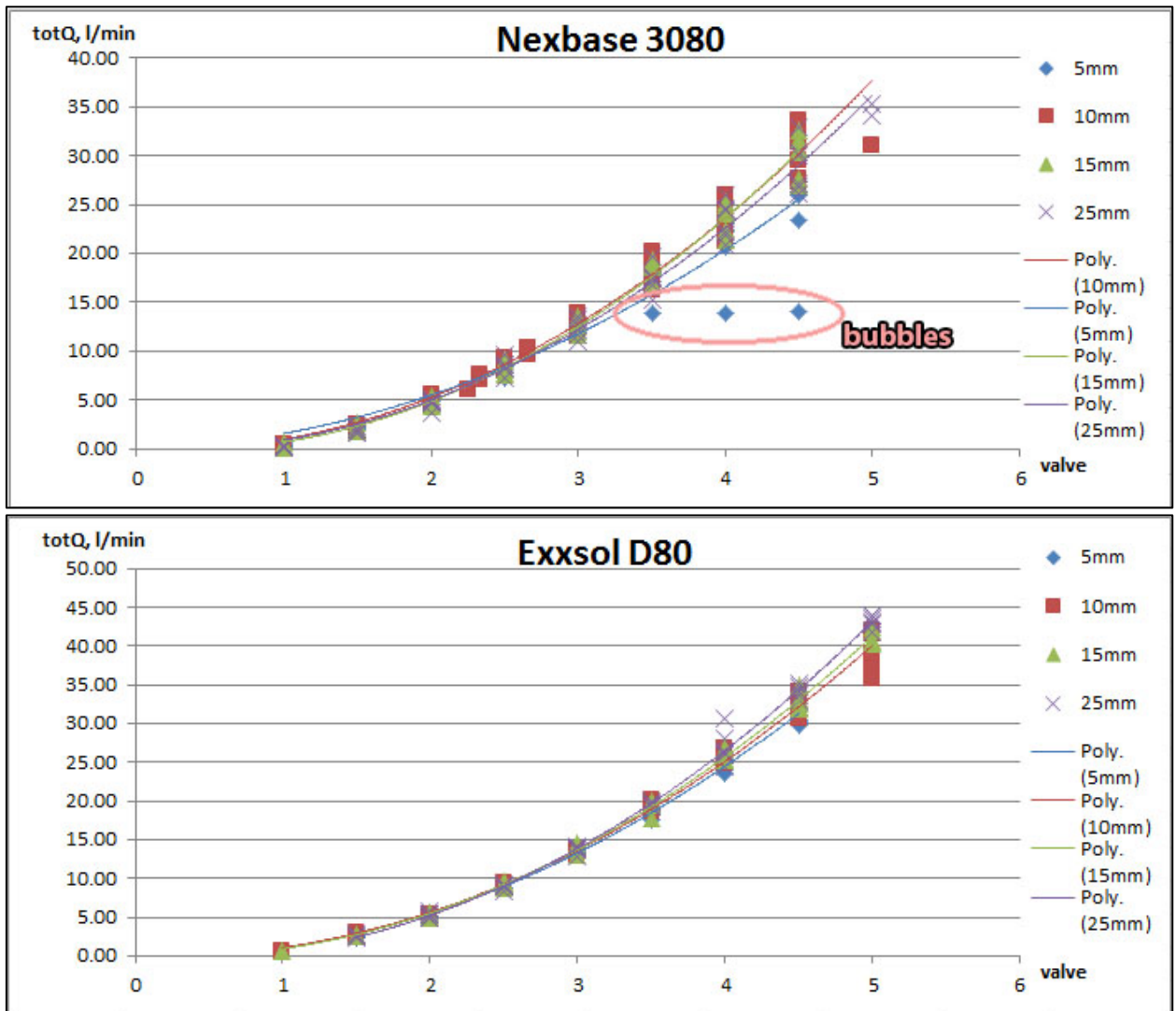


Figure 6.5 – Total flowrate vs. Valve correlations, Nexbase (top) and Exxsol (bottom).

One series in the case “Nexbase oil, 5mm gap” fell out of the trend because air bubbles were coming into the tube (shown in Figure 6.6).



Figure 6.6 – Air coming into the tube. Nexbase 5 mm gap flow development.

When comparing flowrates for different oils one can see a similar flow pattern, but it is clear that a less viscous oil (Exxsol D80) flows easier and achieves higher rates than Nexbase 3080. In Figure 6.7 the comparison is done for 10 mm gap for the sake of demonstration, but more detailed picture with a single graph for each gap is presented in Appendix E.

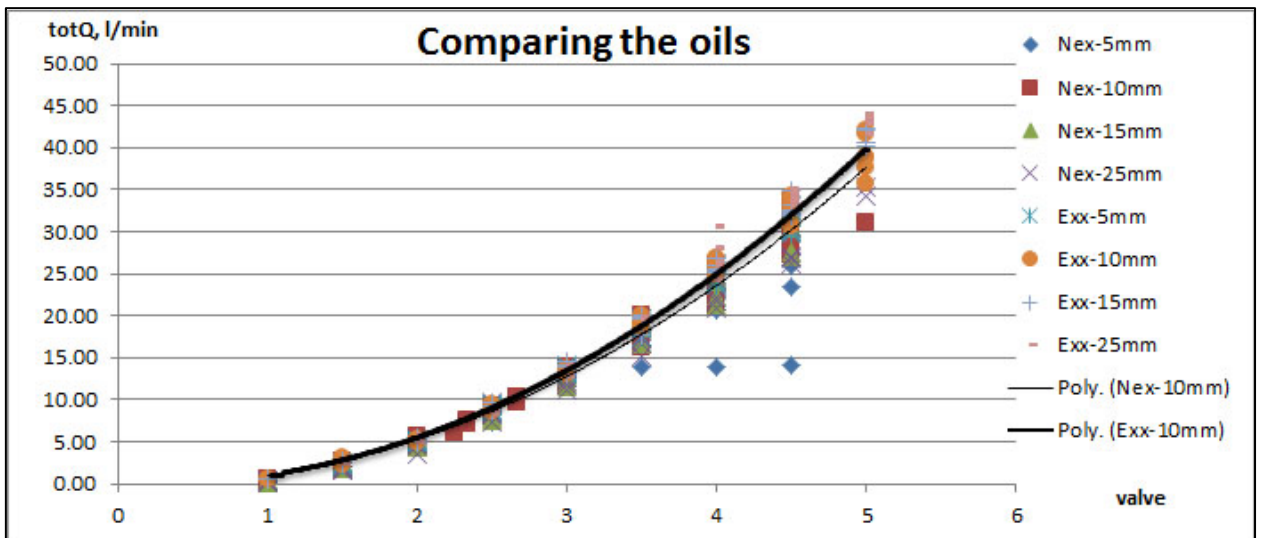


Figure 6.7 – Flowrates comparison for different oils.

It is explained by the following. Torricelli's law, which was discovered in 1643, relates the speed of fluid flowing out of an opening to the height of fluid above the opening (Wikipedia, 2013). $v = \sqrt{2gh}$, where g – gravity acceleration, h – height of the liquid level. In other words, the flow speed is the same for all liquids and actually equals the free fall speed. This is not really true, because the speed depends also on the shape and size of an opening, and on fluid viscosity.

To account for that a correction coefficient φ is introduced: $v = \varphi\sqrt{2gh}$, which is a called speed coefficient for fluid flowing out of an opening. The value of φ (among ε – compression coefficient, and μ – flowrate coefficient) for a round opening can be found by empirical correlations. The Figure 6.8, “Altshul's graph”, shows the correlations between the coefficients and Reynolds number, calculated for ideal speed, $Re = \frac{d\sqrt{2gh}}{\nu}$, where ν – kinematic viscosity.

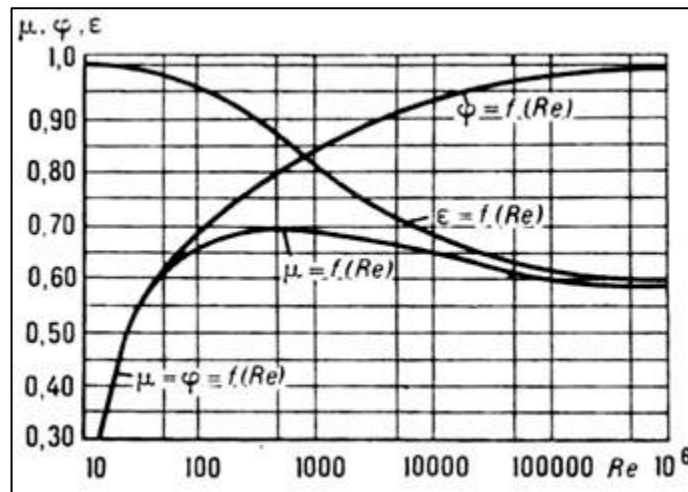


Figure 6.8 – Correlation between ε , μ , φ and Re . Also called “Altshul's graph” (Femto, 2013).

Torricelli's speed is roughly calculated as: $v = \sqrt{2gH} = \sqrt{2 \cdot 9,8 \cdot 0,2} \cong 2$ (m/s). Calculating with the correction coefficients is below, note that 30 mm (downstream flow valve outlet diameter) is used as d .

- Nexbase 3080: $Re = \frac{d\sqrt{2gh}}{\nu} = \frac{0,030 \cdot \sqrt{2 \cdot 9,8 \cdot 0,2}}{48 \cdot 10^{-6}} \cong 1200$, it gives $\varphi \cong 0.85$ and speed $v = 0.85 \cdot \sqrt{2 \cdot 9,8 \cdot 0,2} \cong 1.7$ (m/s).
- Exxsol D80: $Re = \frac{d\sqrt{2gh}}{\nu} = \frac{0,030 \cdot \sqrt{2 \cdot 9,8 \cdot 0,2}}{2,16 \cdot 10^{-6}} \cong 27500$, it gives $\varphi \cong 0.95$ and speed $v = 0.95 \cdot \sqrt{2 \cdot 9,8 \cdot 0,2} \cong 1.9$ (m/s).

According to calculated φ values, it appears that Nexbase speed must be approximately equal to 90% of Exxsol speed. That's exactly what's seen in Figure 6.9 – fully open valve corresponds to ~1 m/s for Exxsol speed and ~0.9 m/s for Nexbase. The speeds are not precisely as calculated above though, because the flow is not just through the

opening in a wall, there are additional losses in the tubing, in the bend, in the gap (discussed above), oil/water multiphase flow.

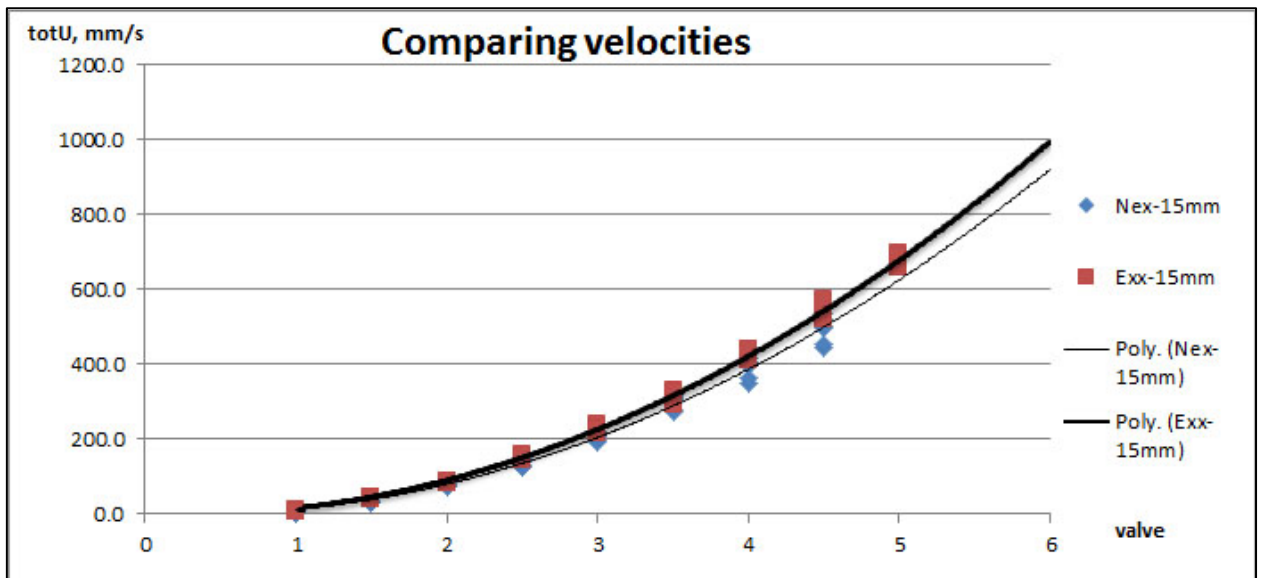


Figure 6.9 – Flow speed comparison for different oils.

The same situation happens when water breaks through to the production orifice. The less viscous water obtains higher speed resulting in total flowrate increase (shown in Figure 6.10). But the rate increase has nothing to do with oil production.

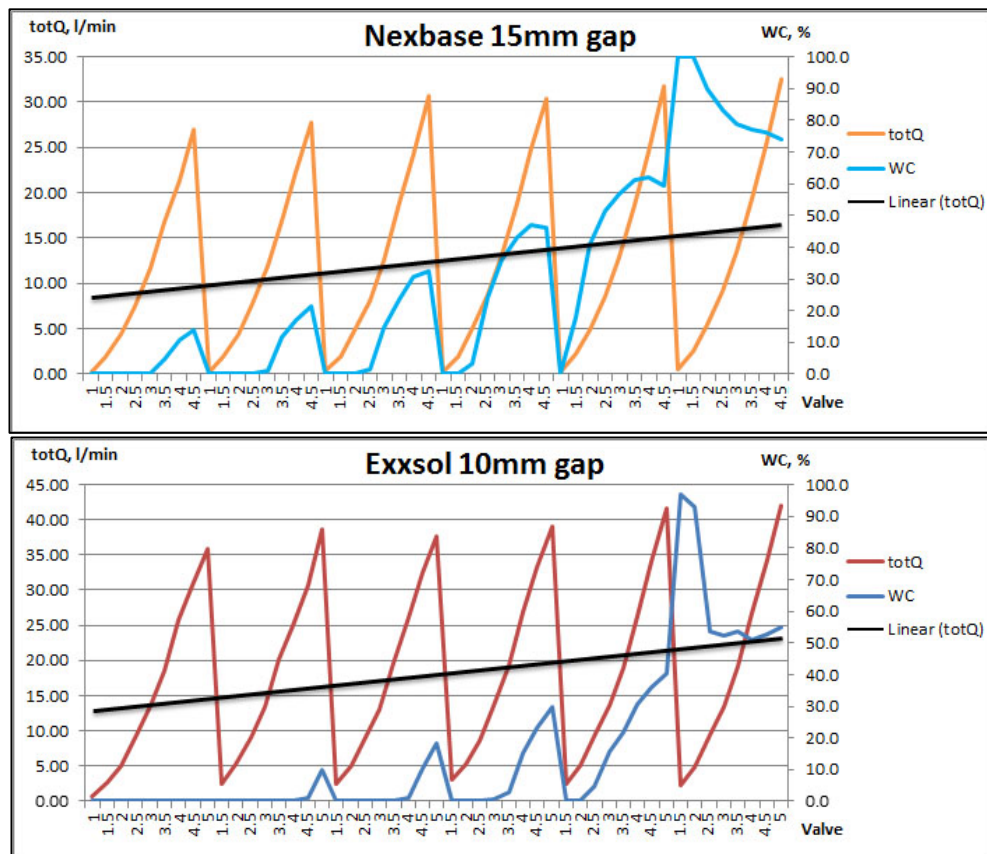


Figure 6.10 – WC influencing the total flowrate, Nexbase (top) and Exxsol (bottom).

Once the water has found its way to the production tubing, its further influence on the flowrate doesn't depend much on the oil beside it (as shown by trends in Figure 6.11). At least, this is the result obtained for the available oil viscosity range of 2.16 – 48 mm²/s.

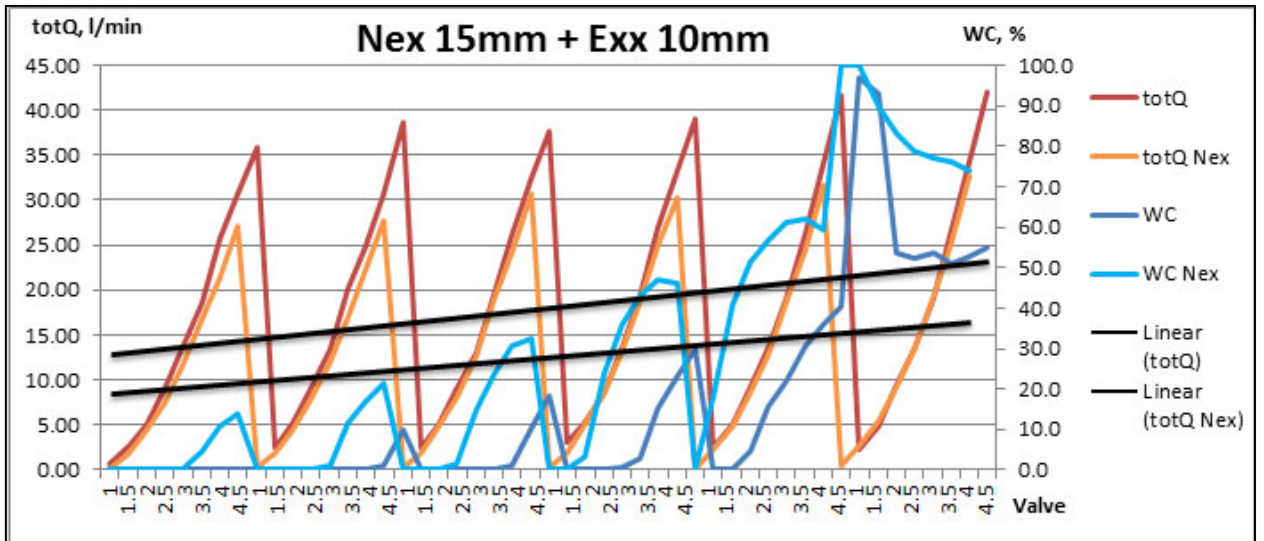


Figure 6.11 – Graphs from Figure 6.10 superimposed.

Additional losses were imposed by partially closing the orifice. As shown in Figure 6.12, leaving it open at 83.5% didn't affect the rate, but further closing reacted in a remarkable drop.

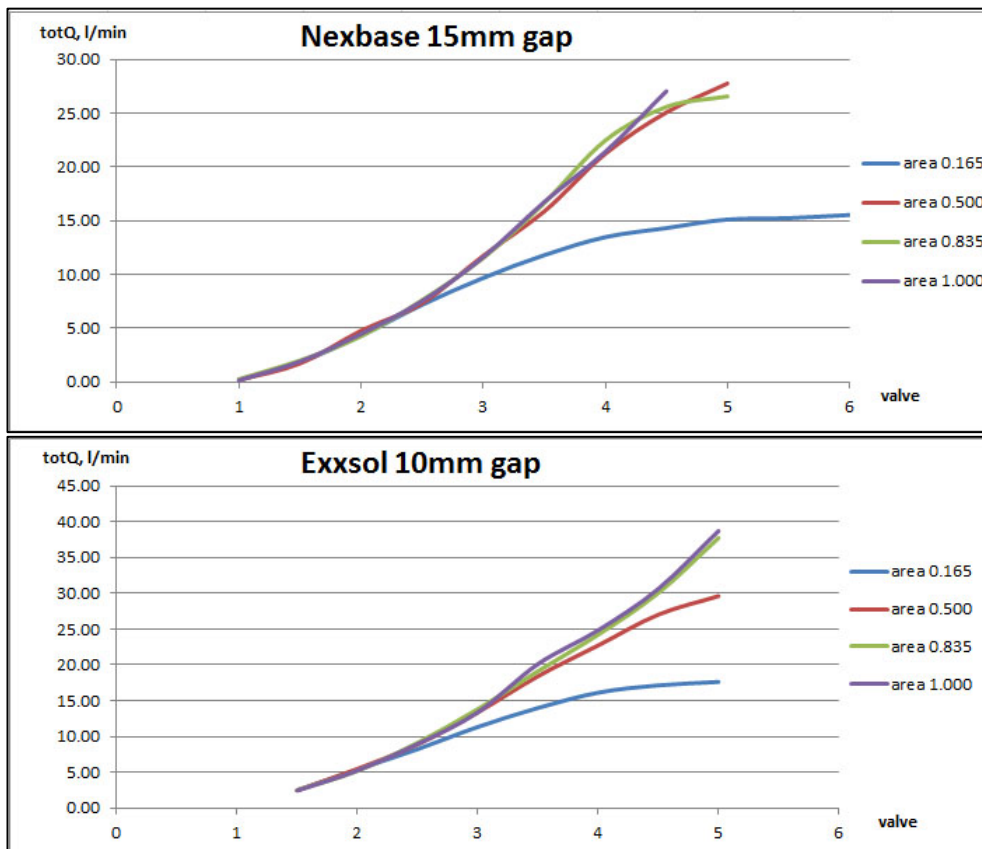


Figure 6.12 – Flowrates correlations with orifice cross-sectional area.

At the same time flow speed in the orifice was steadily rising due to the area shrinkage (see Figure 6.13). Flowrate drop through 16.5% of the area (168 mm² of 1017 mm²) didn't stop the speed to reach almost 1.8 m/s.

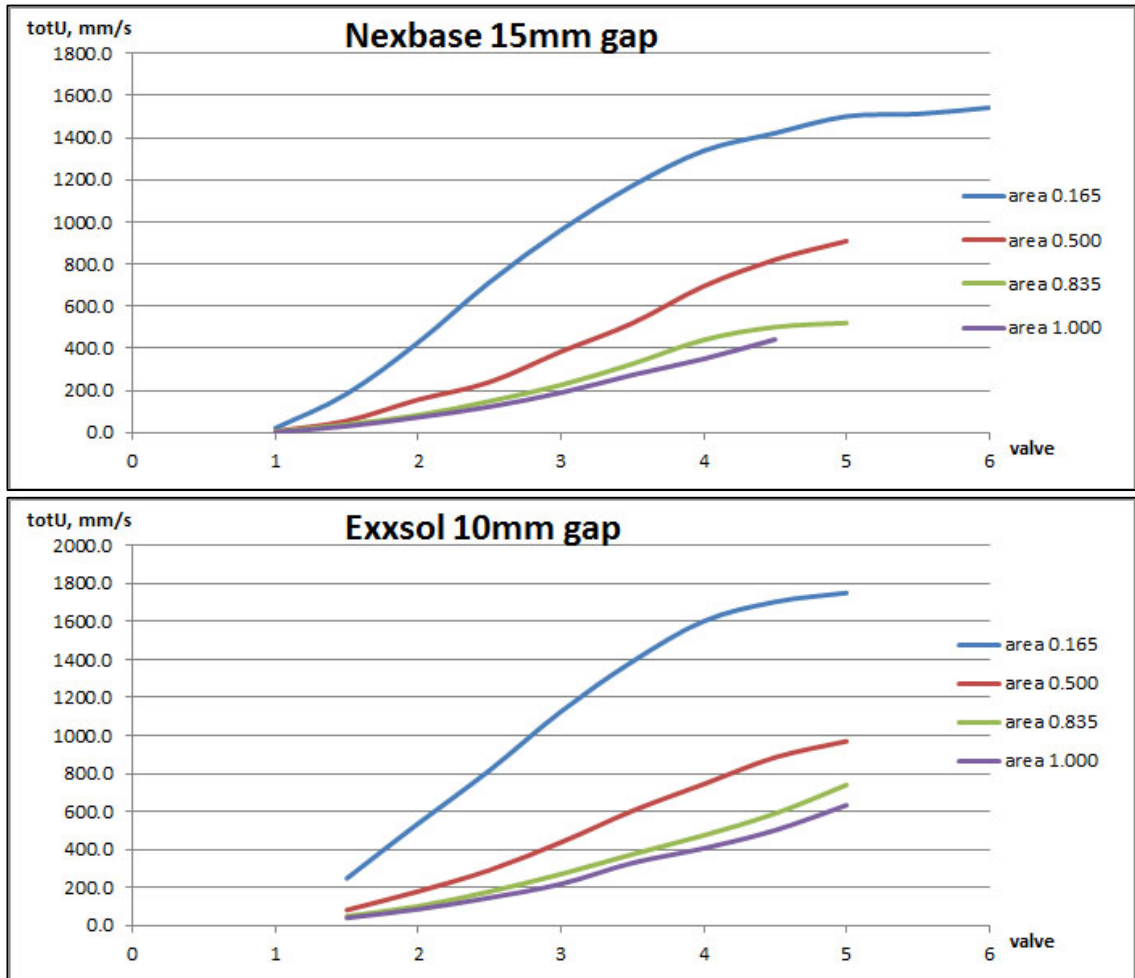


Figure 6.13 – Flow velocity correlations with orifice cross-sectional area.

6.2 Liquid “jumps”, WC

The key correlations related to coning mechanism are described in this chapter. For better comprehension of following trends the rule of thumb is – “jumps” of positive value are for water (straightforward coning) and negative “jumps” are for oil, since oil level sinks downward to the orifice.

The direct dependence of coning over flowrate is shown in Figure 6.14. The flat region means that water reached the orifice, therefore there are steps between different colour lines – the higher the water level, the less place is left for the jump to occur. Oil is less susceptible to coning, its level rarely got to the orifice, for this reason it rarely has flat regions in the plot and it shows a good linear dependence on the flowrate.

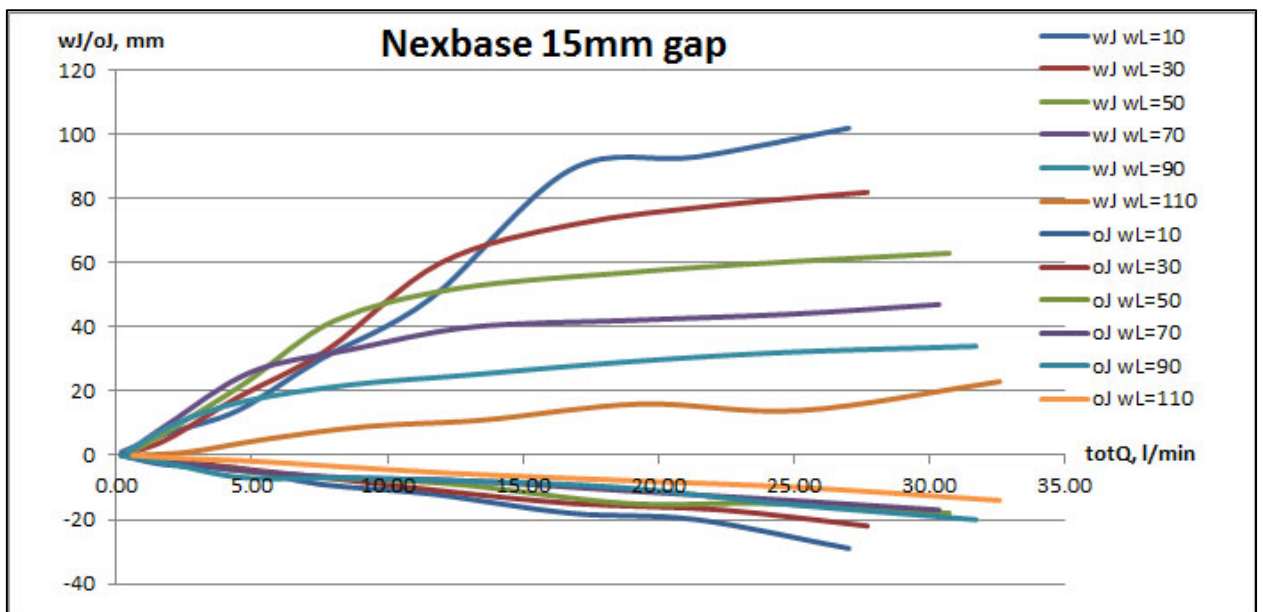


Figure 6.14 – “Jump” vs. flowrate for Nexbase 15 mm gap.

The water coning flow resembles the flow in an injector pump. Injector pump (or ejector pump, Figure 6.15) is a type of pump that uses the Venturi effect of a converging-diverging nozzle to convert the pressure energy of a motive fluid to velocity energy which creates a low pressure zone that draws in and entrains a suction fluid. After passing through the throat of the injector, the mixed fluid expands and the velocity is reduced which results in recompressing the mixed fluids by converting velocity energy back into pressure energy.

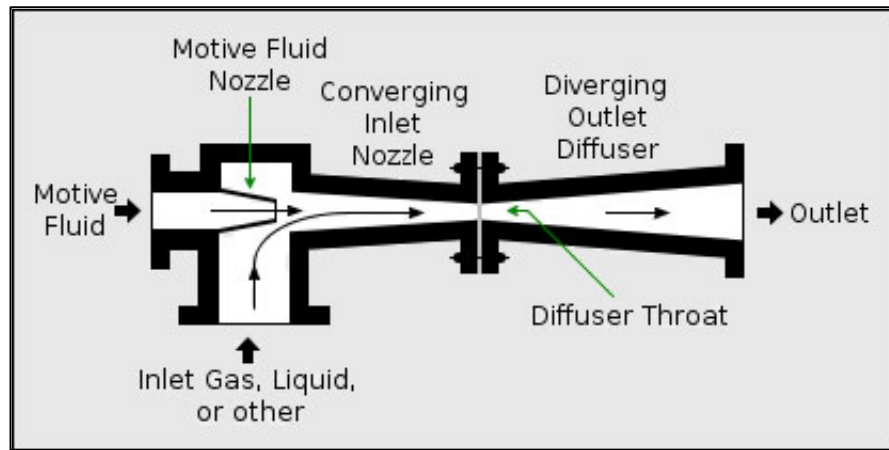


Figure 6.15 – Diagram of a typical modern ejector (Wikipedia, 2013).

Fluid under high pressure is converted into a high-velocity jet at the throat of the convergent-divergent nozzle which creates a low pressure at that point. The low pressure draws the suction fluid into the convergent-divergent nozzle where it mixes with the motive fluid. In essence, the pressure energy of the inlet motive fluid is converted to kinetic energy in the form of velocity head at the throat of the convergent-divergent nozzle.

The same is happening during coning. When fluid starts to flow through the orifice, it creates a low pressure zone according to Bernoulli's principle – increase in the speed of the fluid occurs simultaneously with a decrease in pressure. At the same time, since the interphase level is not flowing, its potential energy is constant. Therefore a pressure drop from the interphase to the orifice appears which causes the coning phenomenon. When a stagnant water cone is formed from the oil-water level toward a valve in the oil zone the total pressure drop is equal to the hydrostatic pressure of the height of the cone (Statoil, 2012).

A common approach to fluid energy is in terms of total head $H = z + \frac{P}{\rho g} + \frac{v^2}{2g}$, but in this application the change in the ρ, g, z term along the streamline is so small compared with the other terms that it can be ignored. This allows the above equation to be presented in the following simplified form:

$$p + q = p_o, \text{ where } p_o \text{ is total pressure, } q \text{ is dynamic pressure and it equals } \frac{1}{2}\rho v^2.$$

So, it feels like the faster the fluid is flowing through the orifice – the higher the water would cone or “jump. However, the experiments don't confirm the suggestion. The Figure 6.16 shows “jump” values for the different cross-sectional area series. It has nothing in common with the speed pattern from Figure 6.13.

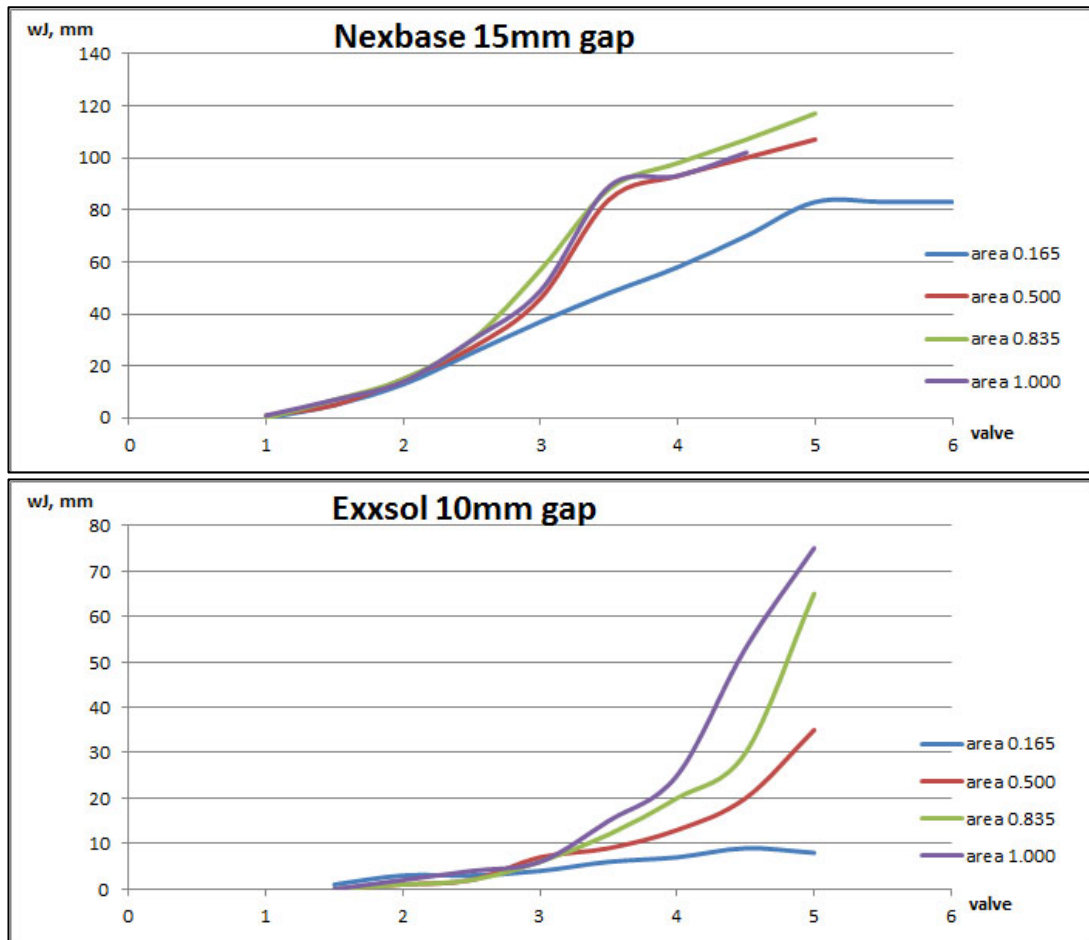


Figure 6.16 – “Jump” pattern in a different cross-sectional area series.

Moreover, changing horizontal axis values from Valve to flowrate in Nexbase case (shown in Figure 6.17) discloses a very direct and strong dependence of coning over flowrate regardless of speed or orifice area.

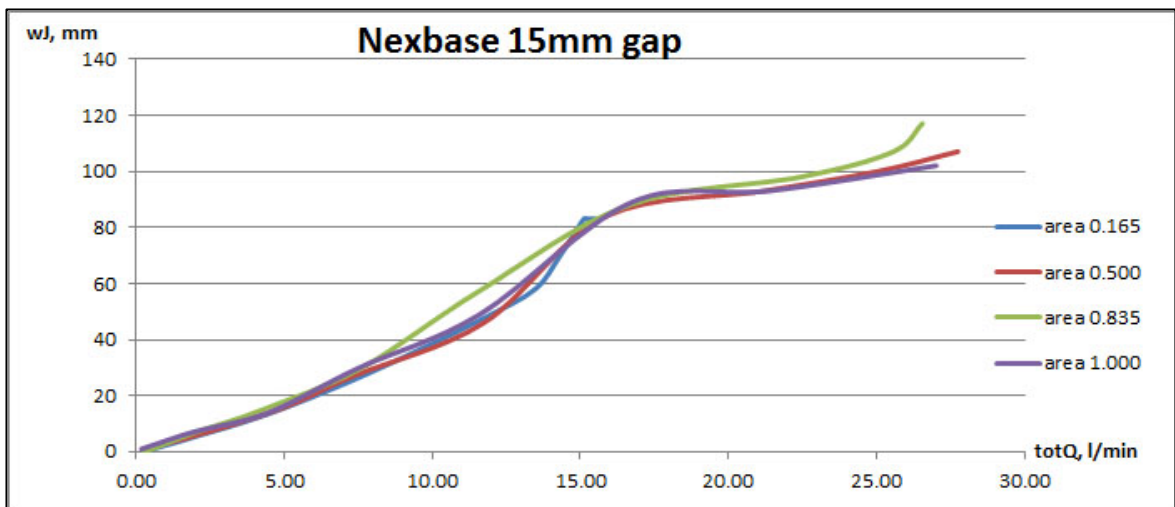


Figure 6.17 – “Jump” values vs. flowrate in different cross-sectional areas.

In order to check if coning is affected by initial water level one has to study regions before the flat ones and to ignore cases with $wL = 90$ mm and 110 mm, since 90 mm is already very close to the orifice perimeter. Studying the colour lines doesn't show a strong perceivable correlation for Nexbase series, however it seems like "jump" slightly grows with a higher initial water level. In other words, the closer the interphase is to the orifice, the easier it is for the water to break through.

More similar plots for different gaps on Nexbase series and Exxsol are shown in Appendix F. Exxsol plots seem a bit more chaotic, but it shows stronger influence of the initial water level on the further coning. The "jump"-gap and "jump"-oil correlation can also be seen from the Appendix, but this is discussed below.

Water coning has a significant dependence on gap width. Figure 6.18 shows "jumps" vs. gap correlations for Nexbase 3080. The inclined trend of the peaks reflects just different initial water levels, from 10 mm to 110 mm. In this figure different colour lines should be compared.

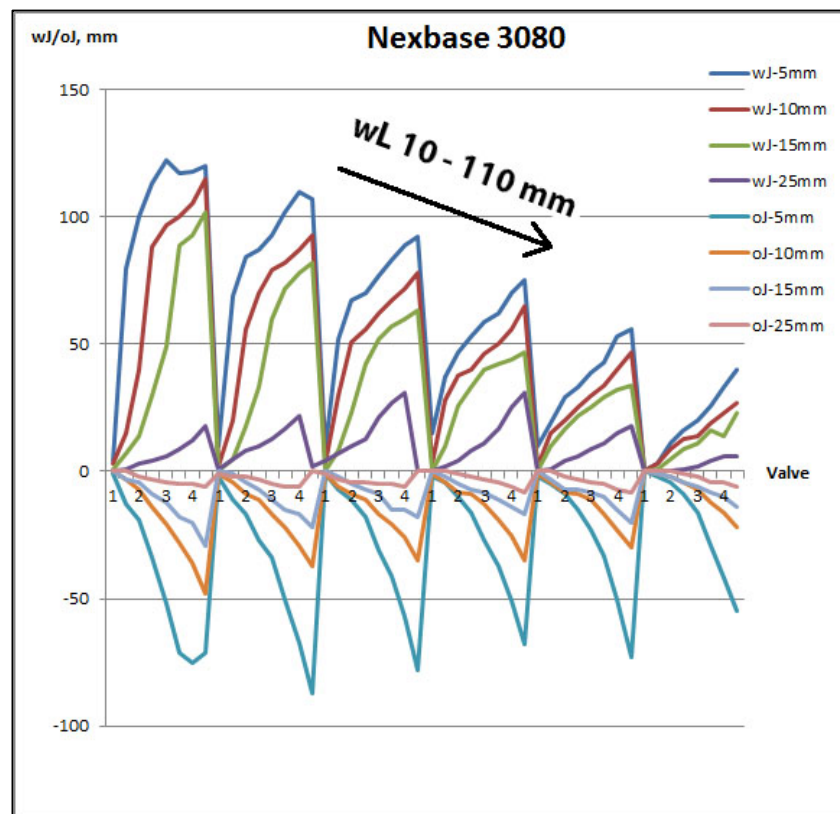


Figure 6.18 – Colour lines show "jump" values for different gap scenarios for Nexbase 3080.

More detailed pattern is presented in Figure 6.19 with "jumps" are plotted against flowrate for all conducted experiments. The "jump"-gap dependence is clearly seen for both oils, for both phases, for all flowrates. In everyday words, during the runs for Nexbase, it could be described by this impression: at 5 mm gap a single touch of the downstream flow valve caused change of water level or even casted it to the orifice, but at 25 mm gap the valve needed to be fully opened to visualize a little change in the interphase line.

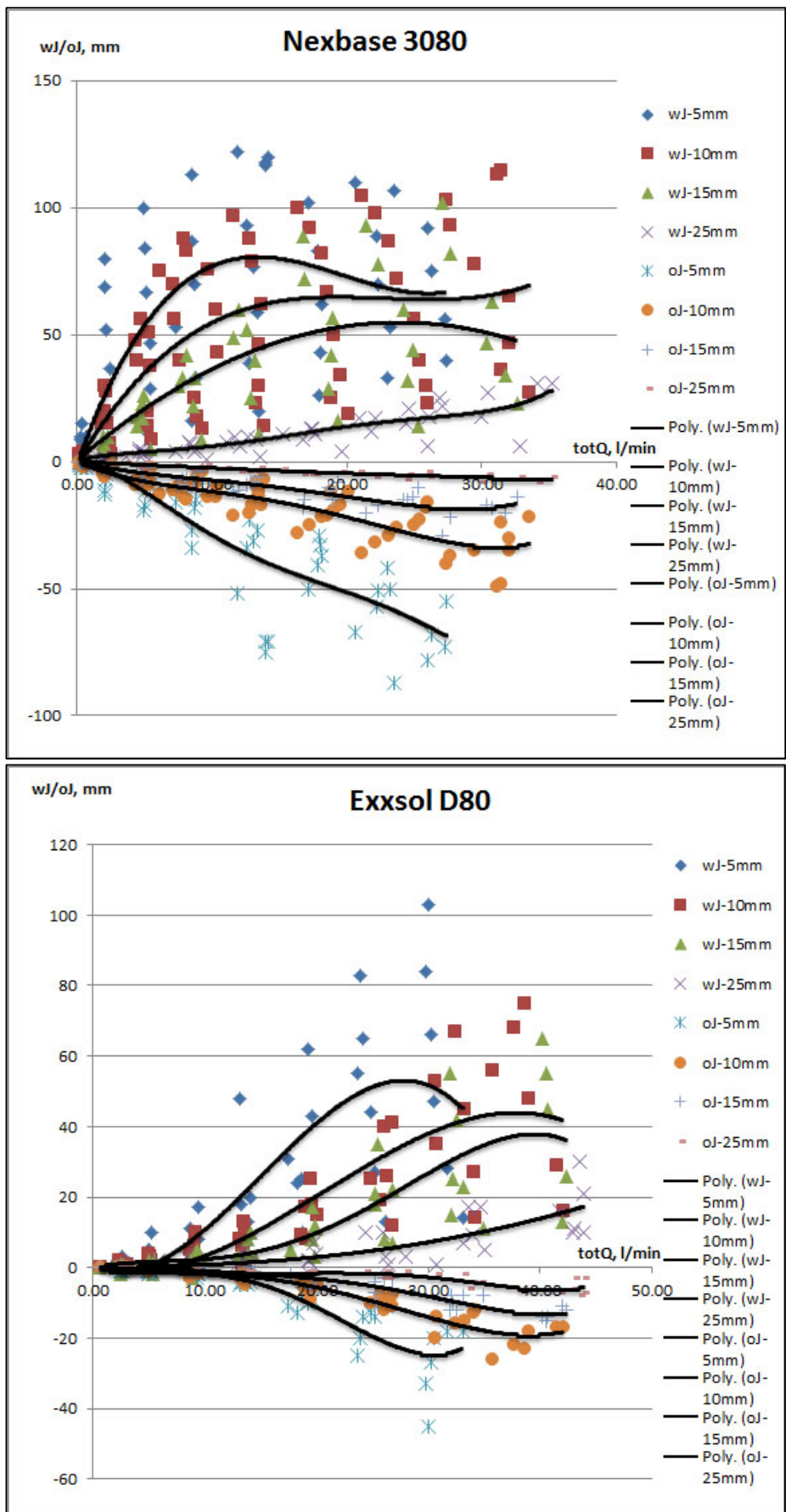


Figure 6.19 – “Jump” values of all runs with trendlines plotted for each single-gap series. Nexbase oil plotted on top, Exxsol – bottom.

This correlation can be explained by a hydraulic press principle (Figure 6.20). Pascal's law, described by a pressure formula $p = F/A$, states that pressure on a confined fluid is transmitted undiminished and acts with equal force on equal areas and at 90 degrees to the container wall. As a consequence: $F_1/A_1 = F_2/A_2$ (eq. 2). It's important, that work being done by F_1 must be equal to the work done against F_2 . If S is a cylinder displacement, then the work equality can be written as $F_1S_1 = F_2S_2$ (eq. 3).

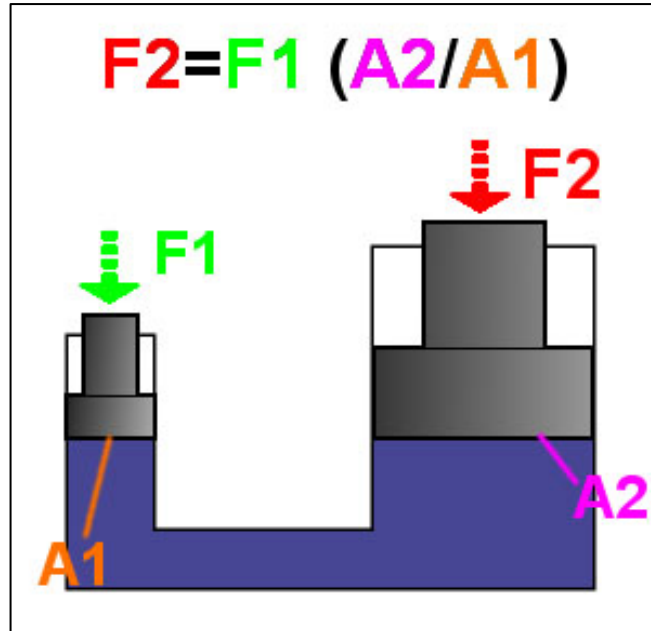


Figure 6.20 – Hydraulic force principle (Wikipedia, 2013).

Let's say, that the second cylinder in a hydraulic press represents the pressure drop to the orifice in the base pipe wall, for example $p = F_2/A_2$, which doesn't change, then F_1S_1 and F_1/A_1 doesn't change as well. It becomes obvious that area increasing leads to proportional displacement decrease. Or in other words, increasing the gap decreases coning phenomenon.

The main conclusion can be said in this way: coning depends on fluids flowrate and on annulus width, what in simple terms means "how strong the water is sucked" and "how much of the water is sucked".

The suggestion to improve an ICD design is to increase the gap between housing and the base pipe wall (shown in Figure 6.21). A thin annulus easily attracts water.

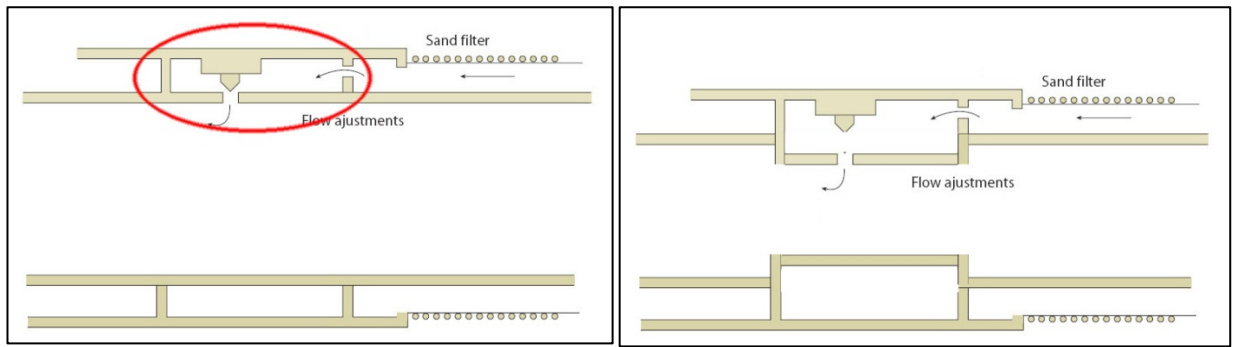


Figure 6.21 – Example suggested increase of annulus width.

When comparing “jumps” for different oils, it is clear that a more viscous oil (Nexbase 3080) increases coning phenomenon resulting in bigger water and oil “jumps”. A 10 mm gap case is compared for Nexbase 3080 and Exxsol D80 in Figure 6.22. More detailed picture with a single graph for each gap is presented in Appendix G.

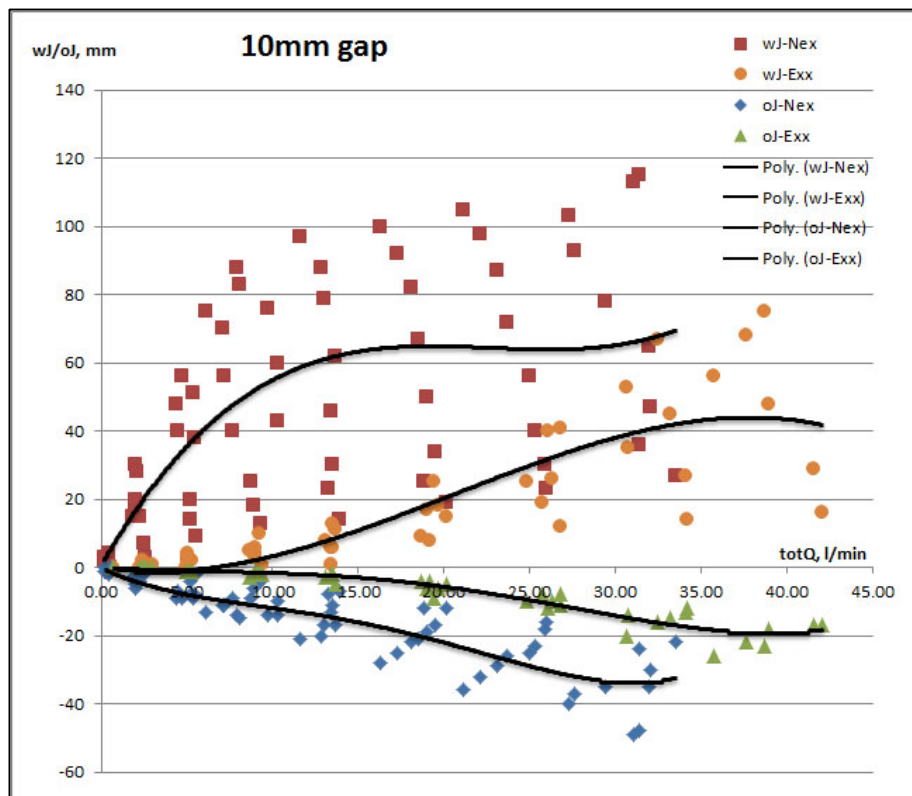


Figure 6.22 – “Jump” comparison for different oils.

Water cut plots are shown in Figure 6.23, more detailed are in Appendix H. It is seen that WC reaches its maximum at 10-15 l/min and then stabilizes or even goes down. That can be explained by a different flow regime in the orifice, as the vortex was clearly observed (shown in Figure 6.24). However, WC grows steadily for Exxsol oil.

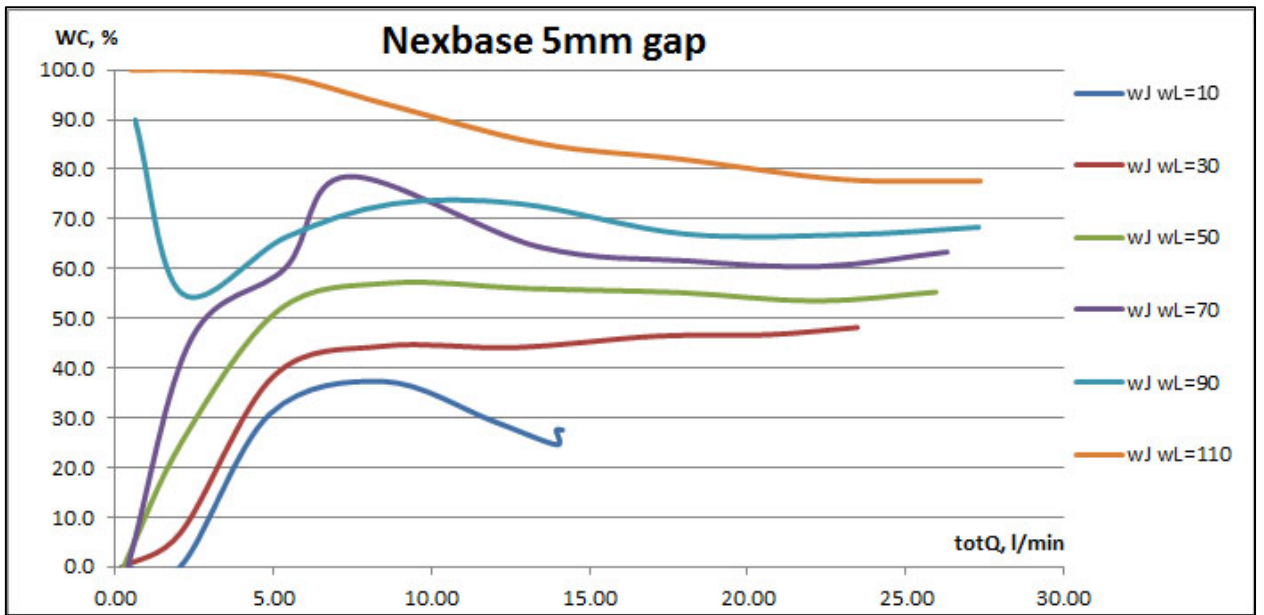


Figure 6.23 – WC vs. flowrate plot for Nexbase 3080, 5mm gap.

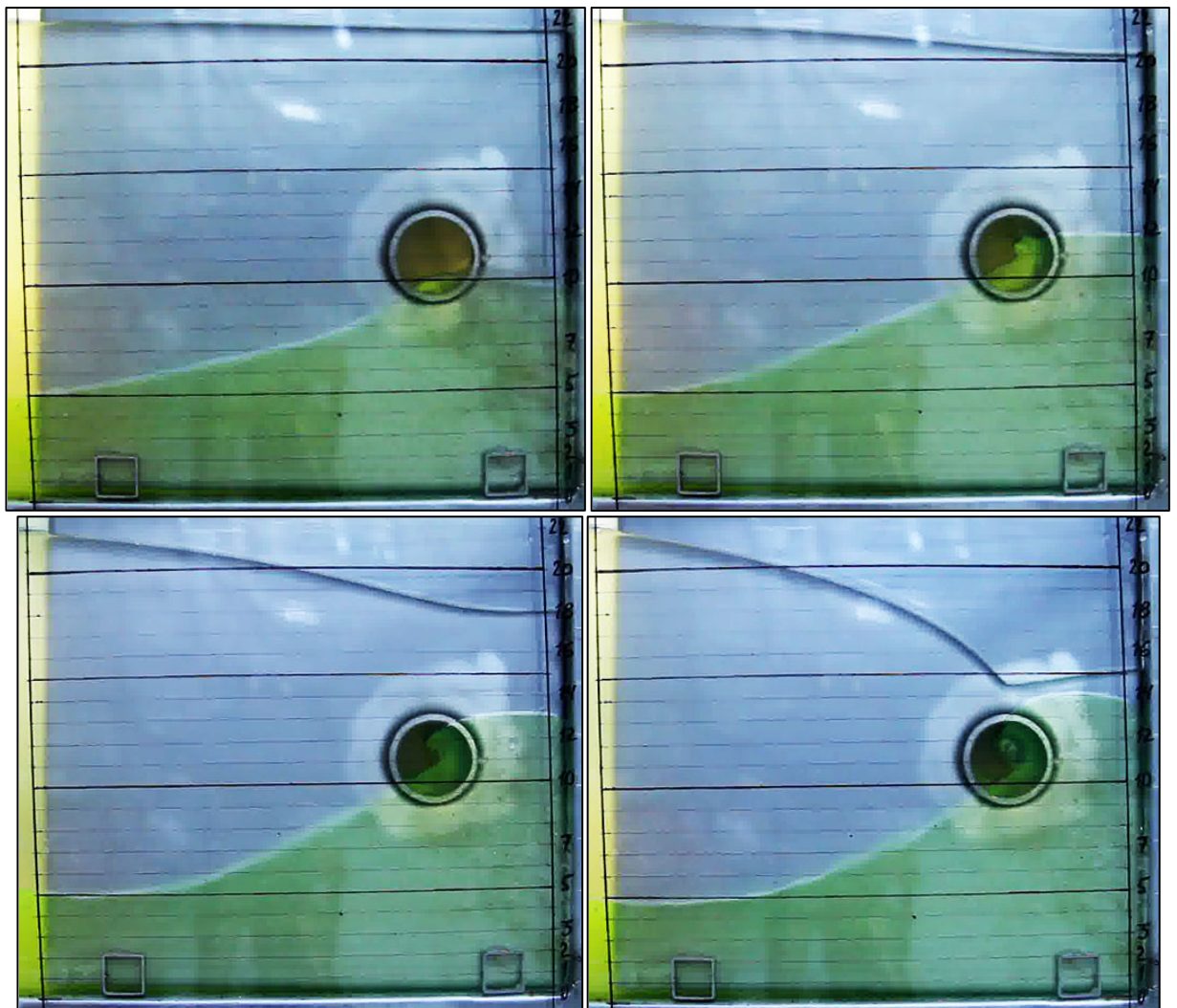


Figure 6.24 – Vortex development in 5mm gap, Nexbase 3080.

7 Conclusions and recommendations

This Master Thesis focuses on the experimental study of the water coning phenomenon in perforated pipe geometry. With the data on horizontal well design, geometry of the ICD/AICD housing, production rates and fluid properties, provided by Statoil Research Centre in Rotvoll, Trondheim, the experimental rig was designed and constructed in NTNU multiphase flow laboratory. It is based on the 2D-configuration setup and was used for flow visualization experiments, all the procedures and key photographs are included in this work. A risk assessment analysis was performed according to the NTNU and SINTEF safety procedures prior to starting of the work in the lab.

The study provides extensive literature review of the problem. Due to the nature of the project overview of research findings on horizontal well cresting and on placement of Inflow Control Devices (ICD) was presented in this chapter.

The total number of 459 experiments with different rig and oil/water flow setup was conducted. Every single flow pattern was recorded on video. All the results, including experimental parameters, graphs, trending analyses, were put down in 1 excel spreadsheet.

The data were carefully analyzed, the correlations between experimental parameters were checked if they meet the objectives of the project. In the end the accent was set on flowrates, liquid “jumps” (coning), water cut dependences from oil characteristics, gap (annulus width), liquid level etc. The explanations to correlations and features were suggested in order to better understand the mechanism of coning formation.

Among other observations the data analysis shows these key features:

- Once the water has found its way to the production tubing it obtains higher speed resulting in total flowrate increase. But the rate increase has nothing to do with oil production.
- Water coning in the annulus geometry directly depends on the fluid flowrate, regardless of speed or orifice area.
- Coning slightly tends to increase when interphase level is closer to the orifice.
- Coning significantly drops with increasing annulus width.
- Coning increases with a higher oil viscosity.

The main conclusion can be said in this way: coning depends on fluids flowrate and on annulus width, what in simple terms means “how strong the water is sucked” and “how much of water is to be sucked”. The suggestion to improve an ICD design is to increase the gap between housing and the base pipe wall.

More coning research is needed to be conducted with pipe geometries instead of flat plates for quantitative studies, because the current 2D-configuration shows just essential relations. More field data should be recovered in order to establish more accurate models and validate the established correlations.

8 References

500px website. 2012. (accessed Dec 2012).

<http://500px.com/photo/7794229>

Aadnoy, B.S. 2008. Autonomous Flow Control Valve or “intelligent” ICD.

http://www.hansenenergy.biz/HANSEN_Energy_Solutions/InflowControl2008B.pdf

Dusseault, M.B. 2001. Comparing Venezuelan and Canadian heavy oil and tar sands.

Calgary, Canada. Canadian International Petroleum Conference (June 12-14, 2001).

http://www.energy.gov.ab.ca/OilSands/pdfs/RPT_Chops_app3.pdf

Ellis, T., Erkal, A., Goh, G. and others. 2010. Inflow Control Devices – raising profiles. Oilfield Review Journal (winter 2009/2010).

http://www.slb.com/~media/Files/resources/oilfield_review/ors09/win09/03_inflow_control_devices.pdf

Femto encyclopedia. 2013. Fluid flowing out of an opening. (accessed Jun 2013).

http://www.femto.com.ua/articles/part_1/1460.html

Guidance to risk assessment – The approval of test rigs in laboratories at NTNU Department of Energy and Process Engineering and SINTEF Energy – Energy Processes

Halliburton. 2008. Developing the heavy oil and oil sands assets.

<http://www.halliburton.com/public/common/Brochures/H06153.pdf>

Halliburton website. 2013. How is heavy oil captured? (accessed Jun 2013).

<http://www.halliburton.com/en-US/ps/solutions/heavy-oil/about-heavy-oil/how-is-heavy-oil-captured/default.page?node-id=hhiyctma>

Inikori, S.O. 2002. Numerical study of water coning control with Downhole Water Sink (DWS) well completions in vertical and horizontal wells. A Dissertation submitted to the Graduate Faculty of the Louisiana State University and Agricultural and Mechanical College in partial fulfillment of the requirements for the Degree of Doctor of Philosophy (August

http://etd.lsu.edu/docs/available/etd-0610102-080619/unrestricted/Inikori_dis.pdf

Maggs, D., Raffn, A.G., Porturas, F., Murison, J. and others. 2008. Production optimization for second stage field development using ICD and Advanced Well Placement technology. SPE 113577. 2008 SPE Europec/EAGE Annual Conference and Exhibition.

<http://www.onepetro.org/mslib/servlet/onepetropreview?id=SPE-113577-MS&soc=SPE>

Makinde, F. A., Adefidipe, O. A., Craig, A. J. 2011. Water coning in horizontal wells: prediction of post-breakthrough performance. Petroleum Engineering Department, Covenant University, Ota, Nigeria. International Journal of Engineering & Technology IJET-IJENS (February, 2011).
<http://www.ijens.org/Vol%2011%201%2001/1110201-4343%20IJET-IJENS.pdf>

Moen, T., Asheim, H. 2008. Inflow Control Device and near-wellbore interaction. SPE 112471. 2008 SPE International Symposium and Exhibition on Formation Damage Control.
<http://www.onepetro.org/mslib/servlet/onepetropreview?id=SPE-112471-MS>

NTNU guidance to handling of waste
<http://www.ntnu.no/hms/retningslinjer/HMSR18B.pdf>

Nurmi, R., Kuchuk, F., Cassell, B., Chardac, J., Maguet, P. 1995. Horizontal highlights. Middle East Well Evaluation Review (Number 16, 1995).
http://www.slb.com/~media/Files/resources/mearr/wer16/rel_pub_mewer16_1.pdf

Porturas, F., Vela, I., Pazos, J., Humbert, O. 2009. Lifting more dry oil by reducing water production with Inflow Control Devices in wells drilled and completed in consolidated reservoirs, Bloque 15, Ecuador. AAPG -ER Newsletter (June 2009)
<http://www.aapg.org/europe/newsletters/2009/06jun/06jun09europe.pdf>

Ratterman, G. 2006. Uniform flow profiles improve horizontal wells. Drilling Contractor journal (March/April 2006)
<http://iadc.org/dcp/dc-marapr06/Mar06-bot.pdf>

Regulations relating to health, environment and safety in the petroleum activities. 2001. The framework regulations (31 August 2001).
http://www.ptil.no/getfile.php/Regelverket/Rammeforskriften-2010_e.PDF

Schlumberger. 2010. ResFlow ICDs in horizontal openhole wells optimize production in thin oil-rim reservoir.
http://www.slb.com/~media/Files/sand_control/case_studies/resflow_malaysia_cs.pdf

Schlumberger Oilfield Glossary website. 2013. Cresting. (accessed Jun 2013)
<http://www.glossary.oilfield.slb.com/en/Terms.aspx?LookIn=term%20name&filter=cresting>

Weatherford. 2010. FloReq Inflow Control Device (ICD).
<http://www.weatherford.com/weatherford/groups/web/documents/weatherfordcorp/wft126939.pdf>

Wikipedia. 2013. Hydraulic press. (accessed Jun 2013)
http://en.wikipedia.org/wiki/Hydraulic_press

Wikipedia. 2013. Injector. (accessed Jun 2013)
<https://en.wikipedia.org/wiki/Injector>

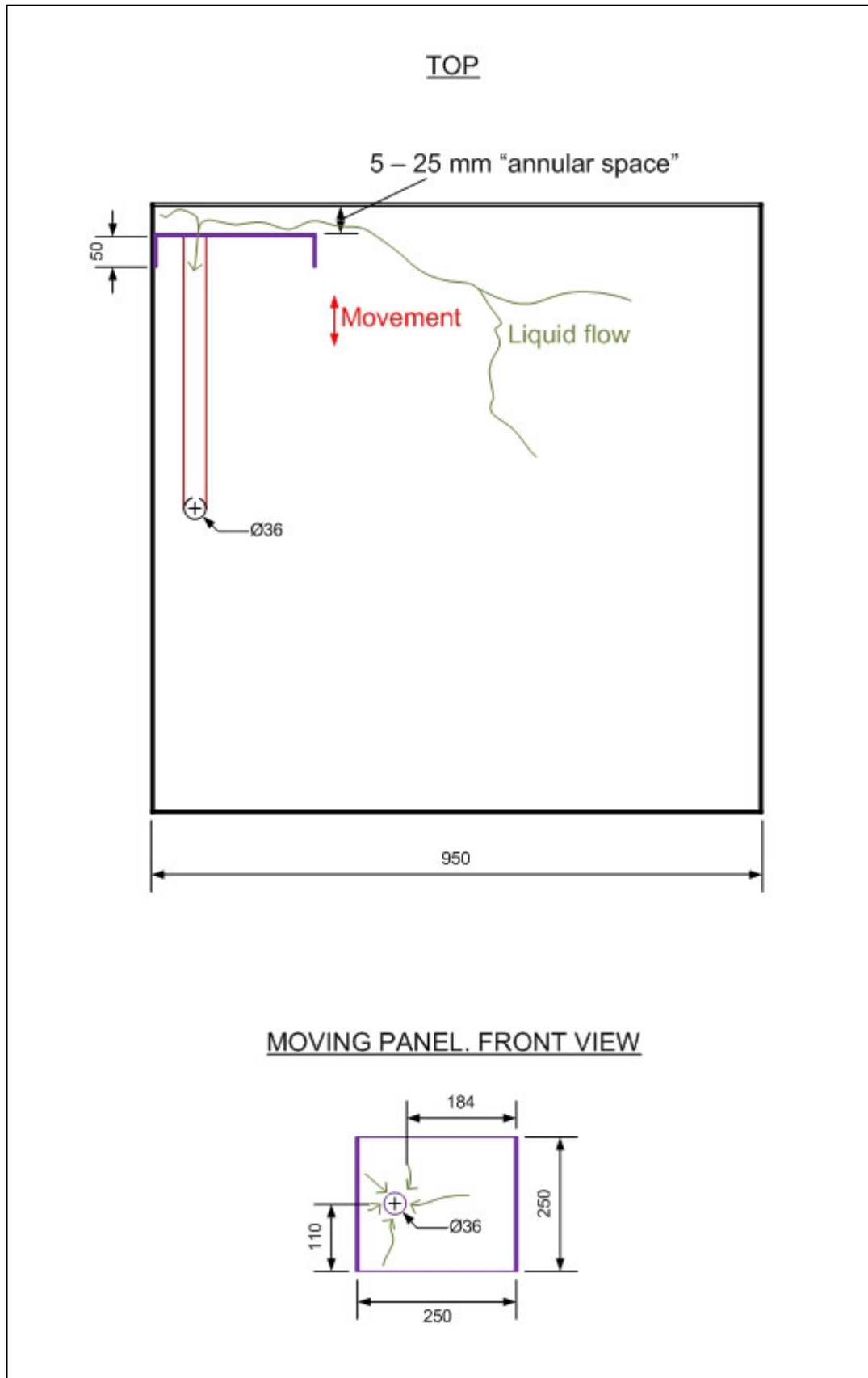
Wikipedia. 2013. Torricelli's law. (accessed Jun 2013).
http://en.wikipedia.org/wiki/Torricelli%27s_law

Zadeh, A. M., Slotte, P. A., Aasheim, R., Gyllensten, A. J., Årland, K. 2012. Optimal Inflow Control Devices configuration for oil rim reservoirs. OTC 22963. 2012 Offshore Technology Conference.
<http://www.onepetro.org/mslib/servlet/onepetropreview?id=OTC-22963-MS>

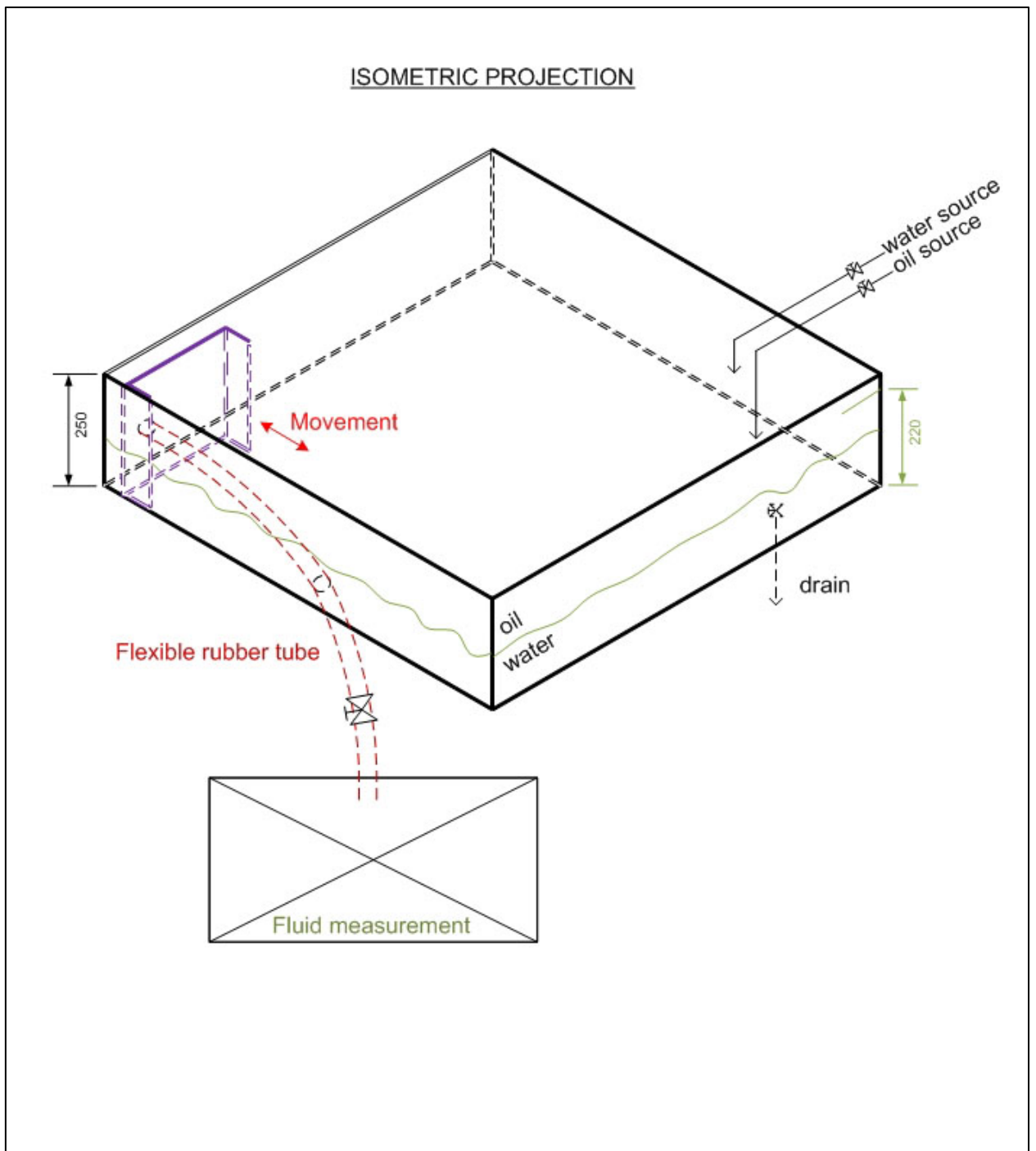
Statoil document. 2012. Oil-water flow patterns upstream and downstream ICD/AICD. Draft.

9 Appendices

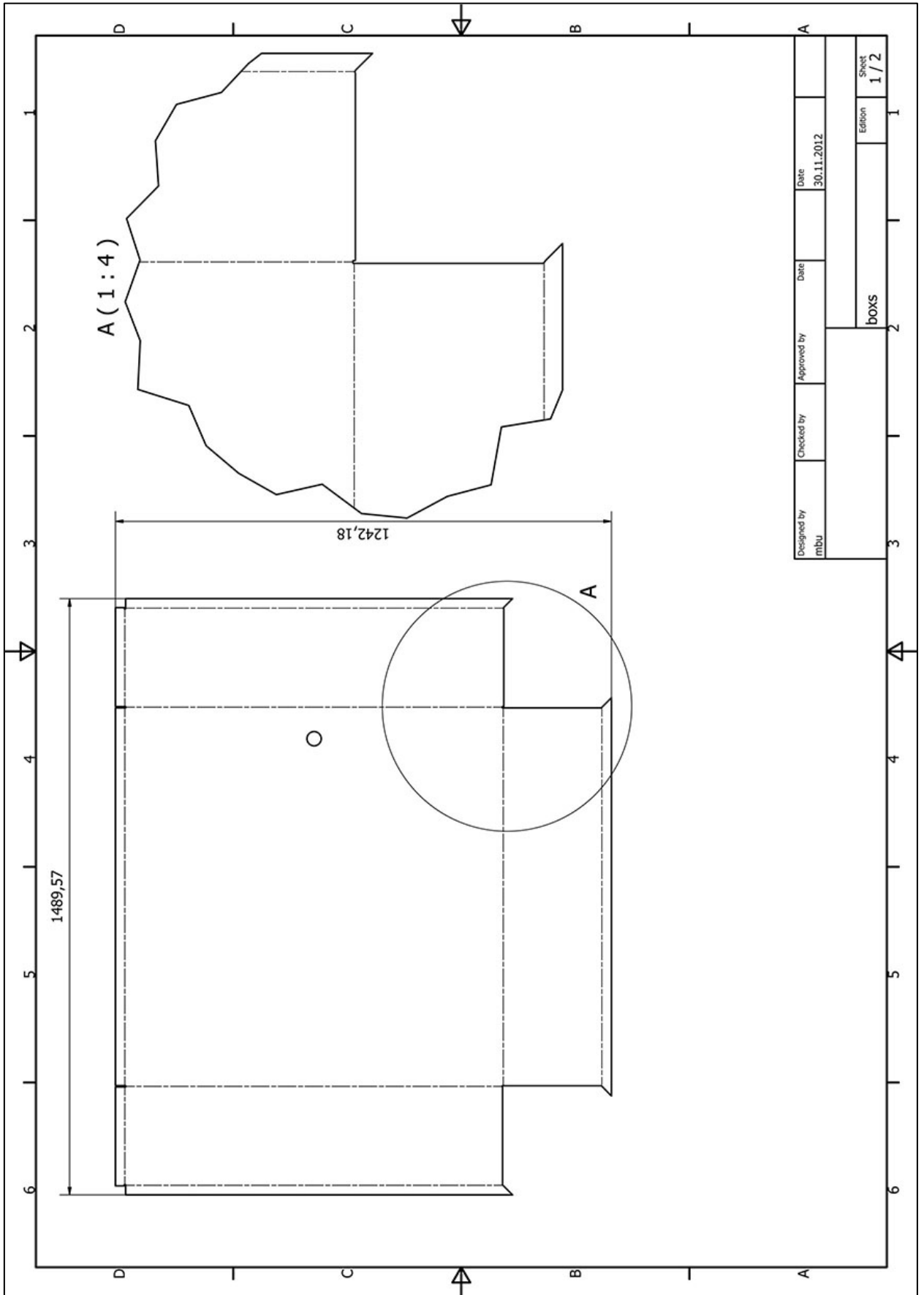
9.1 Appendix A – Full rig design arrangement.



Appendix A – Full rig design arrangement. (2 page out of 2)

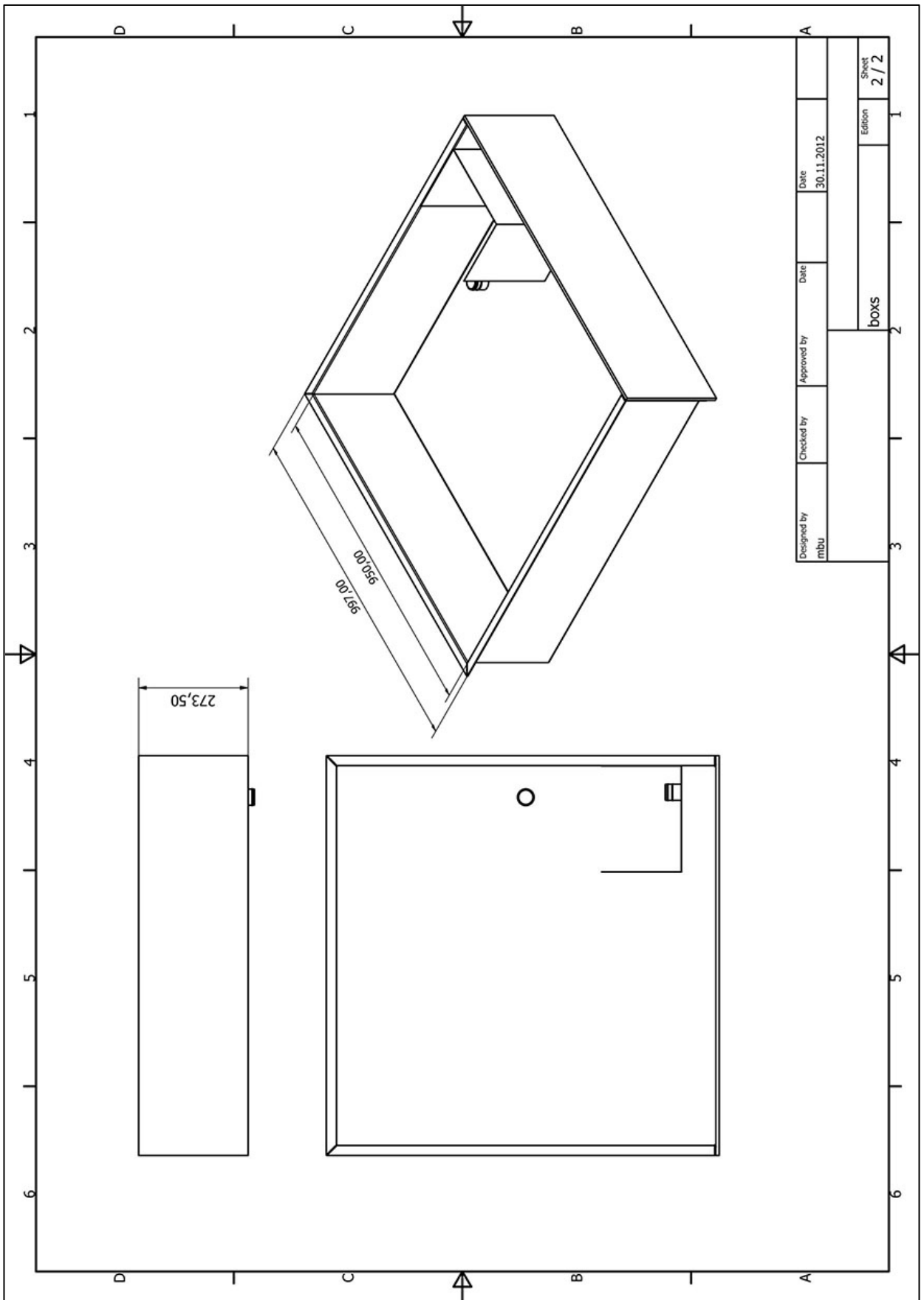


9.2 Appendix B – Drawings for tank manufacturing.



| | | | | |
|--------------------|------------|-------------|------------|-------|
| Designed by mbu | Checked by | Approved by | Date | Date |
| | | | 30.11.2012 | |
| BOXS | | | Edition | Sheet |
| | | | 1 / 2 | 1 / 2 |

Appendix B – Drawings for tank manufacturing. (2 page out of 2)



9.3 Appendix C – The parameters of all experimental runs.

| Oil | Annulus width (gap), mm | Water level, mm | Valve rotation | Orifice area, % | | | |
|--------------|-------------------------|-----------------|----------------|-----------------|------|----|-----------|
| Nexbase 3080 | 5 | 10 | 1 – 4.5 | 100 | | | |
| | | 30 | | | | | |
| | | 50 | | | | | |
| | | 70 | | | | | |
| | | 90 | | | | | |
| | | 110 | | | | | |
| | 10 | 10 | 1 – 5 | | | | |
| | | 20 | 1 – 4.5 | | | | |
| | | 30 | | | | | |
| | | 50 | | | | | |
| | | 70 | | | | | |
| | | 90 | | | | | |
| | | 100 | | | | | |
| | | 110 | | | | | |
| | 15 | 10 | | 1 – 6 | 16.5 | | |
| | | | | 1 – 5 | 50 | | |
| | | | | | 83.5 | | |
| | | 30 | 1 – 4.5 | 100 | | | |
| | | | | | 50 | | |
| | | | | | 70 | | |
| | | | | | 90 | | |
| | | | | | 110 | | |
| | | | | | 25 | 10 | 1.5 – 4.5 |
| | | | | | | 50 | |
| 70 | 1.5 – 5 | | | | | | |
| 90 | 1 – 5 | | | | | | |
| 110 | 1 – 4.5 | | | | | | |

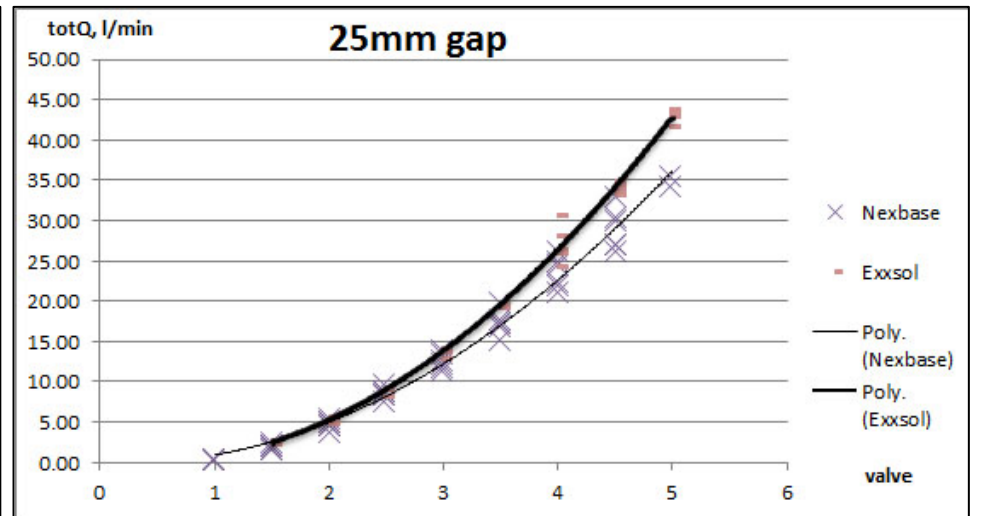
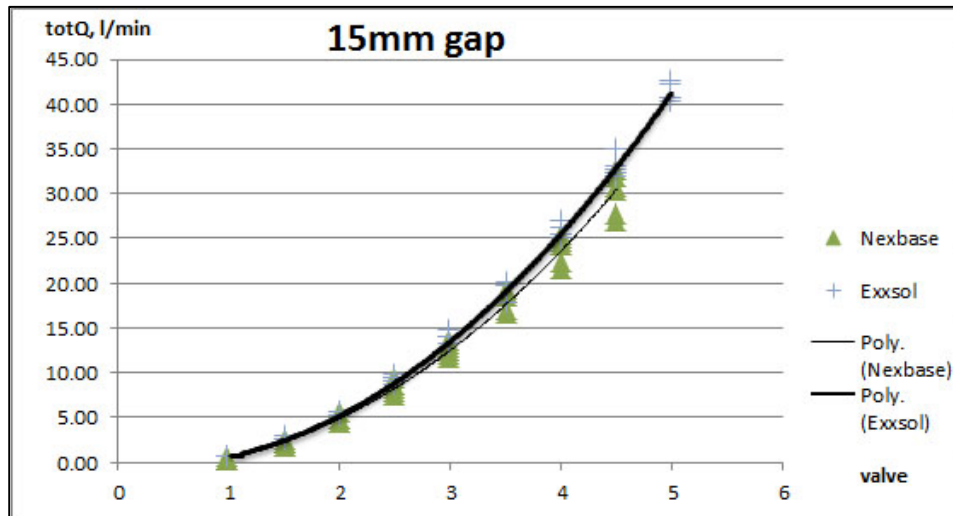
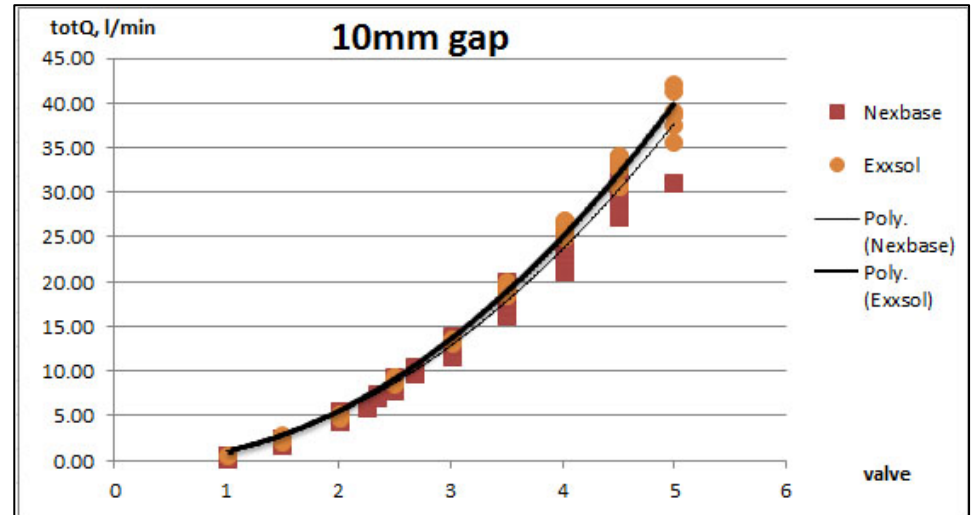
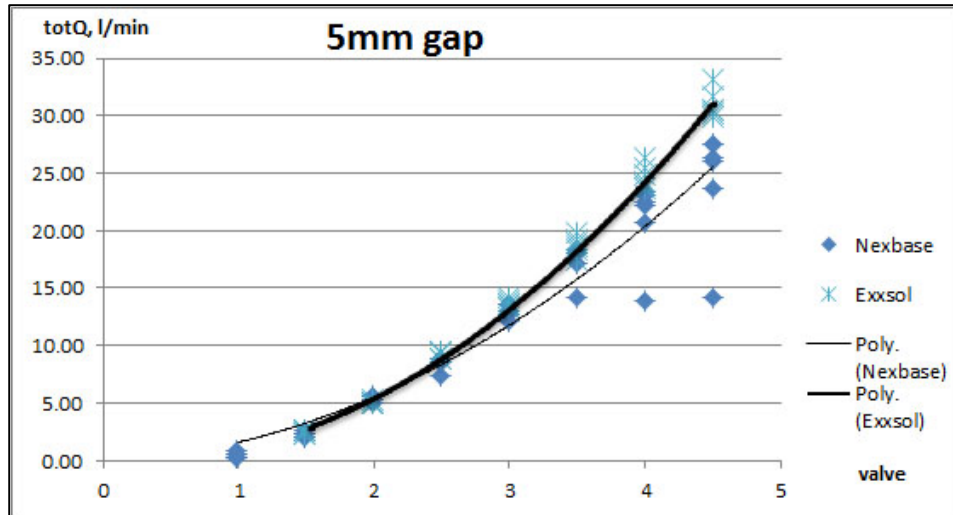
Appendix C – The parameters of all experimental runs. (2 page out of 2)

| Oil | Annulus width (gap), mm | Water level, mm | Valve rotation | Orifice area, % | |
|------------|-------------------------|-----------------|----------------|-----------------|-----|
| Exxsol D80 | 5 | 10 | 1.5 – 4.5 | 100 | |
| | | 30 | | | |
| | | 50 | | | |
| | | 70 | | | |
| | | 90 | | | |
| | | 110 | | | |
| | 10 | 10 | 1 – 5 | 1.5 – 5 | 100 |
| | | 30 | | | |
| | | 30 | 16.5 | | |
| | | 30 | 50 | | |
| | | 30 | 83.5 | | |
| | | 30 | | | |
| | | 50 | | | |
| | | 70 | | | |
| | | 90 | | | |
| | | 110 | | | |
| | 15 | 10 | 1 – 4.5 | 1.5 – 5 | 100 |
| | | 30 | | | |
| | | 50 | | | |
| | | 70 | | | |
| | | 90 | | | |
| | | 110 | 1 – 5 | | |
| | 25 | 10 | 2 – 5 | 1.5 – 4.5 | 100 |
| | | 30 | | | |
| 50 | | | | | |
| 70 | | 1.5 – 4.5 | | | |
| 90 | | 1.5 – 5 | | | |
| 110 | | | | | |

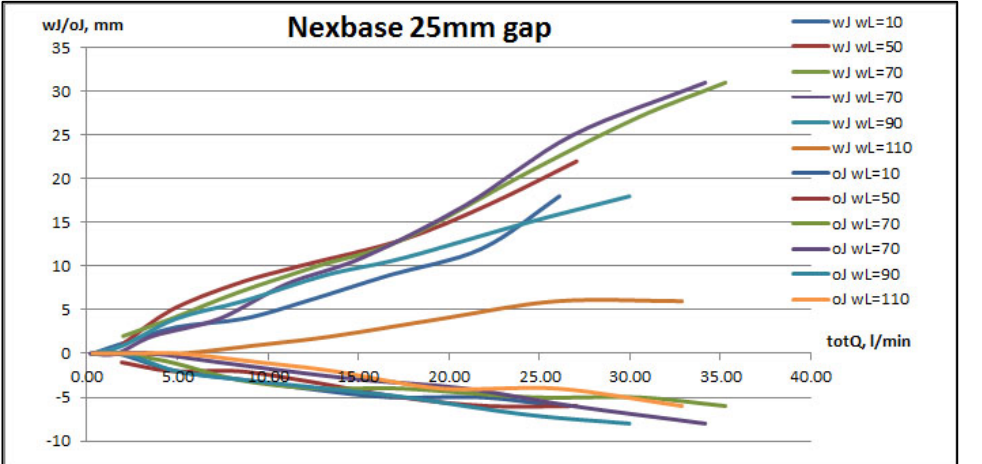
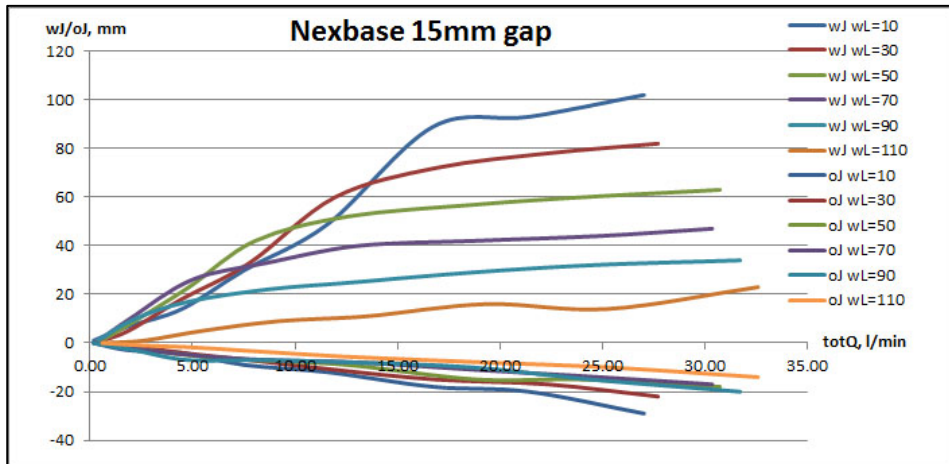
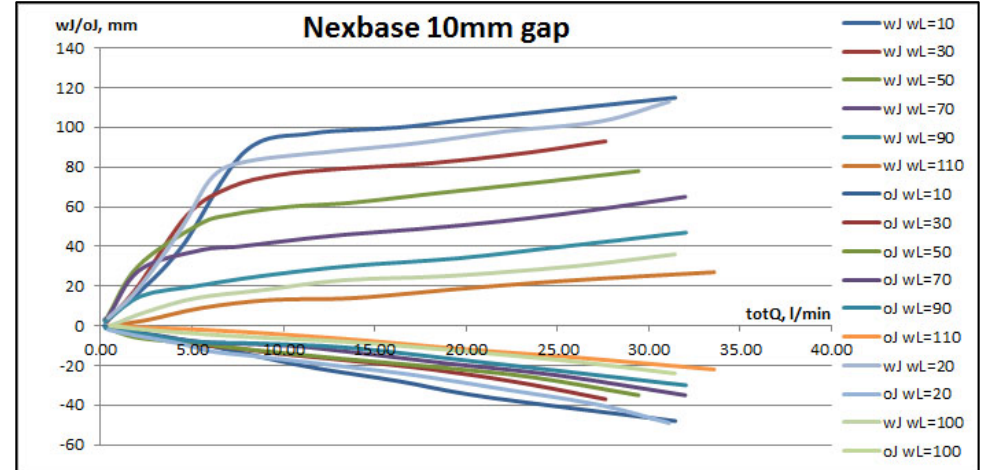
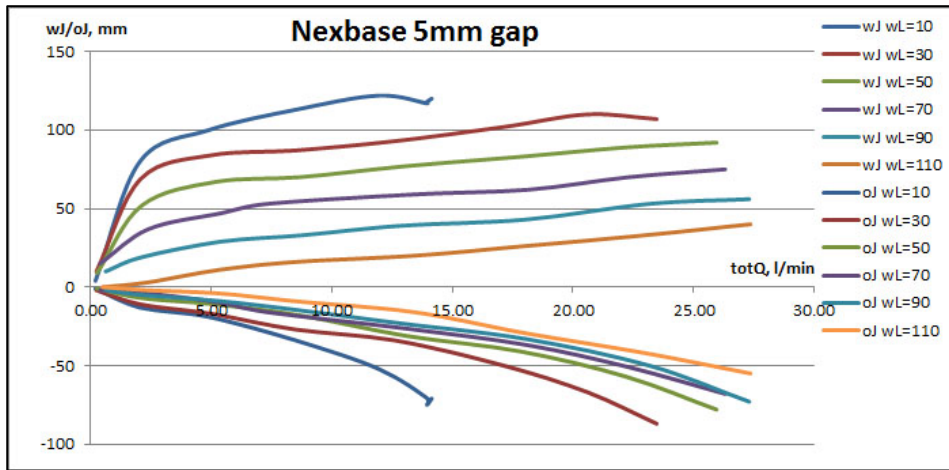
9.4 Appendix D – Spreadsheet acronyms’ identification.

| | | |
|--|--|---|
| H – base pipe height, mm | wL – water level, no flow, mm | wJ – water “jump” (= wL’ - wL), mm |
| B – base pipe width, mm | oL – oil level, no flow, mm | oJ – oil “jump” (= oL’ - oL), mm |
| L – housing distance to the orifice center, mm | ΔL – distance from wL to orifice, no flow, mm | wV – amount of water that flowed, ml |
| h – height of the orifice center, mm | wA – orifice covered with water, no flow, % | oV – amount of oil that flowed, ml |
| d – orifice diameter, mm | wL’ – max water level, during the run, mm | totV – amount of fluids that flowed, ml |
| δ – annulus width (gap), mm | oL’ – min oil level, during the run, mm | WC – percentage of water in the fluids that flowed, % |
| | $\Delta L'$ – distance from wL’ to orifice, during the run, mm | wQ – water flowrate, l/min |
| | wA’ – orifice covered with water, during the run, % | oQ – oil flowrate, l/min |
| | | totQ – total flowrate, l/min |
| | | totU – total velocity, mm/s |

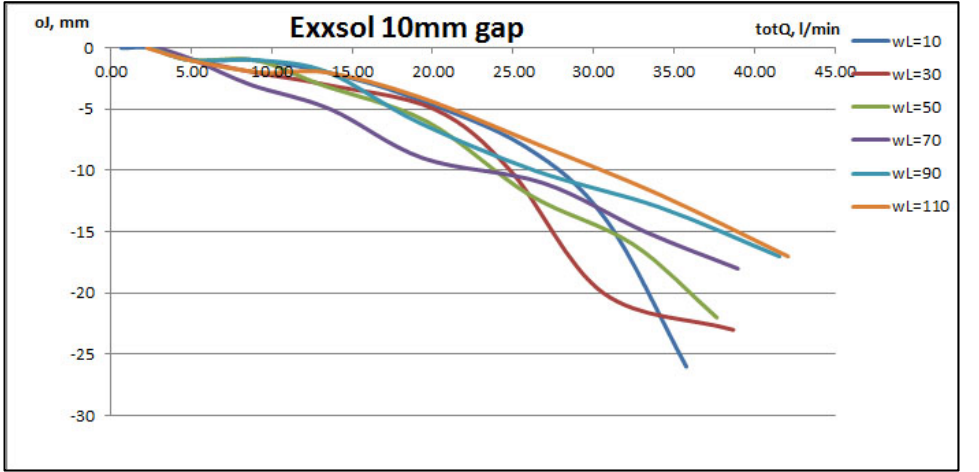
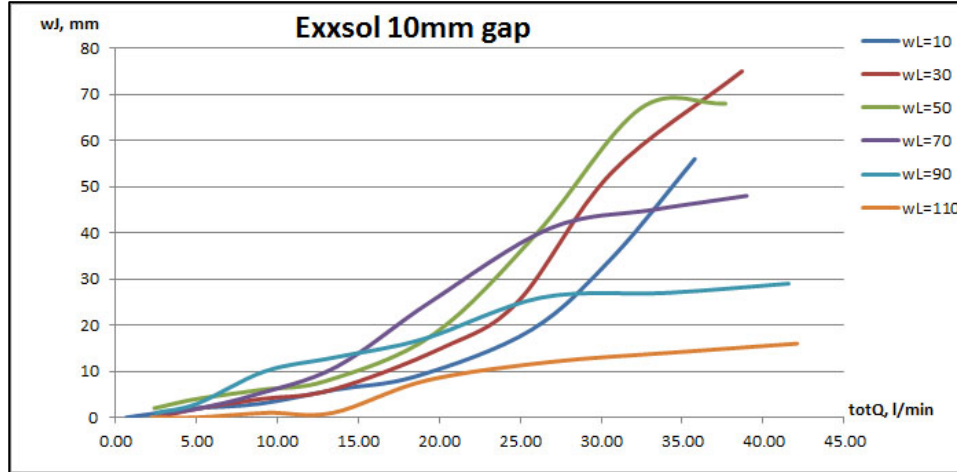
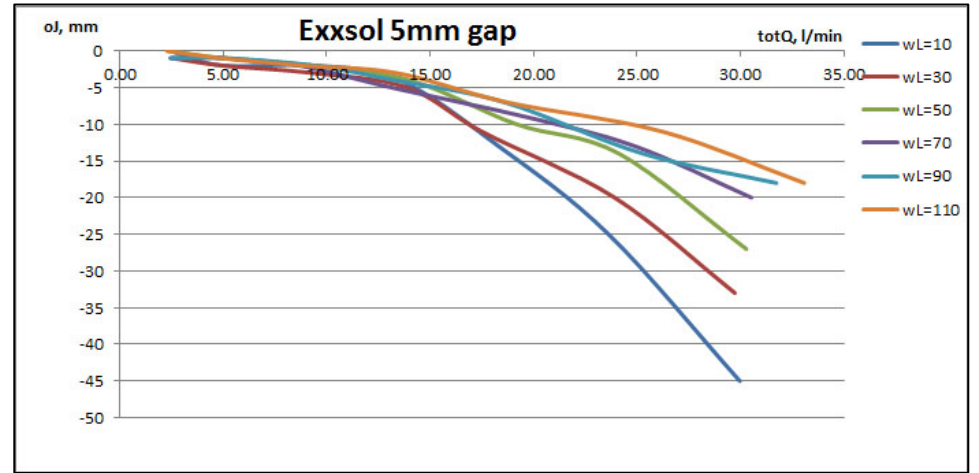
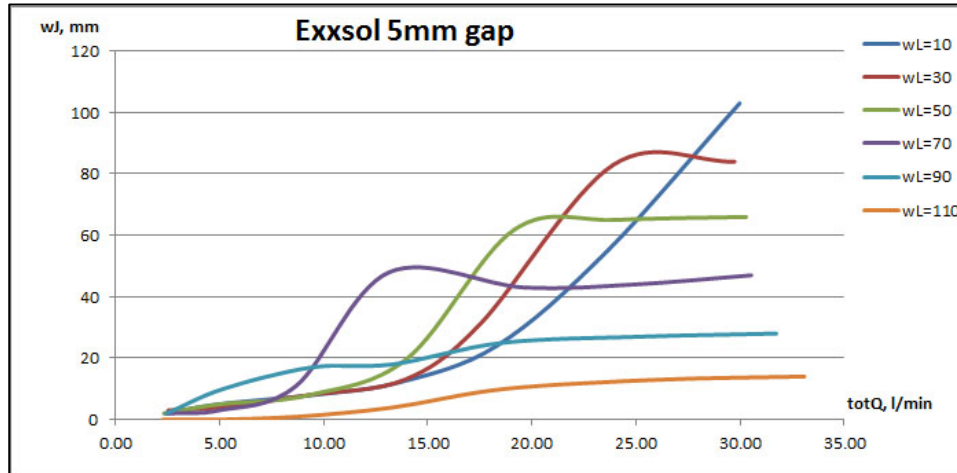
9.5 Appendix E – Detailed oils flowrates comparison with a single graph for each gap.



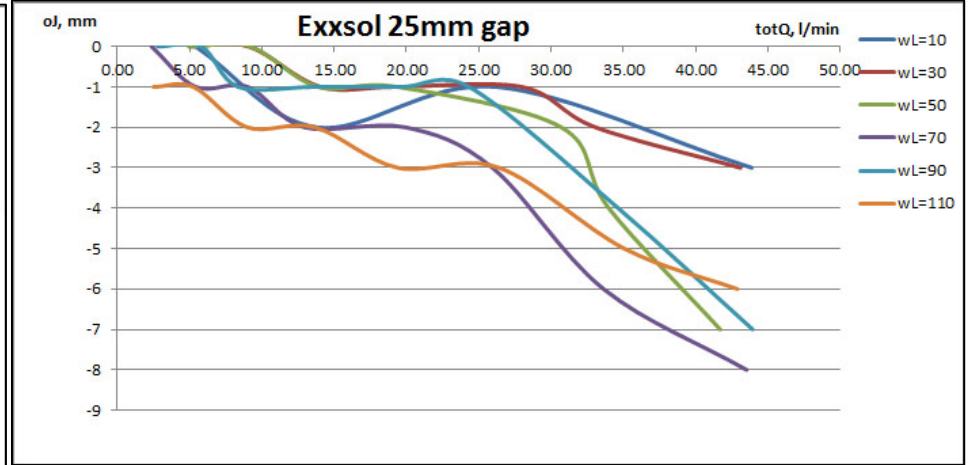
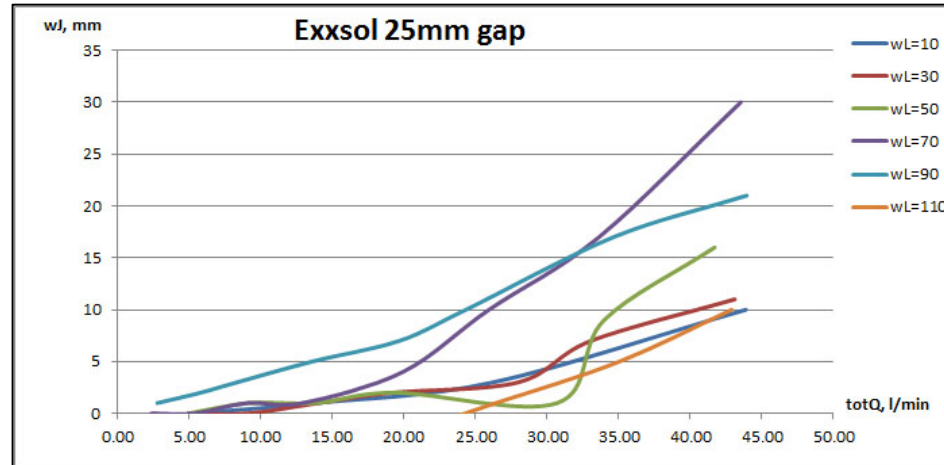
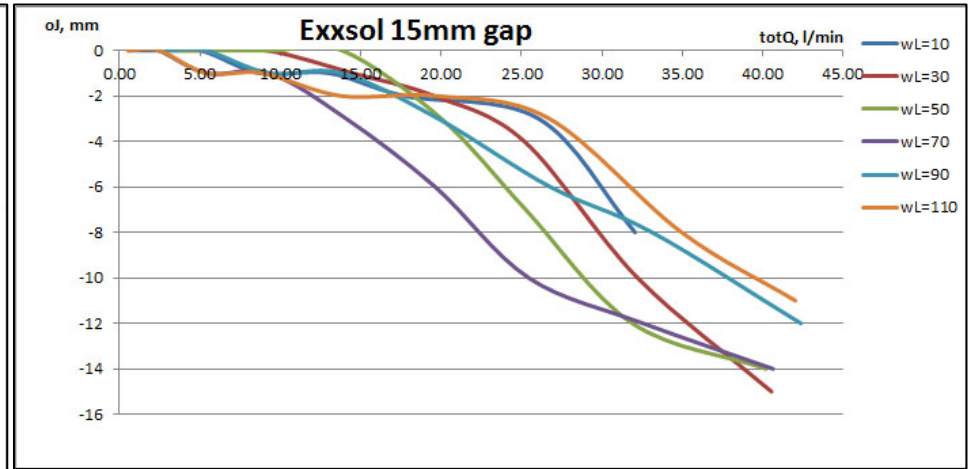
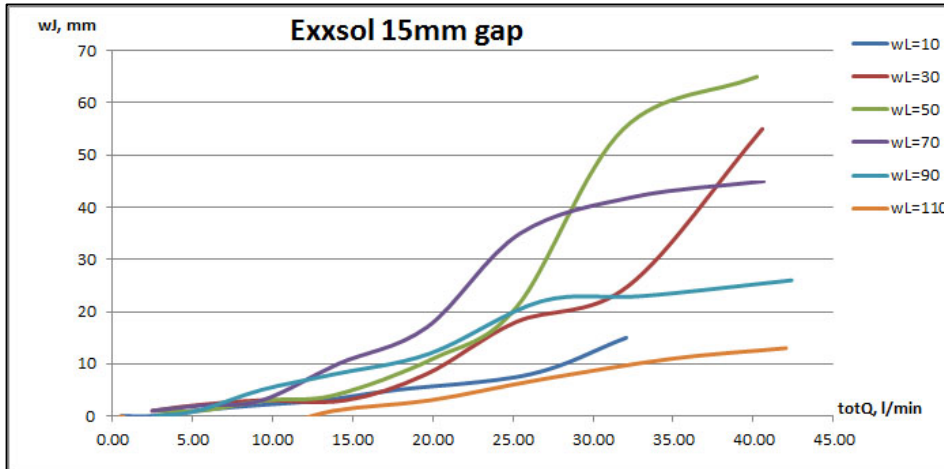
9.6 Appendix F – “Jump” values vs. flowrate for Nexbase 3080 series and Exxsol D80 series for each gap.



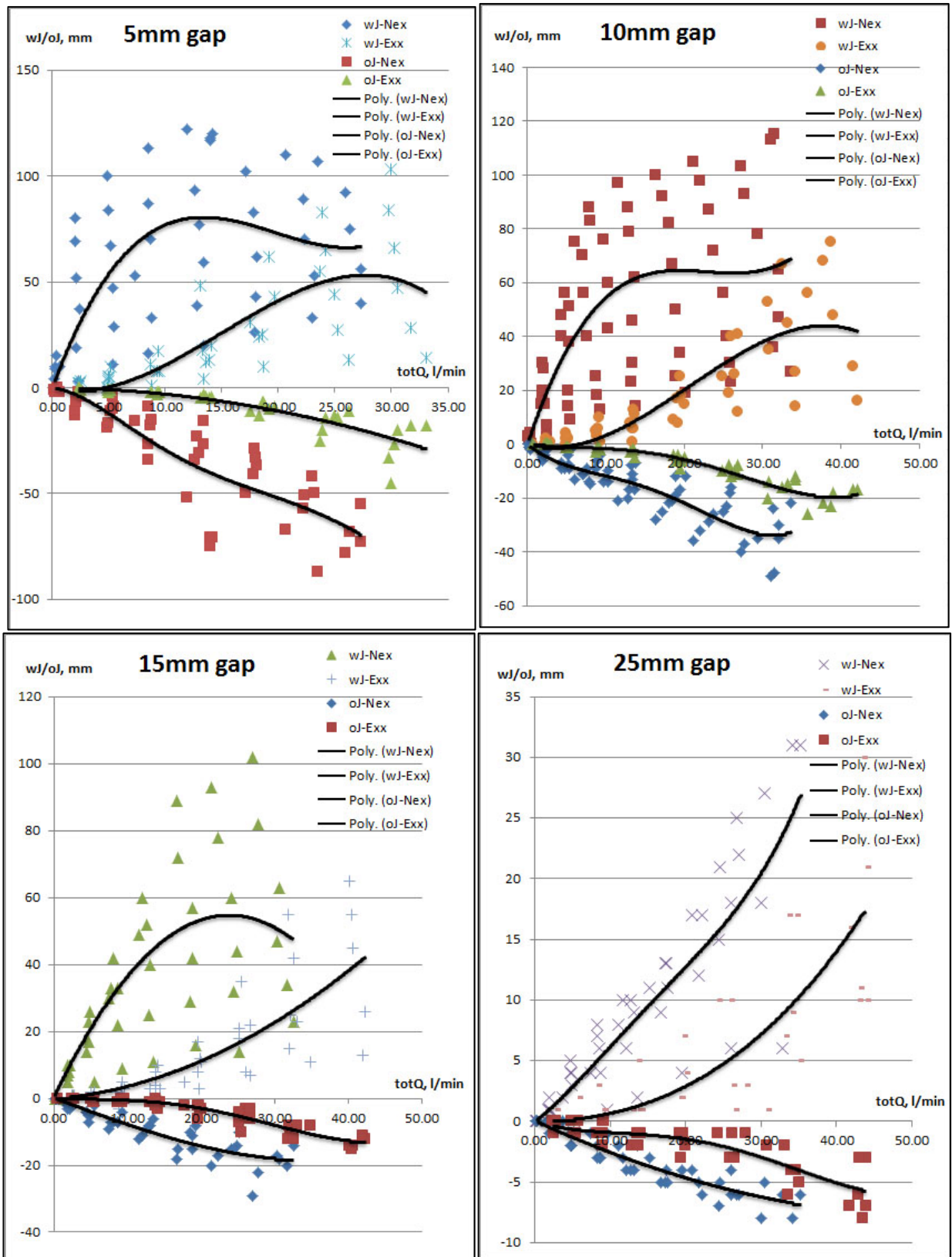
Appendix F – “Jump” values vs. flowrate for Nexbase 3080 series and Exxsol D80 series for each gap. (2 page out of 3)



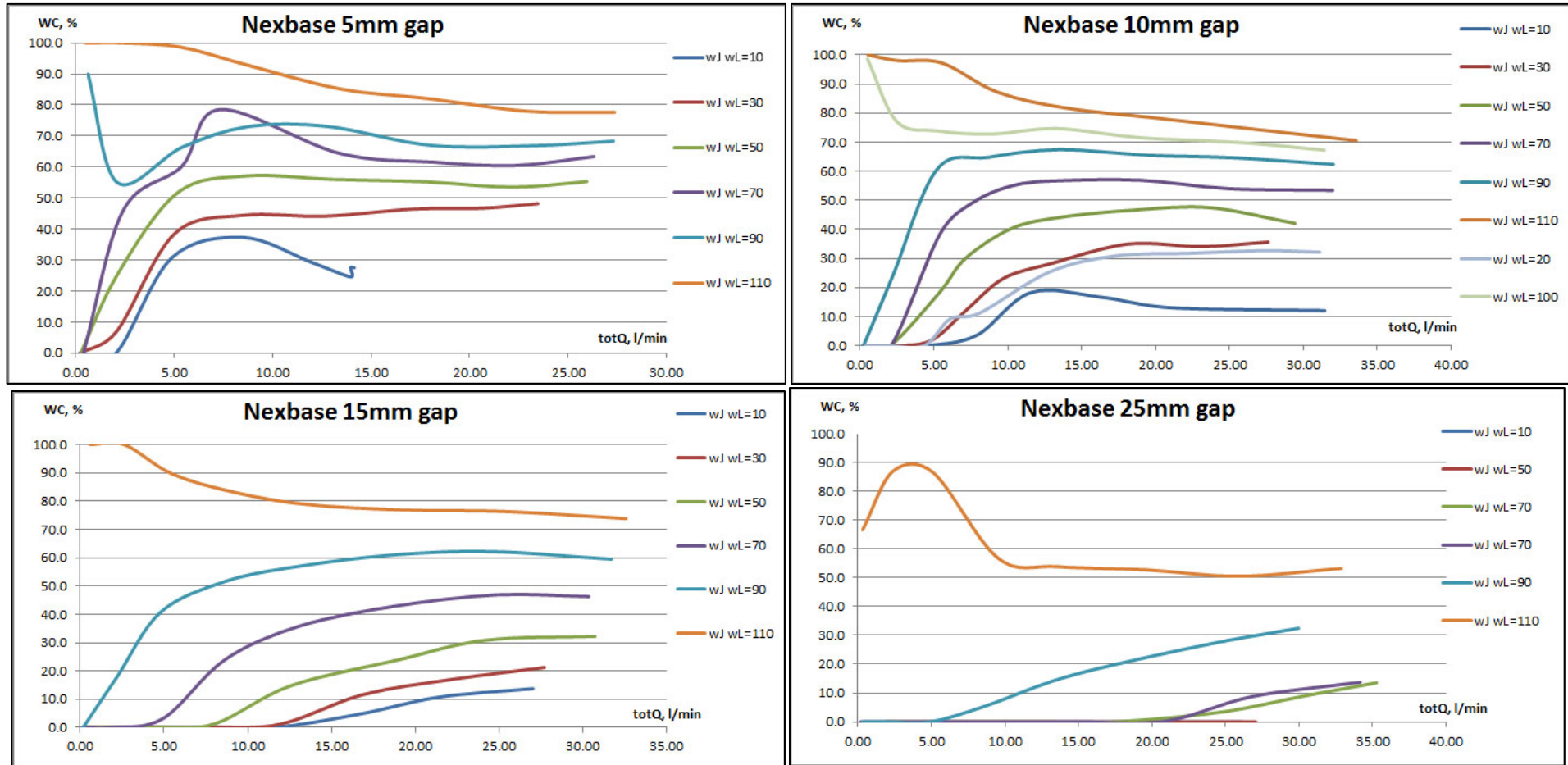
Appendix F – “Jump” values vs. flowrate for Nexbase 3080 series and Exxsol D80 series for each gap. (3 page out of 3)



9.7 Appendix G – Detailed oils “jump” comparison with a single graph for each gap.



9.8 Appendix H – Water cut correlations over flowrate for different water levels.



Appendix H – Water cut correlations over flowrate for different water levels. (2 page out of 2)

